Centre for Geo-Information

Thesis Report GIRS-2007-10

A COMBINED MODEL TO ESTIMATE ACTUAL EVAPOTRANSPIRATION FROM METEOROLOGICAL AND REMOTE SENSING DATA

Raquel Iniesta Ruiz

October 2007

WAGENINGEN UNIVERSITY
WAGENINGEN UR

A Combined Model to Estimate Actual Evapotranspiration from Meteorological and Remote Sensing Data

Raquel Iniesta Ruiz

Registration number 801020-383-020

Supervisors:

Prof. Dr. Lammert Kooistra
Prof. Dr. Jose-Luis Casanova Roque

A thesis submitted in partial fulfilment of the degree of Master of Science at Wageningen University and Research Centre, The Netherlands.

October, 2007
Wageningen, The Netherlands

Thesis code number: GRS-80436
Wageningen University and Research Centre
Laboratory of Geo-Information Science and Remote Sensing
Thesis Report: GIRS-2007-10

ACKNOWLEDGEMENTS

This thesis is dedicated to my parents for their unlimited support. Nothing could be done without their patience and encouragements.

My sincere gratitude to my supervisor in Spain, Jose-Luis Casanova, for trusting in my work and for his support and experience. Thank a lot to my supervisor in Wageningen, Lammert Kooistra, his guidance and experience was essential for the elaboration of this work.

Special thank to Alfredo Romo for everything he has taught me to carry out this work.

To my workmates and friends of the LATUV and Deimos-Imaging, David, David2, Juanjo, Cristina, Silvia, Julia, Julio, Aurelio, Abel, Jorge, Fernando and Mónica, for their patience, support and help. Thanks for making work nicer and easier to take.

I do not want to forget many other friends (MªCarmen, Trini, Bea, Juanma…) who, in spite of the distance, they were supporting me in the bad moments; I like to express my most sincere thanks.

ABSTRACT

This work presents an approach for the calculation of actual evapotranspiration at a regional scale. Using the daily Penman-Monteith equation, the reference evapotranspiration has been estimated by means of a combined model from meteorological stations data and remote sensing data.

Remote sensing data have been used to estimate surface reflectance, cloudiness factor, net radiation and the crop coefficient through the Relative Greenness Index (RGI). To do that MODIS and SEVIRI-MSG data have been use.

The meteorological data were interpolated by different methods determined by a previous study.

The study has been focused in the Autonomic Community of Andalusia, region located in the South of Spain. The chosen months like period of analysis have been July and August because of the greatest evapotranspiration of the year takes place during them and therefore its calculation gains a great importance.

The result of this study shows the usefulness of MODIS to calculate reference and actual evapotranspiration at regional scale. Furthermore, the RGI is shown as a good indicator for characterizing the evolution of crop coefficient.

Keywords: crop coefficient, evapotranspiration, remote sensing.

TABLE OF CONTENTS

LIST OF FIGURES

LIST OF TABLES

1 INTRODUCTION

1.1 Context and background

Spain is the European country in the Mediterranean basin with the largest surface of agricultural lands (20,3 million hectares), of which 84,99 % corresponds to dry-farmed lands with the other remaining 15,01 % to irrigated lands (MAPA, 2004). Spain is also the Mediterranean country with the most number of hectares of irrigation (3,3 millions), ahead of Italy (3,1 millions) and far ahead of France and Greece (1,5 and 0,8 millions, respectively) (FENACORE, 2005).

These irrigated crops consume near 75 % of the approximately 24.094 cubic hectometres of water that are controlled in Spain from the available water resources (MMA, 2005), and they represent 50 % of the whole Spanish agricultural production (MAPA, 2004).

The importance of irrigated lands in the Spanish agrarian economy is not only relevant from a macroeconomic point of view (job-creation, transportation, agro-food industry, fertilizers, crates, machinery, etc.), but also from a microeconomic perspective.

In this way, the transformation of dry-farmed surface into irrigated land has allowed many farmers to improve their yield, competitiveness and quality of life by increasing their production and agrarian revenue. A significant information supports this statement: a hectare of irrigated land produces six times more than a dry-farmed hectare generating incomes four times higher (MAPA, 2004).

Not only do irrigated crops allow higher incomes, but they are also safer enabling a coherent policy of production and market arrangement that guarantees a constant supply to consumers. On the one hand, irrigated lands favour quality and product diversification avoiding the risk that single-crop dry-farmed lands have. On the other hand, the risk of floods caused by torrential rains is also reduced since plants provide cover that intercepts and reduces rainfall and slows wind velocities, the primary mechanism for soil erosion. Irrigation also presents numerous advantages for the environment by favouring oxygen production and avoiding soil erosion (FENACORE, 2005).

With regard to the origin of the water used in Spanish irrigated lands, MAPA estimates that 68 % of the total irrigated surface is supplied by superficial water, whereas 28 % is provided from underground water. The remaining 4 % refers to irrigated water coming from transboundary, filter systems, desalination plants and reuse. In Spain, the reuse water percentage of irrigation water is approximately 20 % of the supply (FENACORE, 2005).

The principal method of irrigation used in 59 % of these surfaces is that of gravity (MAPA, 2004), followed by the spray method (24% of the surfaces) and the drip method (17%). The gravity method is the most wasteful and obsolete, even more so in an arid country. In this method the water is moved from a sector to other one of the zones of irrigation using the natural or artificial slopes of the area.

As a consequence of all this, there is growing social awareness of the necessity of saving water by means of an appropriate integrated management of water resources.

1.2 Problem definition

The place in the world where Spain is situated has a semiarid climate, with relatively scarce rainfall (650 mm per year) (MMA, 2005) and generally irregular, both space and temporally.

Nevertheless, within these general characteristics, the Spanish territory presents an unequal climatology that determines an uneven distribution of water. Mediterranean-climate areas such as Catalonia, Valencia, Murcia, Andalusia, Balearics ... as well as the Canary Isles receive a smaller volume of rainfall. The Segura river basin (located in the South-East of the country) stands out with an average rainfall of only 350 mm per year, being the most extreme case. On the other hand, the Northern basins, with a humid climate, receive an average of 1350 mm per year, a volume similar to other Central European areas (MMA, 2005).

Figure 1. Distribution of water in Spain.

Historically speaking, Spain has been specially affected by the phenomenon of droughts, with an average duration of 4 to 5 years (ONS, 2005). More than half of the years in the period 1880-2000 have been described as dry or very dry. Likewise, in the decades of the 80s and 90s, seven and five years respectively have been considered to be dry or very dry (MMA, 2005).

The droughts that affected Spain in the central years of the 20th century showed the lack of coordination existing among consumption necessities and available water resources. Since then, a policy of public works has been encouraged directed towards increasing water-storage capacity, facilitating the transportation of flows and even the connection among different river basins. As a result, at present, there are 1.187 large reservoirs in Spain, the largest surface per inhabitant in the world (Joaquín Díez-Gascó, 2003).

According to the National Institute of Meteorology, from November 2004 Spain has initiated the most severe drought since 1947, when pluviometric data began to be compiled. A prove of this is the reduction of the hydraulic reserve in Spain (Figure 2).

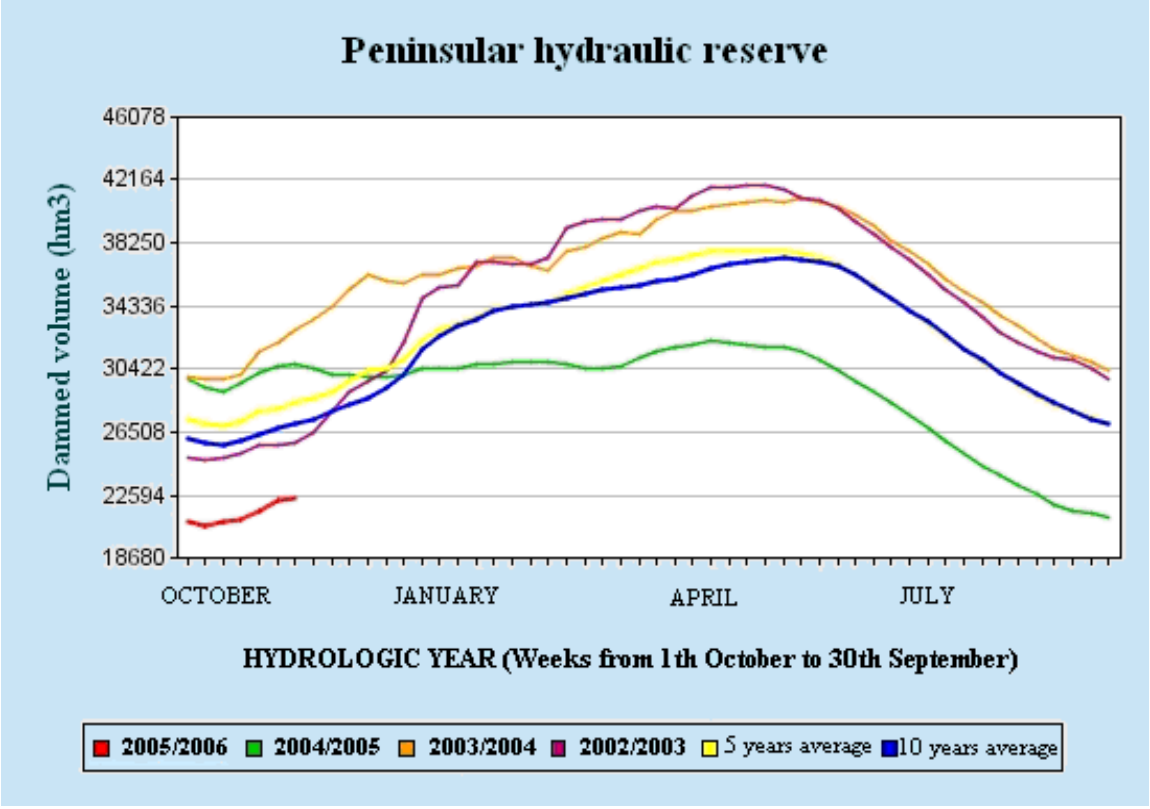

Figure 2. Evolution of the hydraulic reserve in Spain of last hydrologic years.

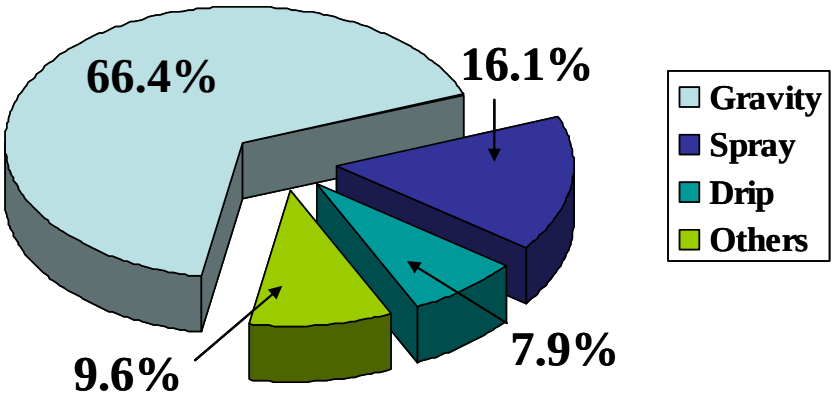

Figure 3. Percentage of water consumption for irrigation system.

It is during these periods of water shortage when most attention is paid to the agriculture sector as the one with the highest percentage of water consumption.

According to the report elaborated in 2005 by FENACORE, in the decade between 1990 and 2000 more than 350.000 new hectares of irrigated land were created. The irrigation method mostly used for this type of agriculture is that of gravity, which, besides, generates the most water wasted (MAPA, 2004), as Figure 3 shows.

Flood irrigation can consume up to 1.500 litters per square meter per year, whereas gravity can use just approximately 1.000 litters per square meter. However, if drip irrigation were used, the volume might go down to half, and lower quantities could be even reached by exudation, which is a microscopic drip (MMA, 2005).

In times of water shortage, to do more with less becomes essential. This is the key for efficiency, and this should be the aim of all water policies, whether it rains or not. A suitable management of water is indispensable to advance in the modernization of irrigation systems based on technologies that allow us to quantify crop water requirements and, consequently, the corresponding endowments of irrigation.

In order to know the quantity of necessary water that has to be supplied for the irrigation, it is essential to know the requirements of the crop (by means of a process called evapotranspiration) and the quantity of water that the rainfalls supply during the growing period. The difference between both is the quantity of water that it must be provided by irrigation.

The evapotranspiration is defined as the combination of two separate processes whereby water is lost on the one hand from the soil surface by evaporation and, on the other hand, from the crop by transpiration (Allen *et al.*, 1998). This concept includes different definitions that will be explained in detail in section 2. Hence, a good

knowledge of evapotranspiration is essential for agronomic studies, as well as other studies related with fields as Hydrology or Climatology.

During the last decades a great variety of methods for the estimation of evapotranspiration has been proposed, from the traditional methods which permit its calculation at local scale by means of field measurements, until the most recent models based on remote sensing techniques. The great advantage that remote sensing provides, regarding traditional methods, is the possibility of carrying out studies at regional scale. The problem of this technique is the fact that satellites only measure received radiation in certain wavelength intervals, after having crossed the atmosphere. These measurements are not directly related in a simple way with the flux of evapotranspiration on the soil but it must be obtained in an indirect way by means of other measurements.

In this work, the estimation of evapotranspiration was carried out using meteorological and remote sensing data, according to the available financial and technical means. Penman-Monteith equation was used according with the methodology established by Allen *et al.*, in 1998, since it is the methodology recommended by the Food and Agricultural Organization of the United Nations (FAO) as standard for calculating crops evapotranspiration.

Previous researches (Brasa *et al.*, 1996; Rivas and Caselles, 2004; Consoli *et al.*, 2006 or Rossi *et al.* 2006) have already combined meteorological and remote sensing data with the aim to estimate evapotranspiration at regional scale. The study of Brasa *et al.* was carried out in Spain in 1996 and NOAA images were used for it. Reference evapotranspiration was calculated according the equation proposed in 1987 by Caselles and Delegido and actual evapotranspiration by means of the Jackson equation (1977). In this methodology empirical coefficients, depending on climatic parameters, must be determined for each region. Rivas and Caselles in 2004, estimated reference evapotranspiration based on a simplified equation of the Penman-Monteith equation. This approach is also of local nature since some parameters must be estimated for a given area from meteorological data. NOAA images were used, too. In 2006, for the study developed by Rossi *et al.* in the South of Italy MODIS and Landsat images were used. Actual evapotranspiration were calculated according to the methodology of Allen *et al.* (1998). The equation used for the calculation of reference evapotranspiration was the Hargreaves equation (1985). This equation has less accuracy that the Penman-Monteith equation but it has the advantage to require less number of data. The last example mentioned, in which meteorological and remote sensing data have been used, is the study carried out by Consoli at al. in 2006 in eastern of Sicily (Italy). Penman-Monteith and Allen methodology were used to estimate reference and actual evapotranspiration, respectively. In this study IKONOS images were used.

In spite of the existing methods for the estimation of evapotranspiration the application of them in the management of agrarian irrigated surfaces is very limited nowadays. The reason is because of the fact that most of these methodologies present problems as the high cost of the required images, low spatial or temporal resolution or the local nature of some methodologies. Hence, the necessity to develop a new methodology.

The proposed methodology in this work tries to solve some of these problems by means of the use of MODIS-TERRA images which have free access by NASA. The medium spatial resolution and high temporal resolution of these images allow a suitable monitoring of crops water requirements in parcels of size higher than 250mx250m.

1.3 Research objectives

- General objective:

- To estimate the daily actual evapotranspiration in the region of Andalusia in Spain by means of a combined model using meteorological and remote sensing data.

- Research sub-objectives:

- To determine the reference evapotranspiration (ETo) using the Penman-Monteith method.
- To determine the crop coefficient (Kc) by means of NDVI.
- To validate the model with meteorological stations of Andalusia.
- To determine daily, tenthly, monthly and yearly actual evapotranspiration.
- To make maps of daily, tenthly and monthly actual evapotranspiration.
- To make a map of actual yearly evapotranspiration.
- To validate reference evapotranspiration.
- To validate crop coefficients.

1.4 Overview of report

This thesis report is structured in six chapters. Chapter 1 is the introductory chapter, in which the background, the research and objectives are detailed. Chapter 2 presents the literature review defining concepts related with evapotranspiration and studying the importance of the evapotranspiration, its estimation with remote sensing and validation. Chapter 3 is divided into seven main parts: the first one describes the study area, the second one makes an overview methodology, the third, forth and fifth ones detail the process followed to calculate reference evapotranspiration, crop coefficient and actual evapotranspiration respectively, the sixth one describes the validation method and the seventh one describes the available data for the implementation of the model. Chapter 4 shows the results obtained in the study area. Chapter 5 presents a discussion on whether the objectives of this research were achieved and some final conclusions are considered in Chapter 6.

2 LITERATURE REVIEW

2.1 Evaporation and transpiration

Evaporation (Ev) and transpiration (T) are two very similar physical processes accounting for the conversion of water from its liquid form to its vapour form, thus escaping to the atmosphere. Both processes only differ from each other in the type of evaporant surface (Brasa, 1997). In nature, they happen simultaneously in soils with vegetation covers so individual estimations are difficult to carry out. For this reason, both processes are very often referred to under the single term evapotranspiration (ET). Water evaporation to the atmosphere occurs from free water surfaces such as oceans, lakes, rivers and marshes, and from soil and humid vegetation. The quantity of evaporation will depend mainly on the following factors:

- Energy availability (solar radiation).
- Atmosphere's capacity to receive humidity (atmosphere evaporating power).

The main factors that control evapotranspiration are (Chorley, 1969):

- Solar radiation. Without doubt, the most important one because is the energy source of this process.
- Air temperature. The colder the air, the higher the thermal convection and consequently the less energy available for the evaporation. On the other hand, the higher the air temperature, the higher its saturation vapour pressure.
- Atmospheric Humidity. Dry air takes longer to get saturated and has lower vapour pressure. The higher the relative humidity is, the lower the saturation deficit. Thus, for instance, when the air relative humidity reaches 100% there is zero evaporation.
- Wind. The evaporation process implies a net movement of water towards the atmosphere. If the process lasts, the air layers closer to the free surface will saturate. For a continuous flow, there must be a vapour pressure gradient in the air. Thus, the more air renovation there is (wind), the higher the evaporation.
- Salinity. This factor depresses the evaporation rate in proportion to the solution concentration. For sea-water the rate is about 2-3% lower than for fresh water.

Most of the water evaporated by plants is water that has passed through the plant, absorbed by the roots, going through the vascular tissues and escaping through the stomates in the leaves and, sometimes, through the cuticles. This evaporation of water produced by means of the plants is known with the name of transpiration. The water absorbed by the roots has the following functions: incorporation to the plant's structure (1%), transportation of nutrients, removal of salts and refrigeration. Transpiration depends on some dynamic aspects of the plant's activity and it is therefore controlled by many variables (Chorley, 1969):

- The type of species. Different crop species may transpire very different quantities of water depending on the nature of the evaporation apertures in the leaves (stomates) especially on their size, density, location and exposition.
- The season. This determines when plants have leaves and for how long.
- The time of the day, which alters the radiation equilibrium, photosynthesis and growing rhythms of the plants and the activity of stomates. At night time, the transpiration rate is about 5-10% of the transpiration during the day time.
- The plant's growing phase. Plants consume much more water during active growing phases, biomass building-up periods or when the radicular system has reached its maximum expansion and efficiency. For certain crop species, the maximum evapotranspiration rate takes place when it has covered the whole soil surface.
- Meteorological factors also influence the opening of stomates. With strong winds, especially if they are hot, stomates close as a mechanism to prevent large water losses. On the contrary, with high humidity plants keep releasing water, even in its liquid form in order to facilitate the sap's movement.
- Soil properties also influence the quantity of water available for the plant. Depending on the lithology, plants will be able to obtain more or less quantity of the water in the soil.

2.2 Concepts of potential, reference and actual evapotranspiration

The concept of potential evapotranspiration (ETp) was first introduced by Penman (1948) and Thornthwaite (1948). In 1956 Penman defined potential evapotranspiration as "the amount of water transpired in unit time by a short green crop, completely shading the ground, of uniform height and never short of water". Thornthwaite (1948) considered that ETp was mainly controlled by meteorological factors with soil and plant factors being secondary.

Later works (Stewart, 1983) have shown that this concept is only applicable to short vegetation. Evapotranspiration measurements in forest species show that the transpiration rate can be much lower than the potential rate even when there is full water supply in the soil as a consequence of biological control, which has a significant effect. On the contrary, when the forest cover is humid, the evaporation rate may be considerably higher than the potential rate.

The concept of reference crop evapotranspiration (ETo) was introduced in order to avoid the ambiguity to which the wide concept of ETp gave place. The concept of ETo is similar to that of ETp and they are even considered as equivalents in certain works (Mckenney and Rosenberg, 1993). The difference is that this is applied to a specific crop (Sánchez-Toribio, 1992). In the last decade, the term potential evapotranspiration is being replaced by that of reference evapotranspiration, which refers to the evapotranspiration of a reference crop under ideal conditions in terms of development, lack of disease and pests, and level of humidity available in the soil. The reference evapotranspiration is the maximum evapotranspiration that can be expected from the reference crop in the prevailing meteorological conditions.

There are two definitions of ETo depending on the type of reference crop considered. Doorenbos & Pruitt (1977) developed for the Food and Agriculture Organization of the United Nations (FAO) the definition of ETo (for a reference crop of grass) as the evapotranspiration rate of an extensive surface covered with green grass of uniform height (8-15cm), actively growing, completely shading the ground and never short of water.

The second definition of ETo takes alfalfa as the reference crop and it was first suggested by Jensen *et al.* (1971). This definition represents the maximum limit or maximum evapotranspiration that takes place under certain weather conditions in a field with a crop well supplied with water that has an aerodynamically rough surface, such as alfalfa, with 30-50cm of top growth.

In an attempt to unify terminology and concepts, a new definition was suggested for the FAO based on Penman-Monteith combination equation (Rivas, 2004). According to this equation, reference evapotranspiration (ETo) would be the evapotranspiration rate from a hypothetic crop with fixed values of height, resistance of the vegetation cover and albedo which must represent the evapotranspiration of an extensive surface covered with green grass, of uniform height, actively growing, completely shading the ground and never short of water (Allen *et al.*, 1998).

Evaporation and transpiration processes depend on the evaporative demand of the atmosphere, the hydric content and the nature of the soil. They also depend on the characteristics of the vegetation cover. Thus, in the first stages of a crop's development the evapotranspiration is mostly evaporation. As the vegetation cover develops (increase of the leaf area index and degree of surface covered) evaporation decreases until transpiration prevails completely over evaporation (De Juan and Martín de Santa Olalla, 1993).

Other concept of evapotranspiration is the crop evapotranspiration, denoted as ETc. This concept make reference to the evapotranspiration produced for any crop under standard conditions. Nowadays, the calculation of crop evapotranspiration (ETc), is usually done from the crop coefficient, kc (no dimension) and a previous estimation of the ETo according to the relation (Doorenbos and Kassam, 1986):

$$ETc = ETo \cdot Kc$$

The crop coefficient shows the relation between crop evapotranspiration and reference evaporation. It is calculated experimentally and according to many factors such as the characteristics of the crop and its phenological state, the weather conditions, water availability of the soil, health state of the crop, farming techniques applied and, especially, the frequency of rain or irrigation, if that is the case (Doorenbos and Pruit, 1977; Hupet and Vanclooster, 2001).

The evapotranspiration process that takes place in a natural surface is not always found under the hypothetical conditions proposed. Thus, it is important to define the concept of actual evapotranspiration (ET).

ET is the real quantity of water lost through the soil and it depends on the atmospheric conditions, the water content in the soil and the vegetation characteristics.

Actual evapotranspiration is, in general, lower than crop evapotranspiration; only when there is maximum water availability in the soil will crop evapotranspiration and actual evapotranspiration coincide.

The most common unit to express water loss through evapotranspiration is expressed in mm of water height, which is equivalent to 10 m^3/Ha. The measure always refers to a concrete interval of time.

2.3 Interest in the estimation of evapotranspiration

The main objective of this thesis is the study of water evaporation in nature. The evapotranspiration is one of the most relevant hydrologic, climatological and agronomic variables (Elias *et al.*, 1996) and its calculation constitutes the base to determine later the water requirements of crops.

In global terms, almost 64% of the water precipitated on the continents is evapotranspirated (Dingman, 2002) reaching up to 90% or even 100% in arid and desert zones (Sánchez-Toribio, 1992). Almost 97% of the total is evapotranspirated from the surface and 3% from bodies of water (Dingman, 2002) (Figure 4). In Figure 5 it is shown the distribution of annual evapotranspiration at global scale, according to the United Nations Environment Programme (UNEP).

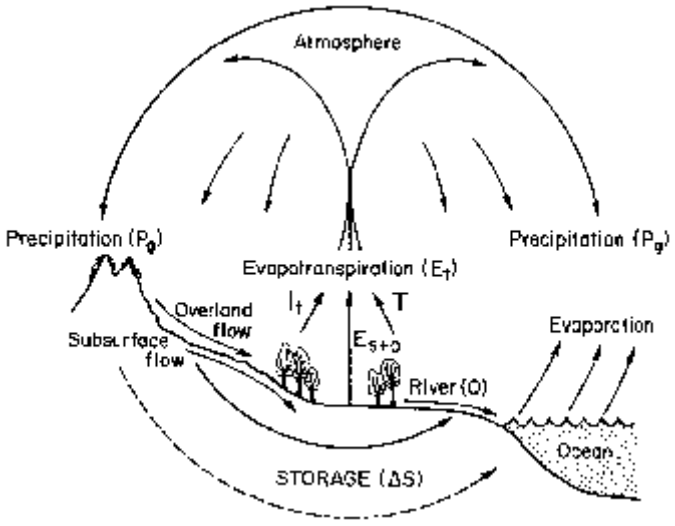

Figure 4. Different fluxes of the hydrologic cycle.

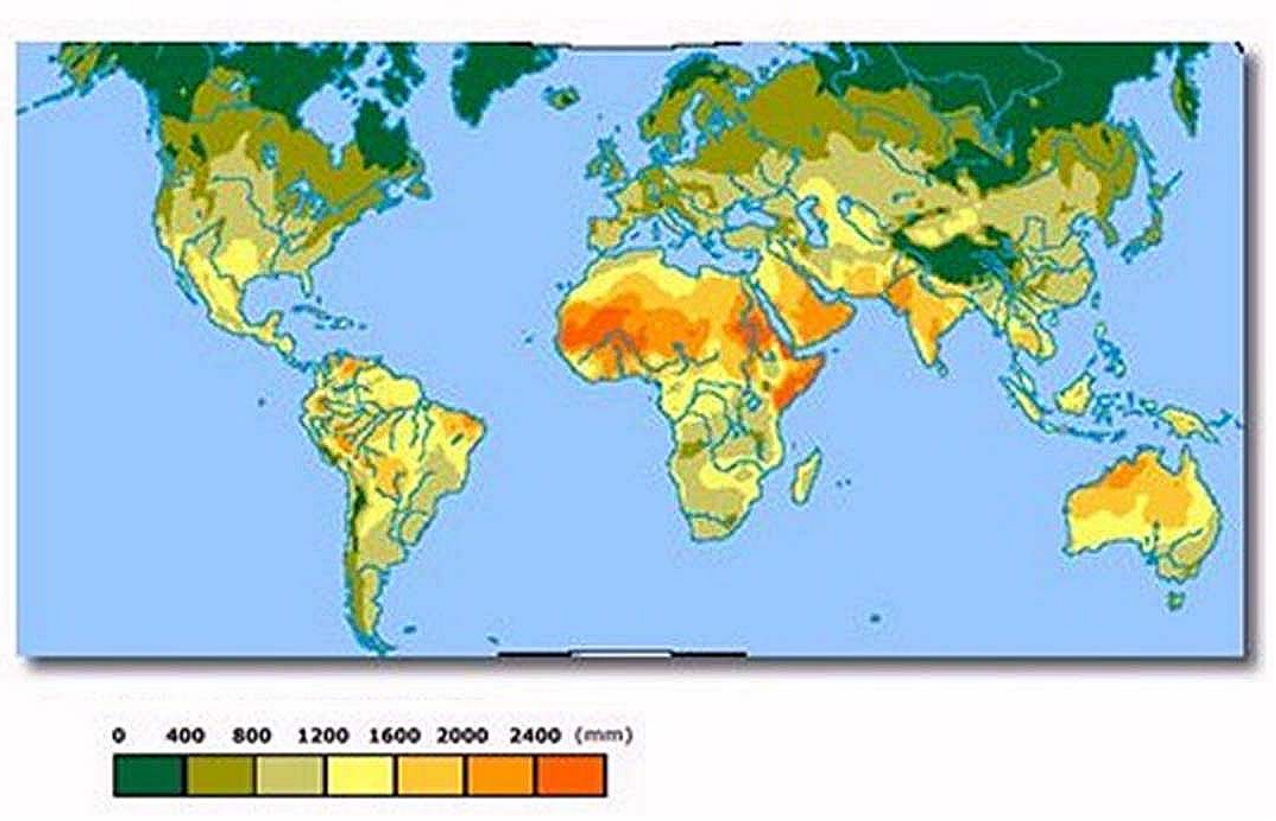

Figure 5. Reference evapotranspiration map (mm/ year) at global scale. Source: UNEP World Atlas of Desertification.

The quantities of water that returns to the atmosphere through this process and the energy necessary for it, reach values really high. On a hot day, evapotranspiration values often oscillate between 3-4 mm/day in some zones, which is equivalent to 30-40 Tm/Ha/day, which requires an energy of 18-24M of kcal. In the Spanish peninsula, the total loss through evapotranspiration is 3 times higher than what is lost to the sea through the rivers.

Certain accuracy in the quantification of ET is essential in:

- In regional hydrological studies the difference between precipitation and evapotranspiration gives us the availability of existing water, making a more rational planning and management of available hydric resources possible.
- Climate models. Most of the water lost through evapotranspiration is used for the growth of plants, which form the base of ecosystems. The understanding of the relation existing between ecosystems and evapotranspiration is a basic requirement to understanding the response to the climate change.
- The large food-producing zones in the world use irrigation (complementary or supplementary) to meet the hydric necessities of crops. A more efficient irrigation and, consequently, better water saving will be possible if we have a better understanding of crop transpiration.
- Models of primary production require an appropriate estimation of evapotranspiration from which the production expected for a concrete region is estimated.

Nowadays, remote sensing is the only technology able to provide the radiometric measurements necessary for the calculation of actual evapotranspiration in a globally consistent and economically feasible manner (Kustas and Norman, 1996).

2.4 Estimation of evapotranspiration at local and regional scale

A great number of equations have been developed for estimating ETP at local scale by means of meteorological data (Thornthwaite, 1948; Turc, 1961; Priestley and Taylor, 1972; Jensen, 1974) with high accuracy. These equations can be included in some of the four groups which are mentioned next, depending on which is the main parameter used: radiation, temperature, evaporation or combination of some of the former.

- *Radiation-based*. Use net radiation and air temperature.
- *Temperature-based*. Use only air temperature (often climatic averages) and sometimes day length (time from sunrise to sunset).
- *Pan*. Use pan evaporation, sometimes with modifications depending on wind speed, temperature, and humidity.
- *Combination*. Based on the Penman combination equation; use net radiation, air temperature, wind speed and relative humidity.

METHODS		ARID CLIMATE			HUMID CLIMATE		
		R	E	SEE	R	E	SEE
RADIATION METHODS	Priestley-Taylor	7	-30%	1.89	3	-3%	0.68
	FAO-24 Radiation	3	+6%	0.62	5	+22%	0.83
TEMPERATURE METHODS	SCS Blaney-Criddle	4	-16%	1.29	7	+17%	1.01
	Thornthwaite	8	-40%	2.40	6	-4%	0.86
	Turc	6	-30%	1.88	2	+5%	0.56
PAN EVAPORATION METHODS	Pan evaporation "Class A"	5	+21%	1.54	8	+14%	1.29
COMBINATION METHODS	Penman-Monteith	1	-1%	0.49	1	+4%	0.32
	Kimberly-Penman	2	+3%	0.54	4	+10%	0.69

Table 1. Evaluation of estimating methods of evapotranspiration at local scale in different climatic regions (summarized in Jensen, *et al.* 1990).

In Table 1, R is the position of the ranking for each method, E is the overestimation or underestimation of 11 lysimeters (%) and SEE is the standard error of estimate (mm/day), calculated according to the equation:

$$SEE = \left[\frac{\sum_{i=1}^{n} (Y_i - \hat{Y}_i)^2}{n-1} \right]^{0.5}$$

where Y_i is the average i th month lysimeter ET, $\hat{Y}_i$, is the corresponding ET estimate, and *n* is the total number of observations.

According to Table 1, the best method to estimate the ETo is Penman-Monteith combined method, both for humid and arid climates. For this reason Penman-Monteith method was taken as the standard method for ETo calculation for FAO.

Other research works carried out by Gavilán and Berengena (2000) or López-Urrea *et al.* (2006) have also demonstrated in Spain the highest accuracy of the Penman–Monteith FAO equation over other methods, if we compare them with lysimetric measurements.

The Penman-Monteith method as well as the other methods used in Table 1 for the calculation of evapotranspiration have a local character, which means that the ET estimation can only be considered representative of the plot where it has been measured and can only be extrapolated in very specific situations (flat, homogenous zones, for instance).

However, the analysis of the evapotranspiration as a regional or hydrological basin variable is required for several reasons. On the one hand, hydrological processes happen very often at a scale which implies the analysis of a basin or region. On the other, the development and use of hydrological resources for agriculture, water supply and other uses usually requires large-scale research. Remote sensing is an attractive tool for the detection of regional, even plot-scale, changes or anomalies of land (Boegh *et al.*, 2002). These allow us to extend evapotranspiration calculation models to large zones where there are not even meteorological data available.

Most of these ET estimation models use physical algorithms with different degree of difficulty which have been discussed by authors such as Choudhury (1989), Bailey (1990), Humes *et al.* (1994), Moran and Jackson (1991), etc.

With the publication of the simplified energy balance in the works of Idso *et al.* (1975) and Jackson *et al.* (1977) a new line was opened in the estimation of ET. Subsequent methods based on these offer calculation alternatives but differ basically on the type of field information required, the wavelength, the auxiliary micro-meteorological information and the necessity of numerical models (Bastiaanssen, 1998). Many of these algorithms have been developed on basins and concrete zones, which limits their use to other zones in the planet. In order to generalise results, authors

such as Seguin *et al.* (1989) and Hurtado *et al.*(1995) developed the simplified model of energy balance and applied it to different zones of the USA, Spain, France and Morocco.

In the last decade, more advanced, complex versions of the energy balance in the surface have been proposed and later validated. Kustas *et al.* (1994), Bastiaanssen *et al.* (2000) validated the SEBAL algorithm in large zones throughout the planet (Egypt, Spain, Italy, Niger, USA, Pakistan...). Tasumi *et al.* (2003) applied an extended versión of SEBAL under the acronym METRIC in the USA and Spain. Menenti *et al.* (2003) validated the SEBI-SEBS algorithm in similar zones. All of them present a very important limitation in the temporal ET monitoring, which depends on the availability of satellite images as a result of the presence of clouds or the programming of passes (Duchemin *et al.*, 2006).

In order to obtain continuous evapotranspiration simulations, process monitoring models in ecosystems or SVAT models are used, which include the soil-plant-atmosphere water transference process (Olioso *et al.*, 1999; Seen *et al.*, 1995). Once combined with remote-sensing data, these models provide continuous estimations of the water and energy balance distributed in space (Courault *et al.*, 2003). It is also important to point out that to obtain accurate ET values, all models previously proposed require their local parametization.

In general terms, and as a conclusion, it can be said that there is a wide variety of methods for the estimation of ET. Using one or other will depend on the accuracy required (spatial or temporal) and on the expense of the data and measures used in each method.

The present work suggests establishing the evapotranspiration by combining conventional meteorological information with satellite data. For this purpose, we have used the methodology suggested by Allen *et al.* (1998) based in the Penman-Monteith method to calculate the actual evapotranspiration at regional scale.

This approach has already been used in different research works (Brasa *et al.*, 1996; Caselles *et al.* 1998; Rivas *et al.* 2004; Consoli *et al.*, 2006; Rossi *et al.* 2006; Cleugh *et al.* 2007) using sensors of different spectral resolutions, depending on the work.

To derive the crop coefficient Kc from satellite data the simplest approach used is a linear relationship between Normalized Difference Vegetation Index (NDVI) and *K*c. This approach was introduced by Heilman *et al.* (1982) and used and validated in further case studies by Bausch and Neale (1989), Neale *et al.* (1989) and Bausch (1993, 1995). The theoretical basis of this approach was established by Choudhury *et al.* (1994). Moran *et al.* (1997) conclude that this approach is one of the most promising ways for operational application.

In this research work an index derived from the NDVI called Relative Greenness (RGI) was used to determine the crop coefficient. This index was proposed in 1990 by Eidenshink *et al*. Up to now most of the studies where it has been used have been related to the calculation of live fuel moisture (Oldford *et al.*, 2006, Chuvieco *et al.* 2003) and, in general, assessment of forest fires danger (Gabban *et at*. 2006, Aguado *et*

al., 2003, Hardy *et al.*, 2000). But, there are also some studies (Burgan and Hartford, 1993) that have used the RGI to determine crop progress, crop maturation and climate event impact.

2.5 Different methods of validation

Reference evapotranspiration can be determined through different methods. Below are the most commonly applied:

- Lysimeter method.
- Tank evaporimeter method.
- Empirical methods.
- Semi-empirical methods.

A. Lysimeter method

A lysimeter is a buried vessel closed on the sides so that the water drained through gravity (which would have seeped into the aquifer) is captured by a drain. During its construction, special care must be taken to restore the soil back to the state in which it was found before the excavation. Next to the lysimeter there must be a pluviometer.

The ETo is calculated from the following hydric balance equation in the lysimeter.

Precipitation = ETo + Infiltration + Δ storage

In order to calculate Δ storage, the soil humidity is usually measured first and from this, a sheet of water expressed in mm is calculated.

B. Tank evaporimeter method

This method consists of finding a relation between the evapotranspiration rate produced in a lysimeter and the evaporation rate produced in an evaporation tank class A, according to which an empirical coefficient is established. Evaporation readings are carried out later according to this coefficient and thus the potential evapotranspiration for specific environmental conditions is obtained indirectly.

Tank class A allows us to estimate the integrated effects of the climate (radiation, temperature, wind and relative humidity) according to the evaporation registered of a free water surface of standard size.

C. Emperical methods

c.1) Thornthwaite method

It was developed from precipitation and runoff data for different drainage basins. The result is basically an empirical relation between the ETP and the air temperature. In spite of its simplicity and obvious limitations, this method offers acceptable results in humid regions. However, the data obtained in dry regions are too low, getting worse in desertic regions.

Thornthwaite formula is as follows:

$ETp = 16\ (10T/I)^{a}$

where:

ETp = reference evapotranspiration (mm).

I = annual caloric index, the sum of 12 monthly "i" indexes, where "i" is function of the mean monthly temperature ($i= (t/5)^{1,514}$).

T = mean monthly temperature (ºC).

A = empirical exponent, function of I .

c.2) Blaney-Criddle method (Modified by FAO)

The original Blaney-Criddle formula (Blaney & Criddle, 1950), was developed in an arid region west of the United States in order to calculate the potential evapotranspiration during a given period of time.

This formula takes into account the mean temperature of the period considered and the hours of daylight, expressed as a percentage of the total annual daylight hours. This simple and easy to apply formula is the most appropriate one for arid and semi-arid zones as well as for periods of time superior to a month.

In order to be able to apply this method, it is necessary to obtain the following data (through measuring or estimation) of diurnal wind speed (during daylight hours exclusively), minimum relative humidity, number of actual isolation hours and maximum hours of isolation possible.

It is not recommendable for high regions (with very low minimum daily temperatures) nor for equatorial regions (where there is little variation of the daily temperature).

c.3) Hargreaves method

The formula below was developed by Hargreaves (Hargreaves & Samani, 1985), according to the measurements carried out in lysimeters.

$ETo = 0.0023*Ra*(Tm + 17.8)*\sqrt{TD}$
where:

ETo = crop reference evapotranspiration (mm/day)

Ra = Extraterrestrial radiation (mm/day)

Tm = Mean daily temperature (ºC)

TD = Mean daily temperature difference in the period considered (ºC)

c.4) Turc method

Turc (1961) proposed a simple method, based on temperature and precipitation. As it happens with other methods based in the correlation between precipitation, as the only recharge, and the evaporation, they can be very useful in some river basins. However, their application in other regions, where the depth of no saturated zone, land use, topography, climate and, specially, type of rain are differents to the location where these correlation have been carried out, its application is very doubtful.

The equation for the Turc method is:

$$ETo = \frac{P}{\sqrt{0.9 + \frac{P^2}{L^2}}}$$

where:

P = total annual precipitation (mm/year)

$L = 300 + 25T + 0.05T^3$

T = mean annual temperature (ºC)

D. Semi-empírical method

d.1) Penman-Monteith method (FAO)

It estimates the reference crop consumptive use and predicts the ETo both in cold, humid regions and in hot, arid zones.

This will be the equation used to validate the ETo calculation in the model suggested and it will be described in more detail in section 3.3.

Below are the most common methods used to establish the actual evapotranspiration (that is, the real quantity of water that returns to the atmosphere through evaporation and transpiration under actual meteorological and soil humidity conditions):

- Hydric balance method.
- Energy balance method.

- Hydric balance method

This method is based on the principle of mass conservation applied to part of the hydrologic cycle (Dingman, 2002).

In order to calculate the actual evapotranspiration, it must be taken into account the quantity of water to be evapotranspirated that does actually exist in the study zone. The hydric balance equation for an established interval will be:

$P = ET + Q + \Delta R$

where:

P = precipitated sheet (mm)

ET = actual evapotranspiration (mm)

Q = water surplus, runoff and infiltration (mm)

ΔR = increase or decrease in the water supplies used by vegetation (mm)

If the values of the supplies at the beginning and at the end of the period are considered to be the same or negligible in comparison to the values of P and Q for a long interval of time (a year, for example), then:

$ET = P – Q$

- Energy balance method

This method is based on the principle of energy conservation. From the energetic point of view, the evapotranspiration, represented by the symbol LE, can be described by an energy balance which, in a simplified way, corresponds to the following equation:

$Rn + G + LE + H = 0$

This balance shows that the radiative energy (Rn) is used to evaporate water (LE) and heat surfaces (ground and vegetation), which is called "latent heat" and "sensitive heat" respectively. "Sensitive heat" represents both the heat which is emitted from the surfaces to the air through conduction or convection (H), and the heat that goes from conduction to the ground (symbol G is used in this case). The inverted energy in the photosynthesis is not taken into account in the energy balance equation since it is negligible in comparison to these other energetic fluxes. Thus, from the energetic point of view, and once the other components in the balance are known, it would be easy to calculate the LE through the difference. However, considering the difficulty in establishing the other components in the balance, this task is too complex to carry out in practice.

In this study, due to technical, economic and time limitations, actual evapotranspiration could not be validated. However, since ET is calculated by means of ETo and Kc and these parameters are validated, we can suppose that the accuracy of the ET measurements will be determined by the accuracy of these two parameters.

3 METHOD AND MATERIALS

3.1 Study area

The study has focused on the Autonomous Community of Andalusia, region located in the South of Spain. The coordinates are shown in Table 2.

This region (Figure 6) has a total surface of 87.597 km^2 ,of which 9,3% are dedicated to irrigated land, which 24,5% of the useful farming surface (MAPA, 2004). At a national level, Andalusia is the region with the largest irrigated surface, 23,6% of the national irrigated land (FENACORE, 2005).

Coordenates	UTM-30n	Latitude/Longitude
X minimum	90000	7.7º West
X maximum	630000	1.5º West
Y minimum	3970000	35.8º North
Y maximum	4300000	38.8º North

Table 2. Coordinates of Andalusia.

Figure 6. Map of Spain with the Community of Andalusia enhanced in red.

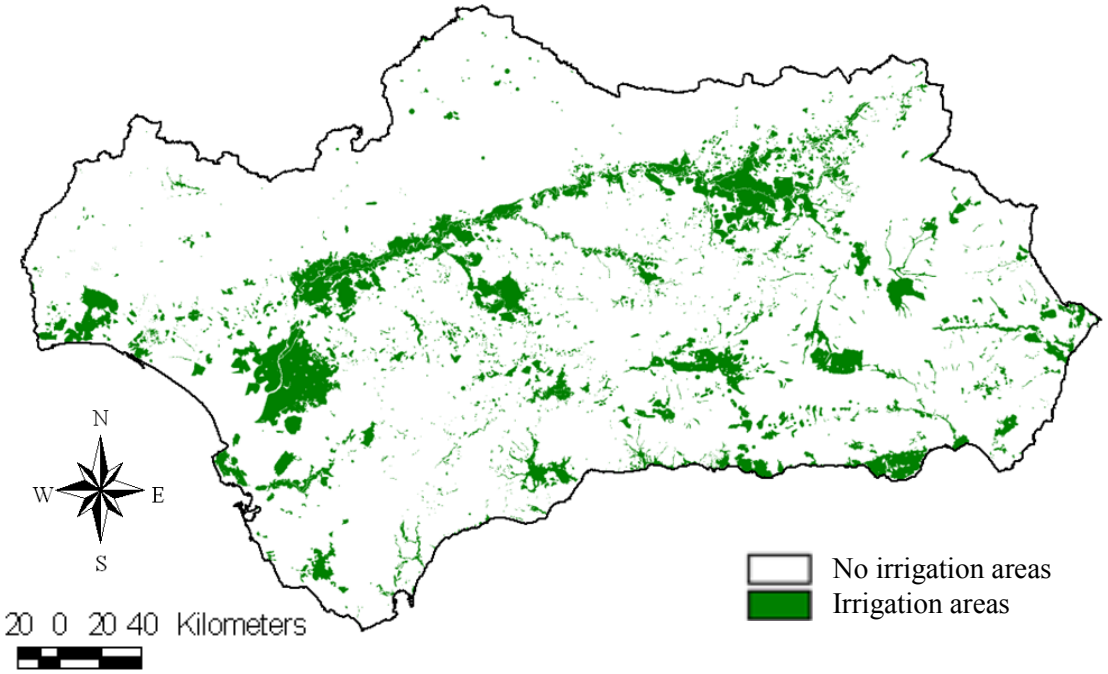

Figure 7. Distribution of irrigated surface in Andalusia (source*:* Inventory and Characterization of irrigated land in Andalusia, 2002).

Most of this irrigated surface is found in the meadows of the main rivers and seashore areas of the region, especially in the basin of the river Guadalquivir (Figure 7), with 72% of the surface (Inventory and Characterization of irrigated land in Andalusia, 2002).

The most important irrigated crops are rice, sugar beet, cotton, fruits and vegetables. Among these, olive trees are the first irrigated crop in Andalusia, with a surface of 320,000 hectares which produce 80% of Spanish olive oil, 37.4% of the EU and 26.8% of the worldwide production. (Inventory and Characterization of irrigated land in Andalusia, 2002).

With respect to the origin of irrigation water, 27% comes from subterranean water (up to 50% in the coast of Andalusia), 71,5% from surface water and 1,5% from treated sewage water (Inventory and Characterization of irrigated land in Andalusia, 2002).

Water resources in Andalusia are greatly influenced by the quantity of rain and the rainfall pattern, which fluctuates between 600 mm/year in the western zone and 200 mm/year approximately in the south-east, with great interannual variability and severe, periodic droughts (Andalusian Department of Environment website: http://www.juntadeandalucia.es/medioambiente/web/Bloques_Tematicos/Publicaciones_Divulgacion_Y_Noticias/Publicaciones_Periodicas/IMA/2005/pdfs/007_Capitulo_02_Clima.pdf).

In all cases, the rainfall distribution is characteristic of the Mediterranean climate, where most of the rain falls between November and March, and not during the summer months.

Evaporation is very high in most of the interior zones of Andalusia with a reference evapotranspiration more than 1.200 mm/year. The Guadalquivir Valley, the largest basin in the region, represents 60% of the water resources available, and there are five other smaller basins. In 2002, the demand of water for different uses went up to 5.661hm^3, while the resources available only reached 5.426hm^3. The quality of water in the region is relatively good with problems of growing salinity in dry and seaside areas. Most water resources, approximately 78% of the total, are used for agriculture (Andalusian Department of Fish and Agriculture, 2003).

3.2 Overview methodology

A diagram with the main steps followed in this work to calculate actual evapotranspiration are presented in Figure 8. The diagram has been grouped in 3 main parts, marked with 3 different colours (purple, green and blue) according to the corresponding section in the report (3.3, 3.4 and 3.5, respectively).

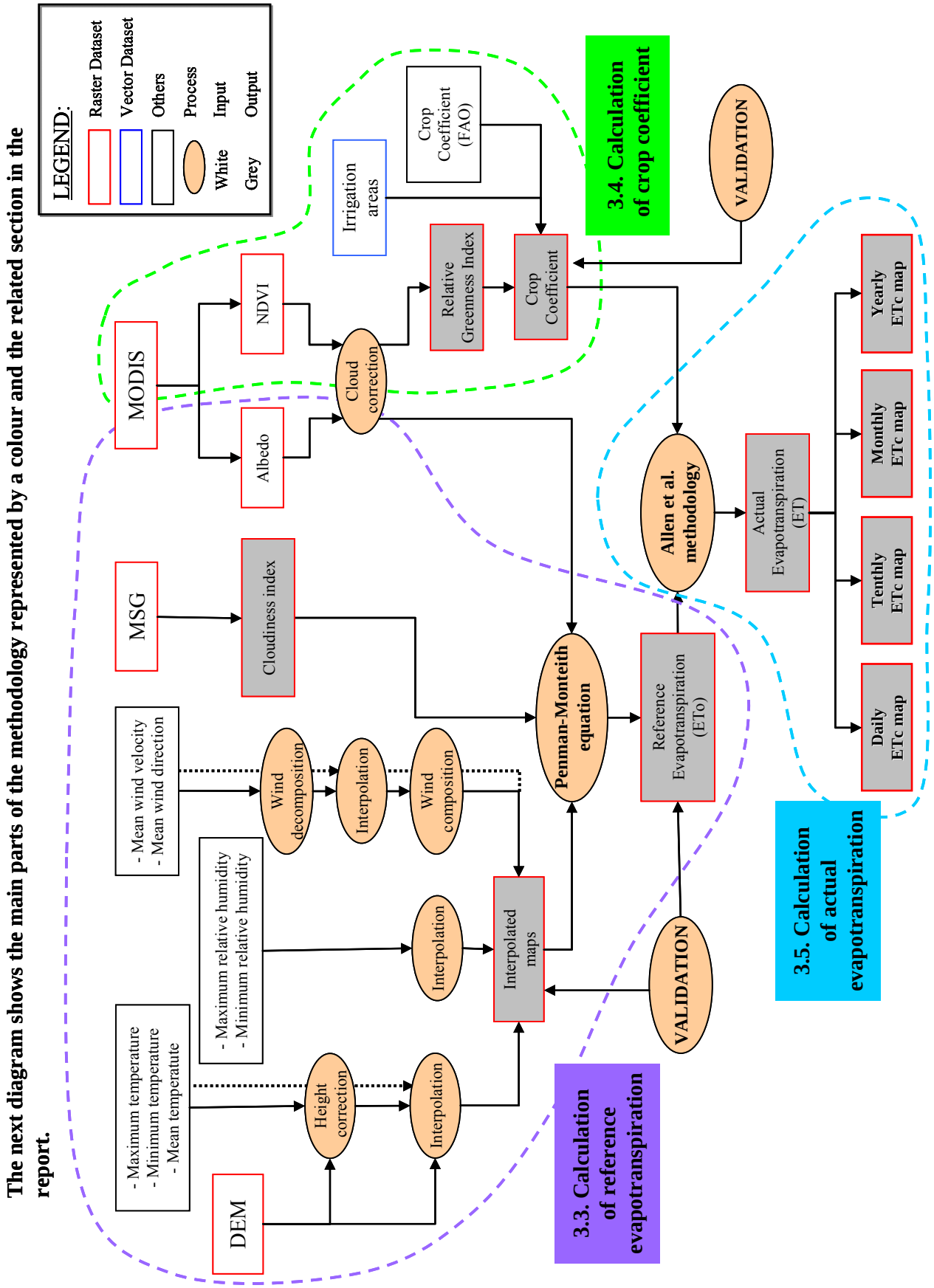

Figure 8. Diagram of the main part of the methodology.

3.3 Calculation of reference evapotranspiration

There are a large number of methods (Table 1) to calculate the reference evapotranspiration indirectly from meteorological data (Thornthwaite, 1948; Turc, 1961; Priestley and Taylor, 1972; Burman *et al.*, 1983; Hargreaves *et al.* 1985, etc) The main one, and without doubt the most accurate one (Jensen *et al.* 1990), is the method developed by Penman-Monteith (Allen et al 1998), although it also needs a larger number of variables comparing with other methods (Sánchez-Toribio, 1992). The equation that Penman-Monteith derived is as follows:

$$ETo = \frac{0.408\Delta(R_n - G) + \gamma \frac{900}{T + 273} u_2 (e_s - e_a)}{\Delta + \gamma(1 + 0.34u_2)}$$

where:

ET_o = reference evapotranspiration [mm day^{-1}],
R_n = net radiation at the crop surface [MJ m^{-2} day^{-1}],
G = soil heat flux density [MJ m^{-2} day^{-1}],
T = mean daily air temperature at 2 m height [°C],
u_2 = wind speed at 2 m height [m s^{-1}],
e_s = saturation vapour pressure [kPa],
e_a = actual vapour pressure [kPa],
e_s - e_a = saturation vapour pressure deficit [kPa],
D = slope vapour pressure curve [kPa $°C^{-1}$],
g = psychrometric constant [kPa $°C^{-1}$].

This study suggests a procedure based on the daily calculation of the reference evapotranspiration by means of Penman-FAO equation. For this purpose, a combination of data from meteorological stations and remote sensing data has been used as inputs of this equation in order to estimate daily measurements of ETo at regional scale.

3.3.1 Processing of meteorological data

The data used, available in all meteorological stations, are:

- maximum daily temperature (ºC),
- mean daily temperature (ºC),
- minimum daily temperature (ºC),
- maximum daily relative humidity (%),
- minimum daily relative humidity (%),
- mean wind velocity (m/S),
- and mean wind direction (º).

The data are obtained from the specific points in the area of study where the meteorological stations are situated. These data (with the exception of mean wind direction) will be interpolated so as to obtain information on the rest of the area.

3.3.1.1 Interpolation methods

Interpolation is defined as the method of predicting values for a whole surface based on sample point values. Spatial interpolation is used to estimate a value of a variable at an unsampled location from measurements made at other sites within a defined area. It is based on the principle of spatial dependence which measures the degree of dependence between near and distant objects (Sakhnovich, 1997).

For spatial interpolation of the meteorological variables required in the calculation of reference evapotranspiration, the SURFER software in its version 8.0 was used. This version contains 12 interpolation methods that have been tested for each of the different meteorological variables.

After the first results (and not having found important differences between the interpolation methods in the study region, see Appendix 1) the five most accurate methods according to the mean bias error (MBE) were selected in order to make the interpolation process more operative. The selected methods were:

- Inverse distance to a power,
- kriging,
- modified Shepard´s method,
- nearest neighbour,
- radial basis function.

Spatial interpolation of the different meteorological variables is going to be implemented in a direct way (that is, applying directly the spatial interpolator over the variables) by means of the mentioned methods. Furthermore, meteorological variables temperature and wind speed will be also interpolated in an alternative way, that is, previous steps to the interpolation process will be developed.

3.3.1.1.1 Height correction

Since there is a relationship between air temperature and ground elevation, a digital elevation model (DEM) has been used in combination with direct interpolation methods to reduce the interpolation error.

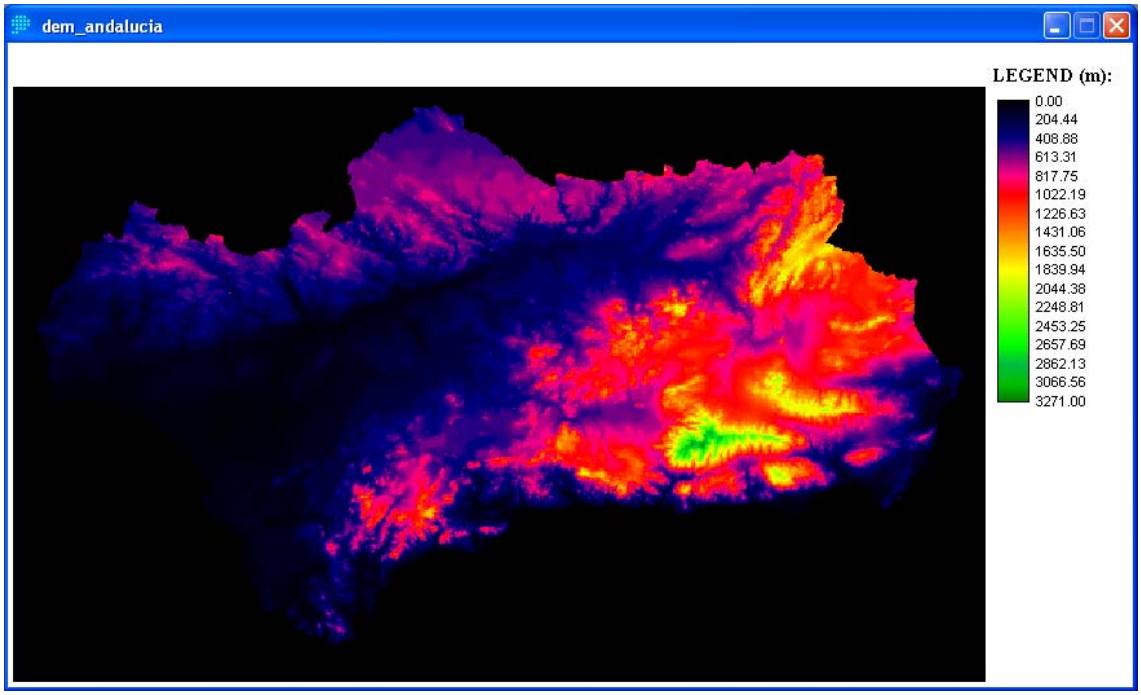

Figure 9. Digital elevation model of Andalusia.

This relation is called vertical gradient of temperature and it is defined as the gradient in which the air temperature changes with height. The vertical gradient of atmosphere temperature ranges in between 0.5ºC (for saturated masses of air) and 1ºC (for non-saturated masses of air) for each 100m of altitude (Lutgens, 1998).

This methodology has already been used in former studies such as the ones carried out by Weng *et al.* (1984) in China, Willmott *et al.* (1995) in the United States, who obtained a 34% reduction of the error initially committed with other interpolation methods.

In our attempt to improve this result, we started by estimating the elevations of the meteorological stations in the study region by means of a DEM. Since in all cases there was a coincidence between this elevation and the datum available in the meteorological station, this DEM was used to calculate the air temperature at sea level. Thus, the temperature at sea level in a station i can be estimated through the equation:

$$T'_i = T_i + GZ_i$$

where T_i is the air temperature measured at station i, G is the vertical gradient of temperature ($\approx 7.5 \cdot 10^{-3}$ ºC m^{-1}), Z the elevation at station i established from the DEM and T'_i air temperature at sea level at station i.

Once the air temperature at sea level was obtained in all available stations, we proceeded to interpolate using the 5 interpolation methods previously mentioned. Finally, actual air temperature at grid point j was estimated from the DEM according to:

$$T_j = T'_j - GZ_j$$

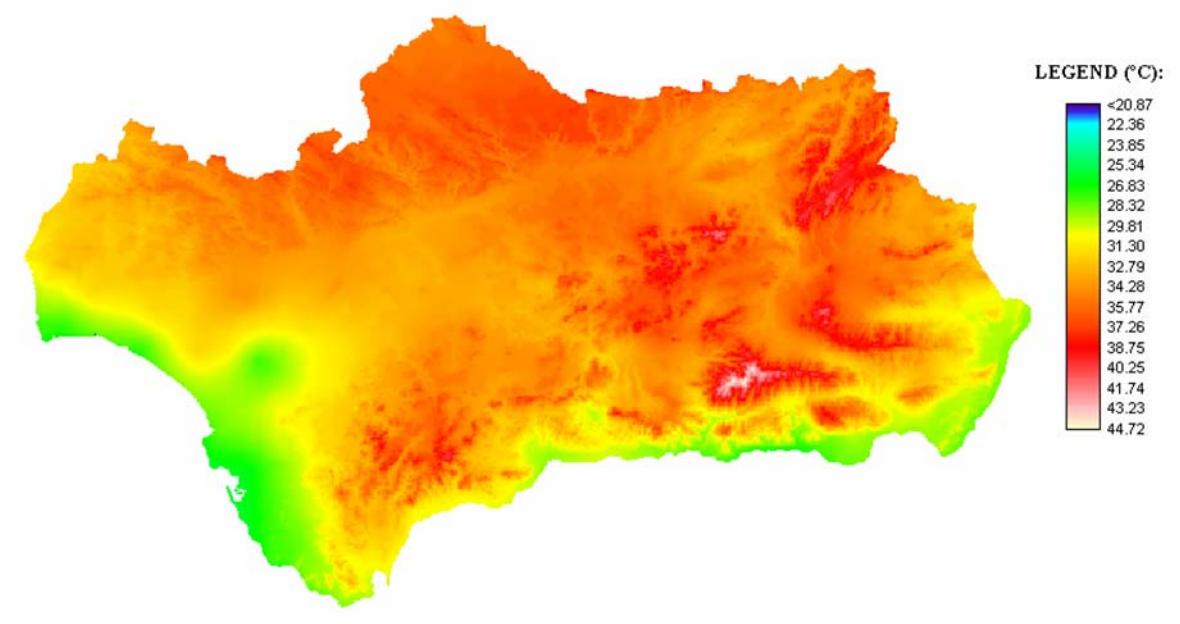

Figure 10. Grid of maximum temperature with the applied DEM.

where T'_j is the air temperature interpolated at station j and Z_j is the elevation estimated from the DEM at grid point j.

3.3.1.1.2 Wind components

Wind can be defined as the natural movement of air and it is measured by means of its direction and velocity (Burton et al, 2004). Therefore, it is a vector often expressed in Cartesian coordinates with components along the X-, Y- (horizontal components) and Z-axes (vertical component), as Figure 11 shows:

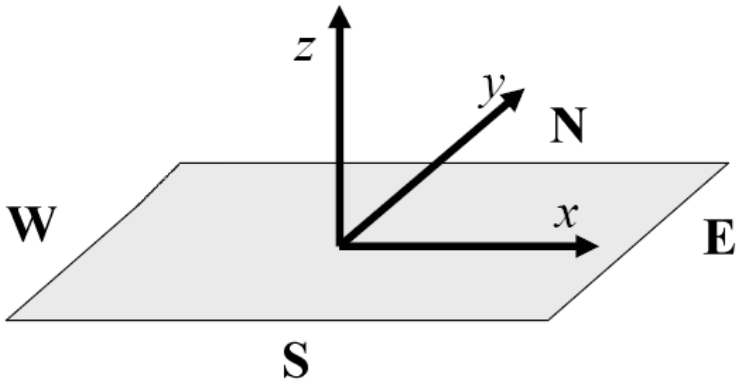

Figure 11. Horizontal and vertical components of wind.

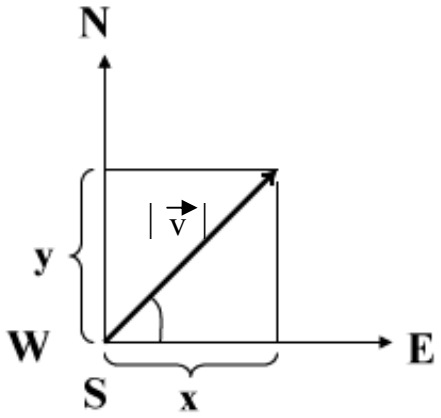

$$x = |\vec{v}| \cos \alpha$$

$$y = |\vec{v}| \text{ sen } \alpha$$

Figure 12. Horizontal components of wind.

where:

$|\vec{v}|$ = vector velocity or magnitude,
α = vector direction or orientation .
x = "x" or zonal component
y = "y" or meridional component.

Since the wind horizontal components are usually much higher than the vertical component, the wind speed is usually given according to its two horizontal components. The x-axis component (from West to East) is usually referred to as zonal component whereas the y-axis component (South to North) is called meridional component. Thus, given the pair (x,y) it is possible to know the horizontal wind direction and speed according to Figure 12.

The velocity or wind magnitude establishes the displacement of the air over a given period of time and it is usually expressed in metres per second (m/s) or kilometres per hour (km/h). The wind direction is defined as the orientation of the wind vector in the horizontal expressed in degrees clockwise from the geographical north. The different wind directions refer to the wind rose marking the cardinal points. The wind direction is observed at weather stations referred to a compass rose of 8 directions (Figure 13).

Figure 13. Wind rose.

The method followed to interpolate the wind is based, therefore, on the fact that the wind is a vector, contrary to other meteorological variables. This methodology was developed and first used by Sánchez *et al.* in 1994.

The novelty of this method with respect to other ones lies on the decomposition of the "x" and "y" wind components that is carried out previously to the interpolation process. Interpolation methods (inverse distance to a power, kriging…) will be actually used in the interpolation of these components once separated. Finally, in order to validate the results obtained in the interpolation, the wind magnitude was calculated once more by means of the equation defined for the module of a vector:

$$|\vec{v}| = \sqrt{x^2 + y^2}$$

where "x" and "y" are the interpolated values of the horizontal wind components.

3.3.2 Processing of remote sensing data

MODIS-TERRA and SEVIRI-MSG data have been used to estimate the cloudiness index, albedo and net radiation.

3.3.2.1 Cloudiness index

This is a key factor for the calculation of the ET, since the solar energy received at the Earth´s surface will be later lost through different ways, one of them, the ET. That's why it is extremely important to know the quantity of energy received by the crop, in order to make an appropriate calculation of the ET.

To measure the cloudiness index, MSG images are used. This satellite acquires and sends images every 15 minutes, which means that there is a perfect monitoring of the insolation received by the crop.

From 7 of its 12 bands, we obtain the cloudiness factor existing in the 24 hours in which the reference evapotranspiration is calculated. In order to discriminate the surface covered by a SEVIRI pixel contaminated or not by a cloud, the method suggested by Casanova (2006) is used.

This method for cloud detection (flow diagram of Figure 14) is based on the fusion of two previous classifications (one carried out on the visible channel obtained according to the quantity of radiation reflected, the other depending on the cloud height) and four subsequent tests:

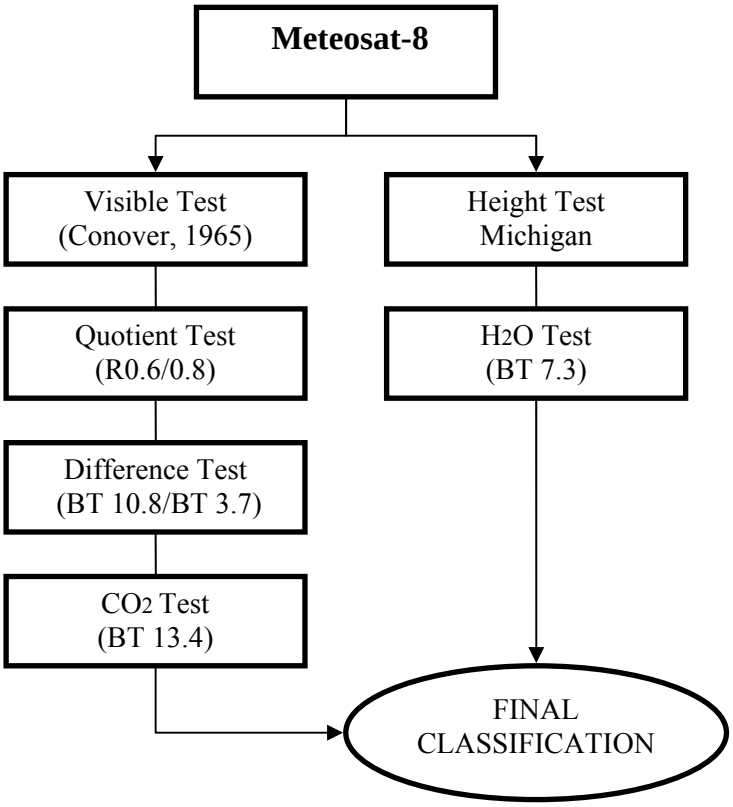

Figure 14. Flow diagram of cloud classification method (Casanova, 2006).

- Difference between the brightness temperature of wavelengths 10.8 and 3.7 μm.
- Quotient between reflectivities 0.6 and 0.8 μm.
- Test in the Carbon Dioxide absorption zone (13.4 μm).
- Test in the Water Vapour absorption zone (6.2 and 7.3 μm).

Table 3 shows a summary of all the tests comprising this method of cloud detection and classification together with their corresponding detection thresholds.

TEST	CONDITION	DIGITAL LEVEL
Visible (R0.6)	Cloud if albedo > 25	If it is cloud = 1 If it is land = 0
Height (Sounding)	–	
Difference ($BT_{10.8} - BT_{3.9}$)	Cloud if difference < -3 K	If it is cloud = 1 If it is land = 0
Quotient (R0.6 / R0.8)	Cloud if quotient < 1.5	If it is cloud = 1 If it is land = 0
Carbon Dioxide ($BT_{13.4}$)	Cloud if $BT_{13.4} < 270$	If it is cloud = 1 If it is land = 0
	"As" if $BT_{13.4} < 245$	–
Water Vapour ($BT_{7.3}$)	Cloud if $BT_{7.3} < T_{400}$	If it is cloud = 1 If it is land = 0

Table 3. Detection tests with their operative values (Casanova, 2005).

The program that generated the cloud masks was implemented in C language. These cloud masks were calculated every fifteen minutes with a spatial resolution of 3 km. For the calculation of the cloudiness index, only the quarters of an hour corresponding to sunlight hours were taken into account since at night time the stomas of the plants are closed and evapotranspiration values are worthless in comparison with the values registered during daytime.

3.3.2.2 Albedo

Albedo is the fraction of incident solar radiation reflected by a surface. In the physical climate system, albedo determines the radiation balance of the surface and affects the surface temperature and boundary-layer structure of the atmosphere. In ecological systems, albedo controls the microclimate conditions of plant canopies and their radiation absorption, which, in turn, affects ecosystem physical, physiological, and biogeochemical processes such as energy balance, evapotranspiration, photosynthesis, and respiration (Wang *et al.*, 2001).

The MODIS algorithm used for the calculation of the albedo is the one suggested by Liang *et al.*, 2002. The albedo is obtained by means of the weighted sum of the visible, near and middle infrared channels:

$$\alpha^{MODIS} = 0{,}160\alpha_1 + 0{,}291\alpha_2 + 0{,}243\alpha_3 + 0{,}116\alpha_4 + 0{,}112\alpha_5 + 0{,}081\alpha_7 - 0{,}0015$$

The coefficients of this equation are specific for the MODIS sensor and they were determined by Liang *et al.* (2002).

MODIS has 36 bands at different spatial resolutions: bands 1-2 at 250 m, bands 3-7 at 500 m and 8-36 at 1 km (King *et al.*, 2000). For the calculation of the albedo we have used the aggregates of bands 1 and 2, and bands 3, 4, 5, 7 all of them with a spatial resolution of 500 meter.

The images required have been processed, that is, geometrically and atmospherically corrected, in the Remote Sensing Laboratory of the University of Valladolid (LATUV) the albedo being one of the products that are generated daily. The LATUV has a receiver antenna of MODIS data from the TERRA and AQUA satellites and is one of the 101 laboratories worldwide that have been recognised by NASA as a "Direct Broadcast Station".

Since the MODIS sensor has a cycle of 16 days, that is, after 16 days the sensor carries out the pass exactly over the same place and at the same time, the value of the daily albedo will be influenced by the Bidirectional Reflectance Distribution Function (BRDF). This function determines that the energy received by the sensor varies depending on both the position of the sun and the position of the sensor.

Studies carry out with the NOAA-AVHRR sensor have demonstrated that the BRDF effect can distorted up to 40% the surface albedo in the visible and near-IR bands when inferred from the nadir reflectance alone (Kimes *et al.*, 1985; Otterman *et al.*, 1985). Hence, to solve the problem of the BRDF effect, the daily albedo has been calculated considering the average albedo values of the whole cycle of MODIS. Thereby, to calculate the albedo of a specific day, it will be necessary to use not only the albedo value corresponding to that day but also the values of the previous 15 days. This methodology is valid in the case of the albedo calculation since its value hardly undergoes changes in periods of time of 16 days.

The image below shows the albedo for the 20th July, 2005. It has been obtained by means of the 16-day images average (from 5 to 20 of July).

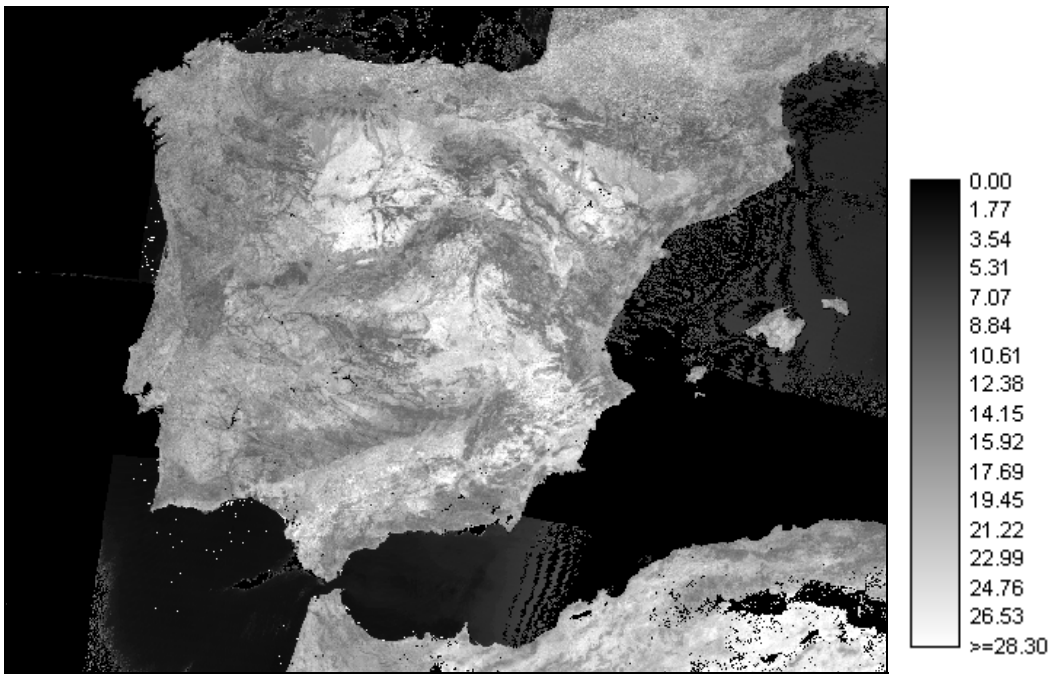

Figure 15. Albedo of the series of MODIS images for 20th of July of 2005.

3.3.2.3 Net radiation

The net radiation (Rn) flux, or available energy, is the most determining factor of water loss of a vegetable canopy when the water in the soil is not limiting. For this reason, Rn flux is the main input variable in Penman-Monteith model: it may represent up to 50 and 60% of ET in humid and subhumid climates respectively (Jensen *et al.*, 1990). Unfortunately, most automatic meteorological stations do not have sensors that measure the Rn flux so it is necessary to calculate it by means of physical models which use solar radiation (Rs), air temperature (Ta) and relative humidity (HR) as input variables (Ortega-Farías *et al.*, 2000a). The present models developed for the estimation of Rn are centred in the so called "reference" crops such as festuca (*Festuca arundinacea*) and alfalfa (*Medicago sativa*) (Allen *et al.*, 1998). For this reason, there is scarce information on models that allow us to estimate the Rn on different vegetable canopies.

The Rn flux represents the balance of short wavelength (0.15 to 3 μm) and long wavelength (3 to 100 μm) that a crop canopy has available to carry out ground-atmosphere water transference processes. This variable can be measured directly by using a net radiometer or by estimating its value through models which integrate the variables which form the long-wavelength and short wavelength energy balance. In the

case of short wavelength, between 20 and 25% of the solar radiation, the main input variable in Rn input models, has been found to be reflected to the atmosphere by the vegetable canopy (Jensen *et al.*, 1990). On the other hand, the long-wavelength radiation balance is measured through Stefan-Boltzmann Law and it depends on the temperature gradient between the air and the crop (Monteith and Unsworth, 1990). Considering all this, the Rn flux of a crop can be measured as follows (Allen *et al.*, 1994, 1998):

$$Rn = R_{ns} - R_{nl}$$

where:

Rn = net radiation flux on a vegetable canopy (MJ m^{-2} d^{-1}),
R_{ns} = short wavelength net radiation (MJ m^{-2} d^{-1}),
R_{nl} = long-wavelenght net radiation (MJ m^{-2} d^{-1}).

The short wavelength net radiation at ground level will depend on the solar radiation and the surface albedo (Brutsaert, 1984) and is expressed as (Allen *et al.*, 1994, 1998):

$$R_{ns} = (1 - \alpha) \cdot Rs$$

where:

Rs = measured solar radiation (MJ m^{-2} d^{-1}),
α = surface albedo (adimensional).

Continuing with the methodology to estimate the Rn used by the Food and Agriculture Organization (FAO), the short wavelength net radiation is determined through the following equation (Allen *et al.*, 1998):

$$R_{nl} = \sigma \left(\frac{T_{max}^{\ 4} + T_{min}^{\ 4}}{2} \right) \left(0.34 - 0.14 \sqrt{e_a} \right) \left(1.35 \frac{R_s}{R_{so}} - 0.35 \right) f$$

where:

σ = constant of Stefan-Boltzman ($4{,}903 \cdot 10^{-9}$ MJ m^{-2} K^{-4} d^{-1}),
Rso = solar radiation calculated for a cloudless day (MJ m^{-2} d^{-1}),
T_{max} = daily absolute maximum temperature (°K),
T_{min} = daily absolute minimum temperature (°K),
e_a = vapor pressure at dew point (kPa)
f = cloudiness factor (adimensional)

Daily comparisons carried out by Howell *et al.*, (1998) between Rn measured with net radiometers (Rno) and Rn calculated following the methodology suggested by FAO, showed the good behaviour of the latter producing an average ratio between both methods equal to 1.01 and a determination coefficient equal to 0.95.

3.4 Calculation of crop coefficient

The crop coefficient (Kc) is defined as the ratio between actual evapotranspiration (ET) and ETo and it is determined and tabulated in field studies. These coefficients integrate the effects of those characteristics that distinguish field crops from reference grass, and can therefore be used to estimate ET. This crop coefficient integrates the effect of both crop transpiration and soil evaporation and it is known as "single coefficient approach".

3.4.1 Processing of remote sensing data

3.4.1.1 Relative Greenness Index

In the Remote Sensing Laboratory of the University of Valladolid (LATUV) there are historical series of NOAA and MODIS images available of 20 and 7 years respectively. By means of these data, we will be able to calculate NDVI values for each pixel rescaled between its maximum and minimum historical values and, thus, to obtain the Relative Greenness Index. This index is indicative about the vegetation condition referred individually to each pixel (Burgan and Hartford, 1993) and it is calculated according to the following equation:

$$RGI = (NDVI - NDVI_{min}) / (NDVI_{max} - NDVI_{min}),$$

where, $NDVI_{min}$ and $NDVI_{max}$ are the minimum and maximum historical values of the NDVI for the analysed pixel. Value range is from 0 to 1.

Thereby, NDVI maps were obtained from band 1 and 2 of MODIS-TERRA and, therefore, with a spatial resolution of 250 meters. The required images were previously processed geometrical and atmospherically in the LATUV. The threshold established in MODIS to detect pixels with clouds is fixed in 0,40 for NDVI (Ackerman *et al.*, 2002) but due to the severe drought that the Iberian Peninsula suffered during the study year 2005, the threshold was reduced to 0,15. This drought produced that the condition of the vegetation in Spain was different to the vegetation surfaces that MODIS has as reference and, thus, most of the surface of the Peninsula appeared cloudy during the whole summer when it was, in fact, cloudless according to MSG images.

Once obtained the NDVI maps, maximum value composites (MVC) were elaborated in period of ten days. Using these composites, maximum and minimum historical values will be calculated for each pixel. With this objective, the first step was to establish the location of the irrigated zones in the study area as well as the type of crop in each pixel. This classification was elaborated and published in CD-ROM by the Andalusian Regional Government in 1999 and later updated in 2003 (Inventory and Characterization of Andalusian irrigated lands, 1999 and 2003). Overlapping both

inventories, only those zones, where the type of crop had remained the same (at least during the 5 years comprising between the two inventories used, from 1999 to 2003), were selected. Thus, we will have a higher certainty that the maximum and minimum historical values (elaborated from the historical series of MODIS from 2000 to 2004), established for each pixel, corresponded to a same type of crop. Hence, it could be stated that the maximum historical value registered in that pixel would correspond to the best state of the plant, that is, it would be in the optimum conditions established by FAO and, therefore, the crop could reach its maximum Kc value (within the vegetative period of each crop) Most maximum values corresponded to the year 2002, an excellent farming year with abundance in crops thanks to the favourable weather conditions registered.

With respect to the calculation of the minimum historical value, the same methodology was used with a small modification. Due to the minimum value of FAO Kc that we use is established within the growing period of the crop, if we would consider periods out of this one, the minimum historical values of NDVI would probably come from bare ground with no vegetation and, as consequence, would not correspond to the minimum Kc value that FAO establishes within crop growing phases. It is because of this, that to calculate the minimum historical value in a pixel with a concrete crop (previously assigned), firstly, there will be selected the time interval corresponding to the vegetative period of that crop and, subsequently, within this period, the minimum value will be obtained. Crops with year-long vegetative periods, such as citrus, do not present this problem when calculating their minimum historical NDVI.

Finally, RGI maps were calculated for the year 2005 as well as RGI maximum and minimum historical values (which will have values of 1 and 0 respectively since, as explained above, this is the range between which their values oscillate). From these maps were derived Kc maps for the year 2005 according to the equation of a straight line, as Figure 16 shows:

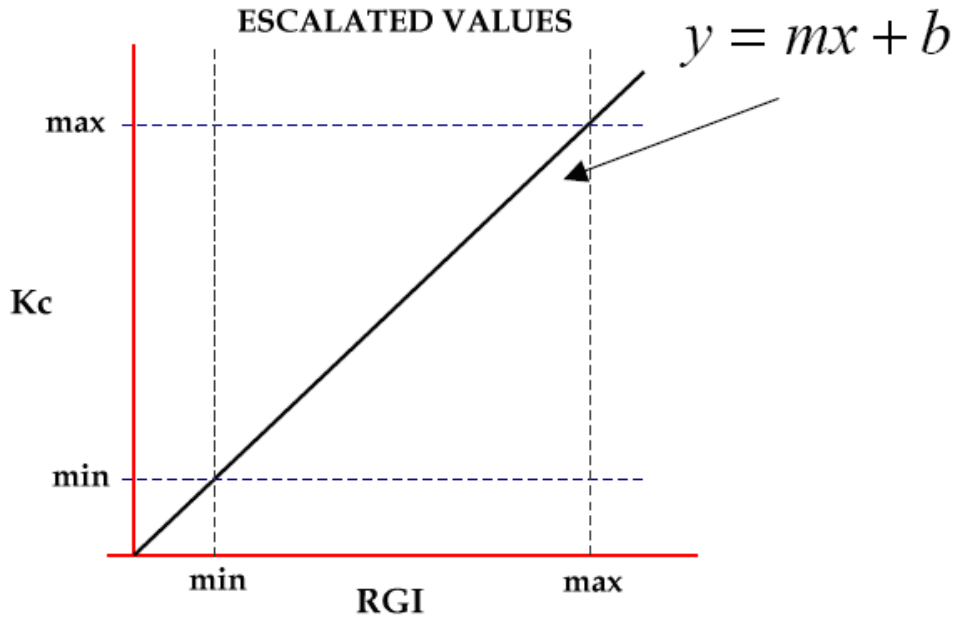

Figure 16. Graphic representation of the mathematical equation to obtain Kc escalated values.

where:

y = Escalated output
m = Rate
x = Input value
b = Offset

The rate and offset are calculated in the following way:

$$m = (Kc_{max} - Kc_{min}) / (RGI_{max} - RGI_{min})$$

$$b = Kc_{min} - (RGI_{min} \cdot m)$$

This methodology will make it possible to consider the real oscillations that a crop will undergo, that is, the crop coefficient curve through its vegetative cycle (due to, for example, strong heat waves, frosts…)

The Kc maps were generated each ten days with a spatial resolution of 250 meters, just like NDVI and RGI maps. The software used to obtain the crop coefficient was IDRISI in its version 14.01 (Kilimanjaro).

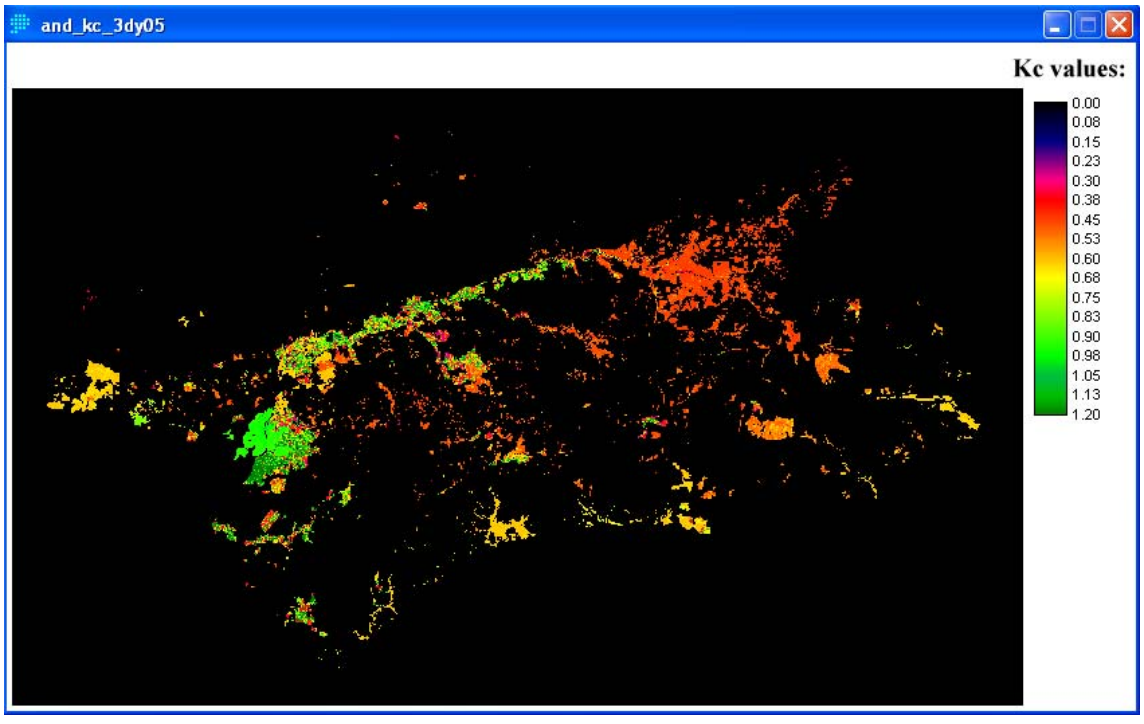

Figure 17. Kc map corresponding to the third tenth of May of 2005.

3.5 Calculation of actual evapotranspiration

As it was detailed in section 2.2., the value of actual evapotranspiration (ET) is, generally, lower than the one of crop coefficient (ETc). Only in case that the water availability in the soil is maximum we can consider that both values are equal. Since our study was carried out in irrigation areas, that is, areas with well-watered crops we can state that ET = ETc and, therefore, henceforth any of these two concepts will be used.

To calculate the crop evapotranspiration, it has been used the most widely accepted methodology in the calculation of water consumption by crops recommended by Allen *et al. (*1998) in the FAO publication. Crop evaporanspiration is calculated according to the reference evapotranspiration (ETo) and a crop coefficient (Kc) (Doorenbos and Kassam, 1986):

$$ETc = ETo \cdot Kc$$

where ETc is the actual evapotranspiration in mm day^{-1}.

Since ETo maps were calculated daily and Kc maps every ten days, daily ET was calculated by multiplying the ETo daily values corresponding to a concrete ten by the crop coefficient value obtained during the previous ten-day period.

3.6 Validation

In order to check the validity of the model suggested we have selected out 30% of the 96 meteorological stations available in Andalusia. These stations are situated in the main irrigation areas of the region as it is shown in Figure 18.

The data of the meteorological stations used for the validation of the meteorological and reference evapotranspiration maps are:

- maximum daily temperature (Tmax),
- mean daily temperature (Tmin),
- minimum daily temperature (Tmean),
- maximum daily relative humidity (Hmax),
- minimum daily relative humidity (Hmin),
- mean wind velocity (WV),
- reference evapotranspiration (ETo).

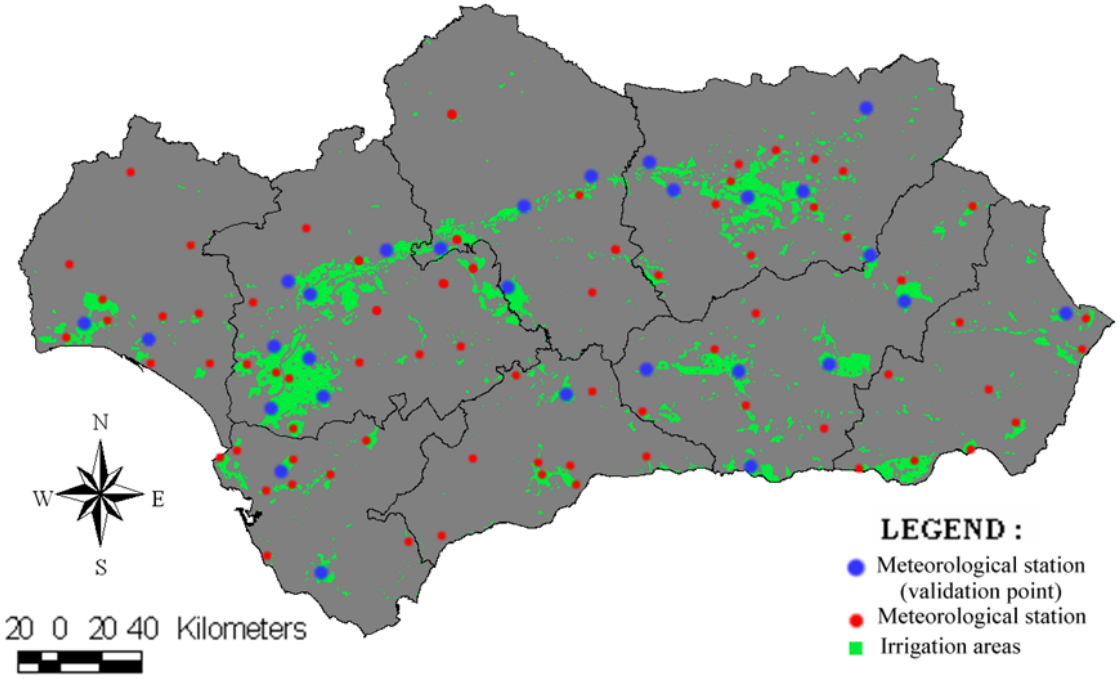

Figure 18. Distribution of meteorological stations.

July and August are the months where the evapotranspiration reaches its maximum level. Because of that, ten days of these months were selected at random to validate the model during the summer of 2005.

The crop coefficient could not be validated through field work due to technical, economic and time limitations. Thus, the validation of each crop classified was carried out by comparing the Kc curves obtained with the curves established by FAO in the paper 56 of the Irrigation and Drainage Serie.

For the same reason, actual evapotranspiration could not be validated either. However, since we started from the premise that the crop coefficient established by FAO is correct, the method used to estimate the ET is considered to obtain as good results as the ones obtained in the calculation of ETo.

The model sensitiveness was analysed by means of two criteria: the root mean square error (RMSE) and the mean bias error (MBE):

$$\text{RMSE} = \sqrt{\frac{\sum_{i=1}^{N}(Es - Eo)^2}{N}}$$

$$\text{MBE} = \frac{\sum_{i=1}^{N}(Es - Eo)}{N}$$

where:

N = number of values,
Es = estimated value,
Eo = observed value and
i = index for the number of data.

The reason of using both is because these two average-error statistics provide complementary information. RMSE indicate the magnitude of the average error, but it does not provide information on the relative size of the average difference between the predicted and observed values. MBE, however, describes the direction of the error bias. A negative MBE occurs when predictions are smaller in value than observations.

3.7 Available data

3.7.1 Meteorological data

The Department of Fish and Agriculture with funds from the European Union has installed in the Andalusian Community a net of automatic meteorological stations and a Regional Center of Data Exploitation (Zonal Centre) that allows us to have agro-meteorological information available for all irrigated lands in Andalusia. The information registered by these meteorological stations is broadcasted freely by the Andalusian Department of Fish and Agriculture through their web page (http://www.juntadeandalucia.es/innovacioncienciayempresa/ifapa/ria/servlet/FrontController).

According to the Guide to meteorological instruments and methods of observation (1997), automatic stations are those in which "instruments carry out and transmit or register observations automatically converting them, if necessary, directly to the corresponding key or carrying out this conversion in a transcription station".

In these stations, manual instruments are substituted by automatic sensors. It can be said that automatic stations arose from the necessity of obtaining information in locations of difficult access, inhospitable places or just to carry out observations during non-working hours.

The first source of data used was the meteorological data from these stations. The data downloaded from the website of the Andalusia Government for the whole year 2005 were the following parameters:

- maximum daily temperature (ºC),
- mean daily temperature (ºC),
- minimum daily temperature (ºC),
- maximum daily relative humidity (%),

- minimum daily relative humidity (%),
- mean wind velocity (m/S),
- reference evapotranspiration (mm day^{-1}).

3.7.2 Remote sensing data

3.7.2.1 MODIS-TERRA

The MODIS (or Moderate Resolution Imaging Spectroradiometer) sensor flies on board of the TERRA and AQUA satellites. The objective of this sensor is to provide comprehensive data about land, ocean, and atmospheric processes simultaneously. TERRA´s orbit around the Earth crosses the equator in the morning from North to South and it provides two-day repeat global coverage, acquiring data in 36 spectral bands with different spatial resolutions (250, 500, or 1000 m, depending on wavelength) (Lillesand and Kiefer, 2000).

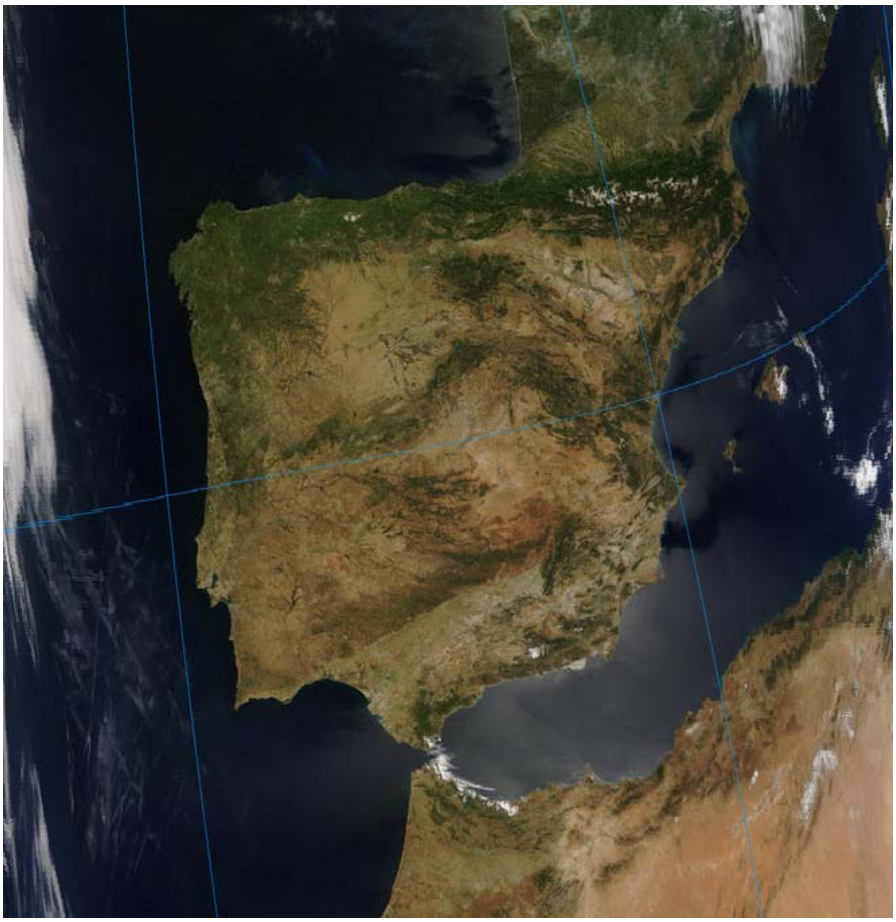

Figure 19. True colour MODIS-TERRA. © 2006 NASA.

Some general information about bands contained in the MODIS sensor is summarized in Appendix I.

MODIS-TERRA images were collected and processed to Level-2, that is, radiometrically, atmospherically and geometrically corrected (Parkinson and Greenstone, 2000) in the Remote Sensing Laboratory of the University of Valladolid (LATUV). The LATUV has a receiver antenna of MODIS data from the TERRA and AQUA satellites and is one of the 101 laboratories worldwide that have been recognised by NASA as a "Direct Broadcast Station".

3.7.2.2 SEVIRI-MSG

The operational Meteosat satellites are positioned in geostationary orbit, above the equator, normally at 0° longitude, i.e. the Greenwich Meridian. The primary payload of the Meteosat Second Generation (MSG) satellites is the Spinning Enhanced Visible and IR Imager (SEVIRI). The SEVIRI takes images of the earth, measuring the radiance at 12 different wavebands of the electromagnetic spectrum. The various channels provide measurements of different physical characteristics of the atmosphere and the earth at a resolution of 3 km at the sub-satellite point. High resolution imagery is acquired by observing the Earth in the visible band and sampling at 1 km resolution. During normal operations the radiometers capture new images of the earth every 15 minutes (EUM TD 07, 2001). The spectral bands of this sensor are summarized in Appendix I.

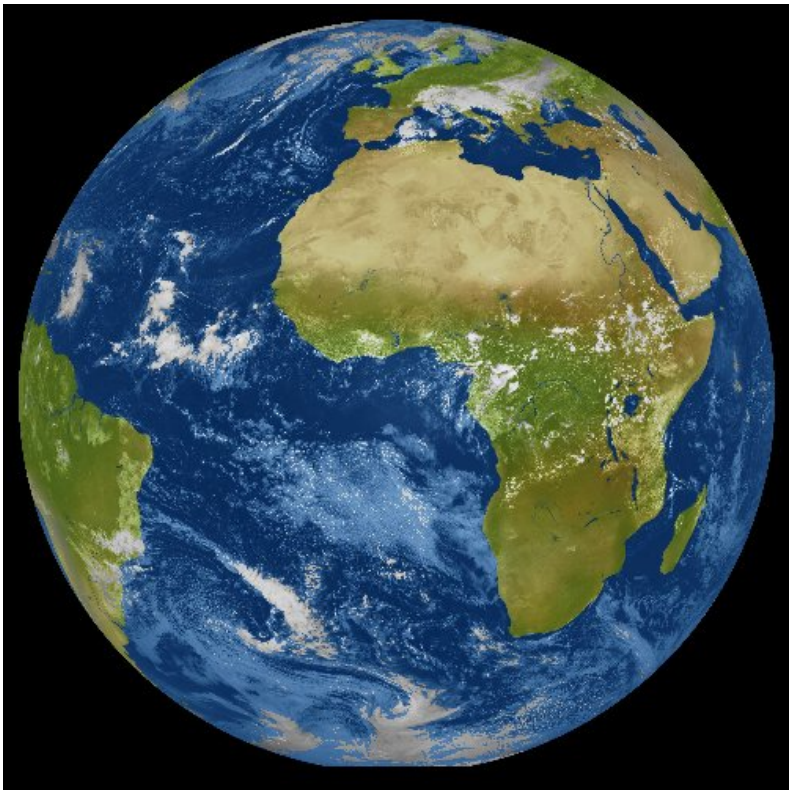

Figure 20 . Artificially coloured image of Meteosat satellite © 2006 EUMETSAT.

SEVIRI images from Meteosat-8 spacecraft have been collected from EUMETCast. The images used for the cloud detection were previously calibrated in the LATUV (EUM TD 15, 2006).

4 RESULTS

In this chapter, it is shown the application of the proposed model in the region of Andalusia. Results have been grouped in 4 main stages developed with our methodology: interpolation of meteorological data, calculation of reference evapotranspiration, calculation of crop coefficient and calculation of actual evapotranspiration.

The model sensitiveness was analysed at 28 meteorological stations using two criteria: the root mean square error (RMSE) and the mean bias error (MBE).

4.1 Interpolated maps

As specified in the interpolation methods section (3.3.1.1), the methods selected to interpolate meteorological data were:

- Inverse distance to a power (ID),
- kriging (KG),
- modified Shepard´s method (MS),
- nearest neighbour (NN),
- radial basis function (RB).

There was an attempt to improve the interpolation of temperature and wind speed by following some steps before and after the interpolation process (see section 3.3.1.1.). Ten days were selected at random between the months of July and August to calculate the mean statistical error of each method. Maximum, minimum and mean values registered for each variable through these days are presented in Table 4.

The results obtained for the MBE and RMSE are shown in Tables 5 and 6. The value of the smallest error has been highlighted in yellow for each one of the meteorological variables (Tmax, Tmin and Tmean).

Value	***Tmax (ºC)***	***Tmin (ºC)***	***Tmean (ºC)***	***Hmax (%)***	***Hmin (%)***	***W V (m/s)***
Maximum	41.8	26.2	31.5	100	61.7	**5.6**
Minimum	25.2	10.6	20.3	25.3	6.1	**0.4**
Mean	**35.1**	**17.38**	**26.23**	**71.03**	**20**	**1.59**

Table 4. Maximum, minimum and mean values for each meteorological variable.

Method	*Tmax (ºC)*	*Tmax_hc(*) (ºC)*	*Tmin (ºC)*	*Tmin_hc (ºC)*	*Tmean (ºC)*	*Tmean_hc (ºC)*
ID	-0.816	-0.685	0.745	0.786	0.141	0.343
KG	-0.278	-0.077	0.449	0.488	0.011	0.052
MS	-0.433	-0.118	-0.533	2.436	0.029	0.036
NN	-0.349	-0.310	0.523	0.725	0.064	0.102
RB	-0.655	-0.516	0.709	0.836	0.091	0.191

Method	*Hmax (%)*	*Hmin (%)*	*W V (m/s)*	*W V_comp(**) (m/s)*
ID	-2.310	2.082	0.240	-0.235
KG	-3.955	0.425	0.258	0.023
MS	-2.825	1.163	0.293	0.218
NN	-2.742	1.626	0.123	0.123
RB	-4.197	0.393	0.264	-0.020

Table 5. MBE of the different interpolation methods for each of the meteorological variables.

Method	*Tmax (ºC)*	*Tmax_hc (ºC)*	*Tmin (ºC)*	*Tmin_hc (ºC)*	*Tmean (ºC)*	*Tmean_hc (ºC)*
ID	1.484	1.364	2.158	2.070	1.014	1.033
KG	1.262	1.068	2.106	2.267	1.098	1.116
MS	1.608	1.256	2.747	4.150	1.516	1.453
NN	2.061	1.833	2.424	2.436	1.502	1.357
RB	1.725	1.521	2.450	2.740	1.173	1.154

Method	*Hmax (%)*	*Hmin (%)*	*W V (m/s)*	*W V_comp (m/s)*
ID	5.705	4.209	0.724	0.711
KG	6.428	3.271	0.790	0.774
MS	6.121	4.004	1.141	1.023
NN	6.087	5.790	0.964	0.964
RB	7.272	2.850	0.718	0.691

Table 6. RMSE of the different interpolation methods for each of the meteorological variables.

(*) ***hc*** means that a previous step of height correction has been applied in the temperature variable according to the process detailed in *section 3.3.1.1.1*.

(**) ***comp*** means that a decomposition of wind components has been carried out as was detailed in *section 3.3.1.1.2*.

A positive value in the MBE means that the method overestimates the true value of the meteorological variable, on the other hand negative value means that the method underestimates the value.

According to these results, the selected methods of interpolation for each of the meteorological variables are presented in Table 7.

Error Statistics	*Tmax*	*Tmin*	*Tmean*	*Hmax*	*Hmin*	*W V*
MBE	KG_hc	KG	KG	ID	RB	RB_comp
RMSE	KG_hc	ID_hc	ID	ID	RB	RB_comp

Table 7. Summary of the most accurate interpolators.

Table 7 shows how the method selected as the best interpolator may vary in some cases depending on the criterion chosen to determine the mean statistical error (MBE or RMSE).

In 2005, Willmott and Matsuura carried out a study to determine the efficiency of the measurements of different statistical errors (MBE and RMSE among them) in order to evaluate different spatial interpolators applied to the obtaining of air temperature maps. They concluded that the mean absolute error (MAE) and MBE are the most natural measures of spatial-average interpolation error, and that (unlike RMSE) they are unambiguous measures of spatial-average error. Consequently, with the dilemma arisen in our study in selecting the most accurate interpolator for Tmin and Tmean, we selected the interpolation method established by the MBE. In spite of that, RMSE has been also calculated since, as it was explained in section 3.6, can provide complementary information about the errors.

Interpolated maps obtained through the spatial interpolators selected are shown in Appendix II. The application of the selected interpolators to other regions, probably, would not be possible with the same accuracy since the accuracy of the interpolation is conditioned by factor like the size of the study area, the geomorphology of the terrain, the oscillation range of the different variables or the distribution and number of available stations.

4.2 Reference evapotranspiration

ETo maps were obtained daily. From these maps we obtained, subsequently, accumulated ETo maps in periods of ten days, months and the whole year. Figure 21 is and example of reference evapotranspiration map obtained for 7th of July of 2005. Other examples of tenth, month and yearly maps are shown in Appendix II.

The comparison between ETo values estimated with the proposed methodology and the values calculated in the meteorological stations is shown in Figure 21. The cloud of points represented in this figure shows the ETo values obtained in 28 meteorological stations. For each station were taken the daily ETo values corresponding to the ten days selected for the validation (detailed in section 3.6).

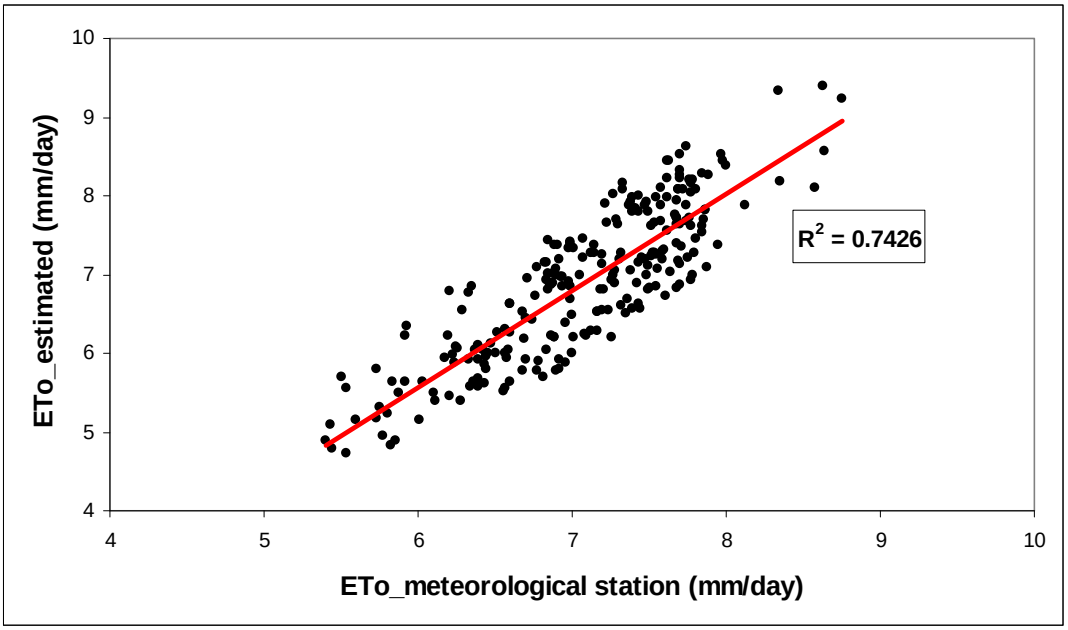

Figure 21. Dispersion between ETo estimated with the proposed model and the one calculated in the stations.

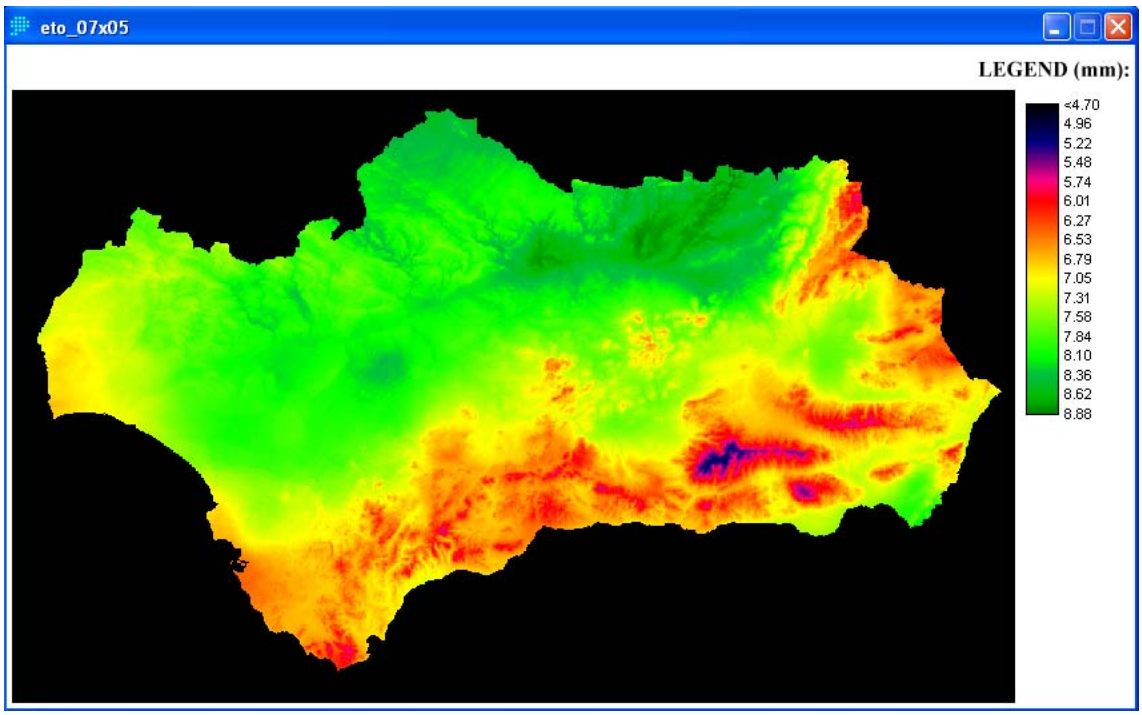

Figure 22. Reference evapotransporation estimated for 7th of July of 2005.

Observing figure 21 we can deduce that lower values of ETo are associated, in general, with areas of higher elevation or coastal areas. This is due to these zones are characterized by having lower temperatures in summer and, therefore, lower evapotranspiration. Furthermore, coastal areas present high humidity values implying a

high water vapour concentration in the atmosphere and, as consequence, the evaporative capacity of the atmosphere will be reduced.

With the aim of carrying out the sensitivity analysis of our model, two criterion were used, the RMSE (equation 4.1) and the MBE (equation 4.2). The estimation error of ETo according to the RMSE was ± 0.537 mm/day, and 0.181 mm/day for MBE. The last error shows that the proposed model tends to overestimate slightly the real value of ETo. The ETo values, along the selected 10 days for the validation, ranged between a maximum of 8.75 mm/day and a minimum of 5.4 mm/day, the mean ETo was 7.04 mm/day.

4.3 Crop coefficient

Below are the crops classified to estimate their crop coefficients:

- sunflowers,
- sugar beet,
- cotton,
- citrus,
- wheat,
- barley,
- rice,
- maize,
- oats,
- alfalfa,
- olives,
- strawberries,
- avocado.

Next are shown some examples of the results obtained in the calculation of the relative greenness index (RGI) and crop coefficient (Kc). Graphs in Figure 23 show the temporal evolution undergone by these two parameters through the year 2005 for pixels with different crops. These pixels were selected at random between pixels situated in central areas inside region with the same crop. Thus, we assure that the selected pixel is not mixed with neighbouring crops. Previously, curves of several pixels of each crop were observed in order to check that, within a same crop, most of curves were similar.

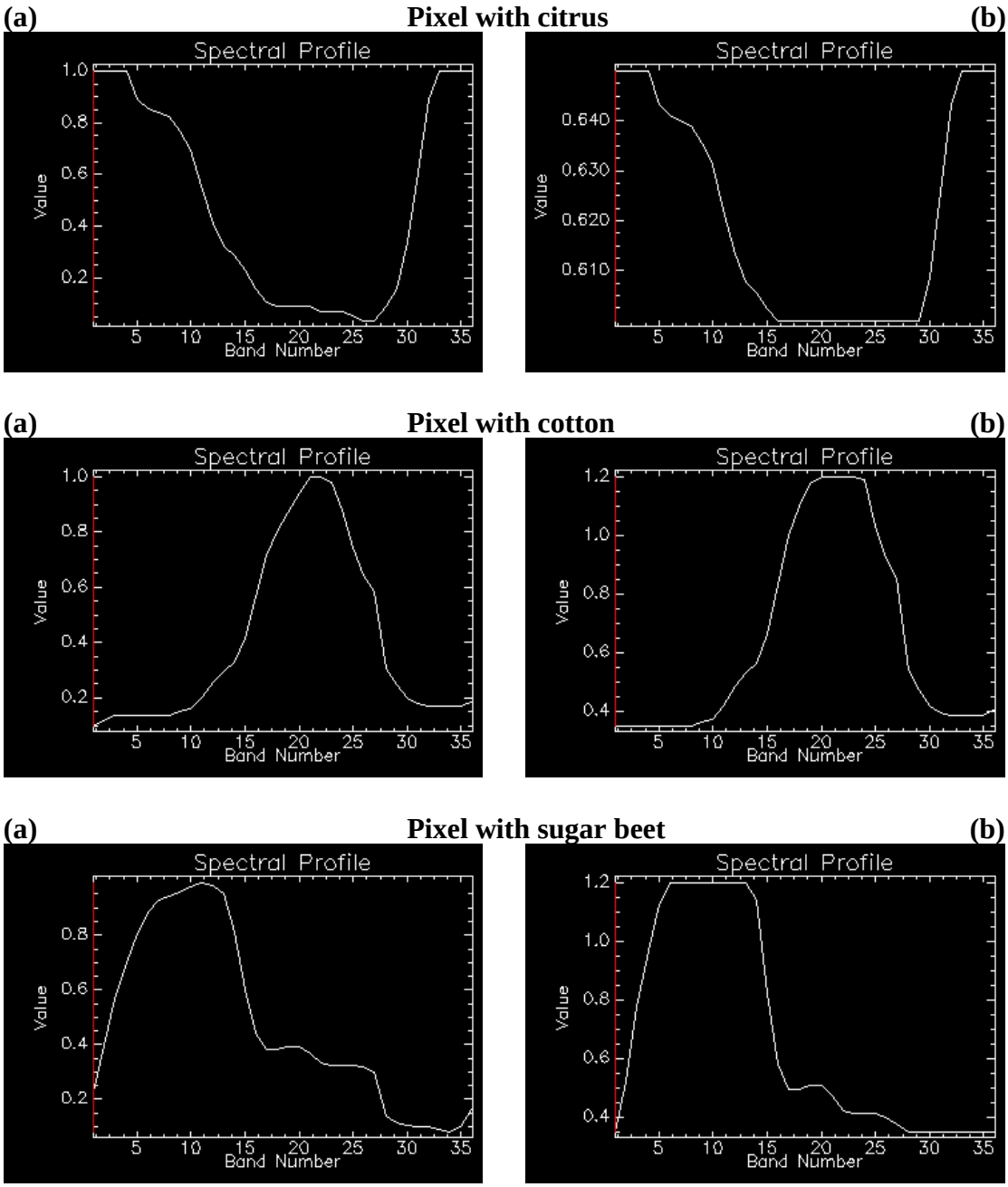

Figure 23. Temporal evolution of RGI (a) and Kc (b) through the year 2005 for pixels with different crops

The "X axis" of the graphs (Figure 23) shows the different tenths in which a year is divided, that is, their value range goes from 0 to 36. The "Y axis" corresponds to the RGI (or Kc) value of a pixel in each of the tenths. The values of this axis for the RGI range between 0 and 1 and, for Kc, they will vary according to the maximum and minimum values established by FAO depending on the type of crop (explained in section 3.4.1.1., see Figure 16).

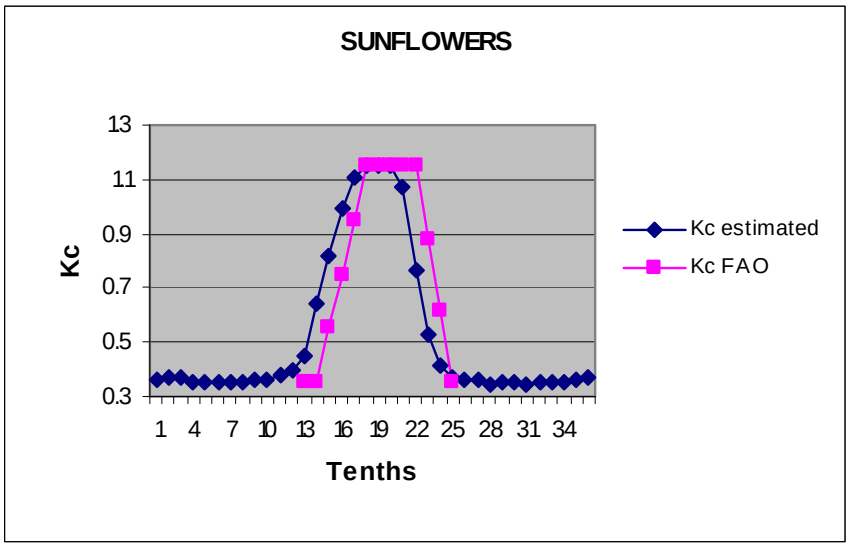

Figure 24. Evolution of sunflower Kc through the year 2005.

To establish the validity of the RGI in the calculation of crop coefficients, we have proceeded to compare the Kc curves estimated (through the whole year 2005, see Figure 24) according to our methodology with the ones established by FAO. Some results are shown in Figures from 24 to 29. The rest of curves are shown in Appendix II.

In order to visualise more accurately the similarity between both curves we have selected exclusively the growing period established by FAO (in the case of sunflower from the first tenth of May to the second tenth of September) and removed the small time displacement between them, that is, both curves will be overlaid as we can observe in Figure 25.

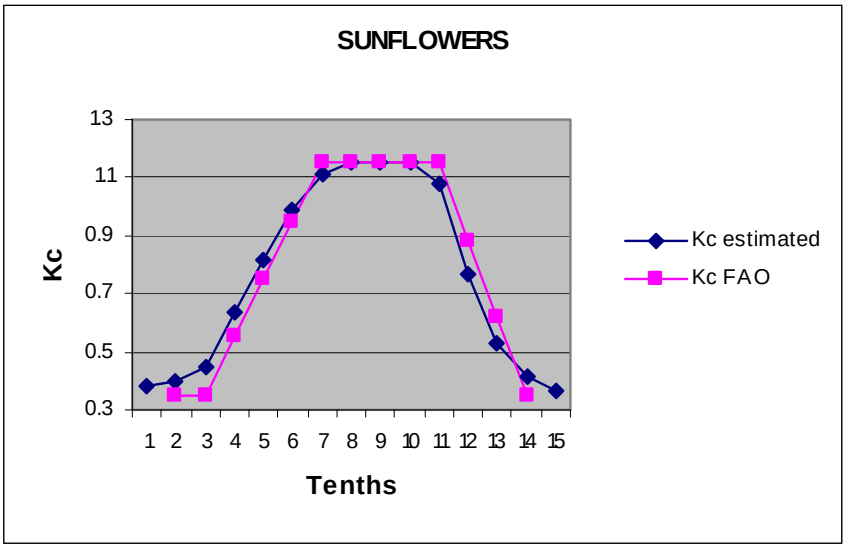

Figure 25. Adjustment between both curves during the growing period (from May to September).

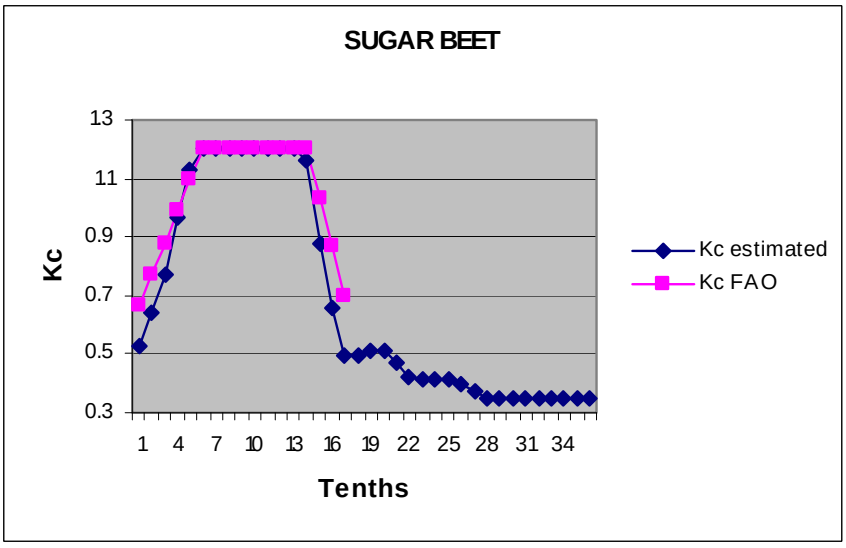

Figure 26. Evolution of sugar beet Kc through the year 2005.

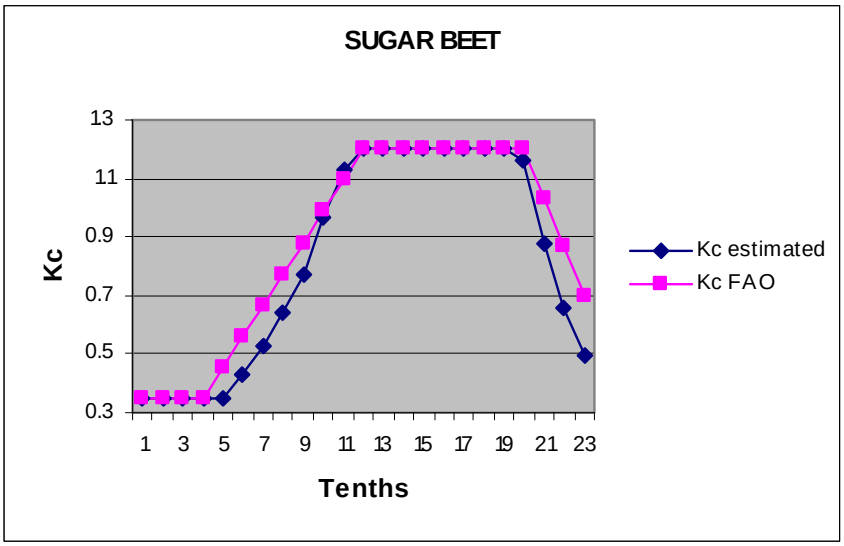

Figure 27. Kc curves during the growing period (from November to June).

Since, according to FAO, the growing period of sugar beet takes place between the first tenth of November and the second tenth of June, Kc values for November and December 2004 were filled with the values corresponding to the same months of 2005. The same thing happened with other crops such as wheat, barley or oats.

As can be observed in Figure 28, the evolution of the crop coefficient estimated is completely different to the one established by FAO, which reveals that the study carried out by FAO to determine Kc values for olives is not valid for our study zone.

Studies carried out by the Andalusian Department of Fish and Agriculture (CAP) have concluded that Kc values for olives in Andalusia range in between 0.50 and 0.65 through their growing period (March to December) (Irrigation Fundaments, 2006). The lowest values are registered during the summer months and the highest ones during spring and autumn/winter. In Figure 29 it can be observed how our estimated curve adjusts quite well to the one established by CAP.

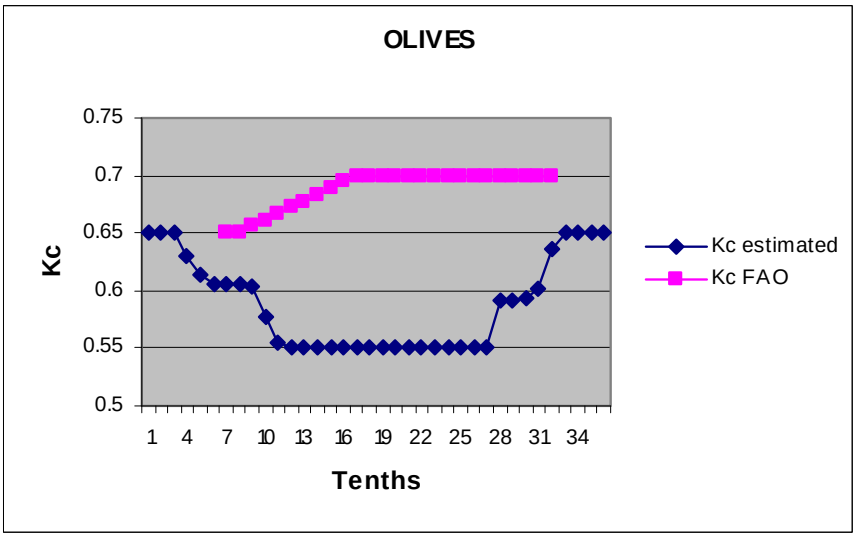

Figure 28. Evolution of olives Kc through the year 2005.

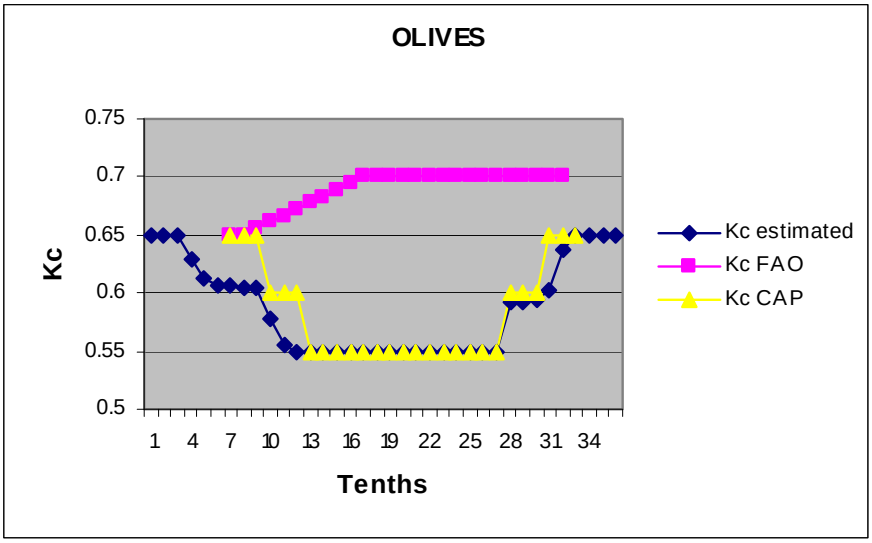

Figure 29. Evolution of olives Kc through the year 2005.

Once the different crop curves have been obtained, we can observe that in most of the cases Kc curve estimated and Kc curve established by FAO fit quite well although, in some cases, the vegetative cycle of the first one is slightly displaced in time with respect to the second one. This is due to the normal oscillations that take place during the vegetative cycles as a consequence of this year's weather conditions. On the other hand, although Andalusia is said to belong, in general term, to a Mediterranean climate with hot and dry summer and mild winter, there are differences within the region. The three most typical distinctions are: coast, inland and mountain climates. These differences may be the cause of advancements and delays of crop cycles with respect to the ones established by FAO for Mediterranean climates. Finally, other important factor to take into account to explain the slight displacement between curves is the variety inside of each crop. Thereby, taking as example, the olive tree, the most characteristic and important crop in Andalusia, we can distinguish a large number of olive varieties exiting in this region. Depending of this variety the vegetative cycle will be able to fluctuate in time in different ways. For instance, the "Picual" variety has the earliest recollection in Andalusia (beginning of November) and, however, the "Lechín de Granada" variety has the latest one (at the end of February).

In order to be able to study in depth the precise causes that generated each one of the oscillations between curves, more data would be necessary. This question will be expounded in section 6.1. as recommendation for future improvements.

4.4 Actual evapotranspiration

Since ETo maps were calculated daily, however, Kc maps were calculated every 10 days (see section 3.4.1.1), actual evapotranspiration was obtained by multiplying the daily ETo value by the crop coefficient value that includes the day for which the actual evapotranspiration is going to be calculated. Thus, for example, to calculate the actual

evapotranspiration on 15th August (Figure 30), we will multiply that day's ETo value by the crop coefficient corresponding to the second tenth of August (between 11 and 20 August, both included). This reveals that when calculating the actual daily evapotranspiration in the same tenth, the crop coefficient will always be the same and only the daily ETo value will change.

Different colours in Figure 30 show the quantity of water that each crop has evapotranspirated for the day 15th of August of 2005. The colour of each pixel only is comparable between pixels with the same crop due to the intensity of evapotranspiration will vary, mainly, depending on the type of crop. Thus, one pixel with rice throughout most of the year will have higher evapotranspiration that one pixel with olive trees, even if the first one is in an initial stage of growing and the second one in its maximum development stage, period when the evapotranspiration is higher.

Figure 31 represents graphically the evolution of actual evapotranspiration through the year 2005 for pixels with different crops. There is shown the large difference of evapotranspiration values between, for instance, a pixel with rice (yellow line) and other with olive trees (dark blue line). This figure has been elaborated in accumulated periods of ten days.

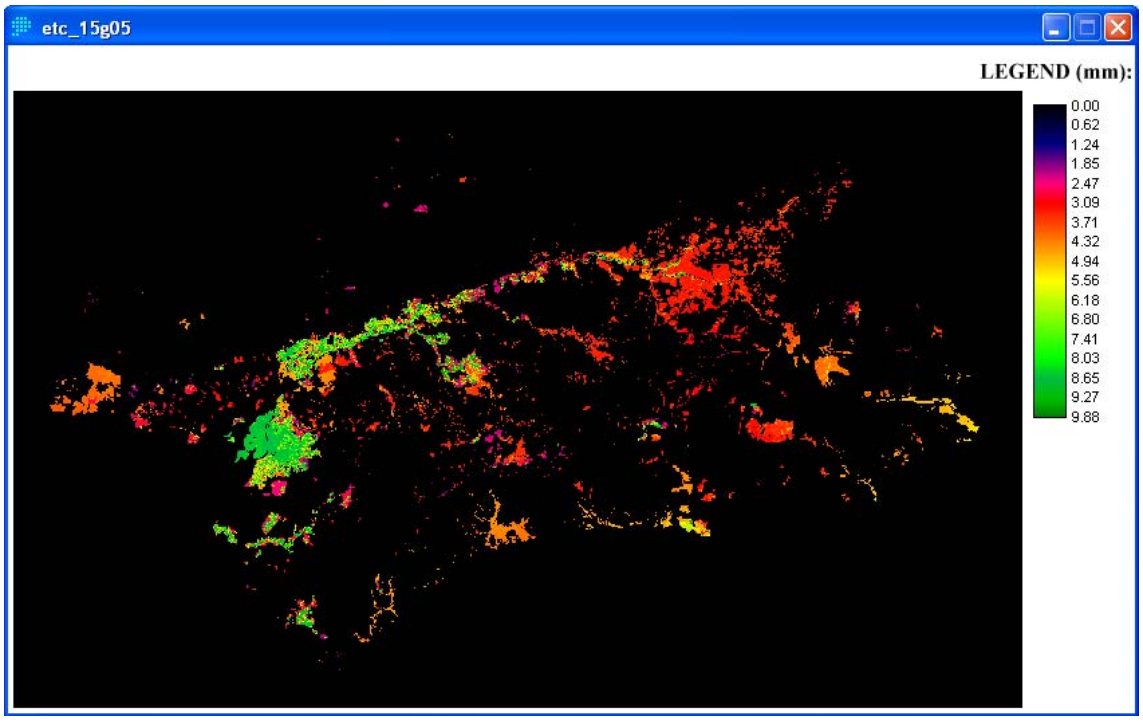

Figure 30. Actual evapotranspiration estimated for 15 August, 2005.

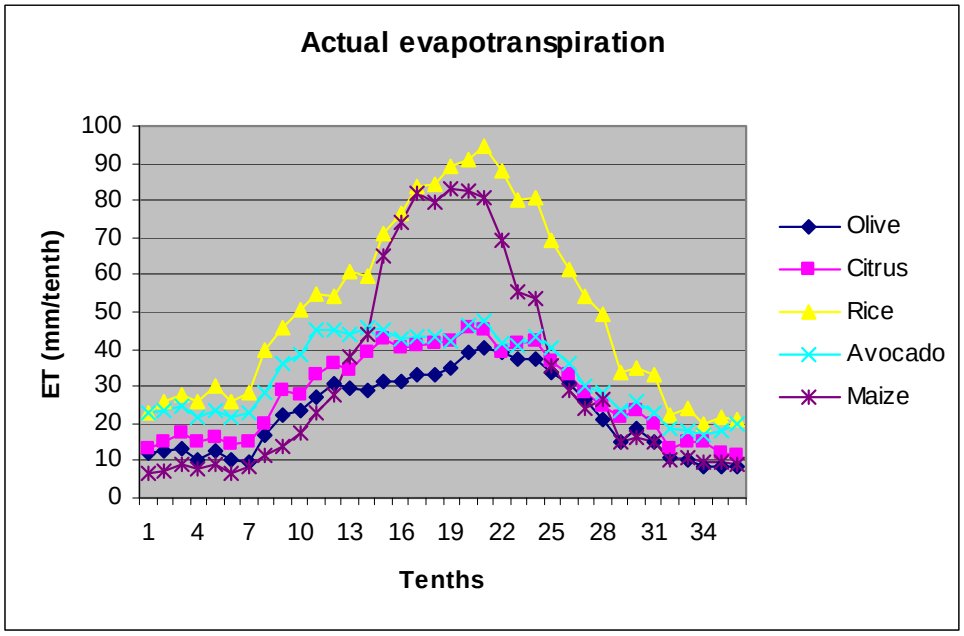

Figure 31. Temporal evolution of actual evapotranspiration for several pixels with different crops.

5 DISCUSSION

With the results obtained for ETo we can observe (Figure 21) that the adjustment between ETo estimated and ETo calculated in the meteorological stations is quite good. In spite of that, the results of reference and actual evapotranspiration have been able to be affected for uncertainties from meteorological and remote sensing data.

Since meteorological data are collected from automatic meteorological stations they can undergo uncertainties from the calibration of the measurement instruments, the location of the meteorological stations, the geographic distributions or the density of stations of the study area. Hence, these uncertainties will influence in the final results of both reference and actual evapotranspiration. In this study the uncertainties could not be taking into account because of technical, economic and time limitations.

Remote sensing uncertainties will be related fundamentally for the crop coefficient due to the high weight of this parameter in the equation used to calculate actual evapotranspiration. These uncertainties are mention in detail below, together with the results obtained for the crop coefficient. They could not be studied for the same reasons that meteorological uncertainties.

The results obtained for the crop coefficient shows, in general term, a good adjustment between Kc curves estimated and Kc curves established by FAO for most of the crops. Therefore, this reveals that the Relative Greenness Index used to obtain crop coefficients is a good indicator of the coefficient's evolution.

Using this index for the establishment of the crop coefficient instead of using directly the values established by the FAO has the advantage of considering the actual oscillations that a crop might undergo throughout its vegetative cycle. Thus, for instance, for woody crops such as almond trees, an early start of the spring weather conditions will influence other aspects such as an earlier flowering period and, consequently, an earlier collection season. This index also allows us to detect meteorological perturbations such as frosts, hail, torrential rain, heat waves, etc, which will affect the plant's growing cycle and which will obviously affect the crop's coefficient value.

It must be also taken into account that within the region of Andalusia, with a predominantely Mediterranean climate, we can find small micro-climate zones which will determine whether the plant development cycles will be different from the ones established by FAO for Mediterranean climates. These small climatological variations within the Mediterranean climate are reflected when the crop coefficient is established through remote-sensing and, in this particular case, through the relative greenness index.

The only exception to this good adjustment between the curves calculated through the RGI and the ones established by the FAO was that of olive-trees. As the results show, the data on the Kc evolution obtained through remote-sensing are completely different to the ones established by FAO for a Mediterranean climate. In the

first curve (Figure 29), we can observe that maximum values are registered in the spring and autumn months, whereas minimum values are registered during summer. However, in the second curve, the one established by FAO, maximum values appear during the summer remaining until the autumn, whereas the minimum value is registered in spring.

In order to try to solve this problem, other sources based on studies carried out directly in Andalusia were consulted. All these studies (Orgaz and Fereres, 1999, Fernández, *et al.* 2006, Barranco, 2004) proved that the actual evolution curve of the olive Kc responded to the curve obtained through remote-sensing. This demonstrated that the Kc value established by FAO for the Mediterranean climate was established under weather conditions different to the ones registered in the interior zone of Andalusia (where most olive tree plantations are found). According to Orgaz and Fereres (1999), these differences in the Kc value appear due to the fact that the FAO values were established in the island of Crete, with a Mediterranean climate which is quite different to the Mediterranean climate characteristic of inland zones. The climate of the island of Crete is, in general terms, a climate with mild temperatures and a high relative humidity very much determined by the influence of the sea. The Inland Mediterranean Andalusian climate, however, presents a lower relative humidity and extreme temperatures during the winter and summer months. With these high temperatures, plants such as olives-trees close their stomates so as to minimize the water loss that takes place through transpiration. For this reason, in Andalusia there is a low crop coefficient during the months of intensive heat, contrary to what happens in other zones with a milder, more favourable climatology for their development.

With respect to the methods used for the interpolation of meteorological data, it is worth mentioning the method selected for the interpolation of the wind speed. Through the decomposition of the "x" and "y" wind variables, this method resulted in an error reduction of 95% with respect to other interpolation methods for the MBE, and of 11% for the RMSE. This means that the application of this method reduces both the level of scatter and the tendency of the model. However, the most important reduction is produced in relation with the tendency of the model to overestimate the values.

Comparing the results of this work with the obtained in previous studies and for meteorological variables (Felicísimo, *et al*., 2001, Vicente-Serrano, *et al.*, 2003, Ninyerola, *et a*l., 2005, Sánchez, et al., 1994), the data varied ± 5 % among all the studies taken as reference.

In order to obtain actual daily evapotranspiration maps (as explained in section 4.4), the daily ETo was multiplied by the Kc obtained for the whole ten-day period. This methodology will be possible as long as the estimation of the actual evapotranspiration is not carried out in real time, as is our case. The obvious reason is that in order to obtain the Kc value for a concrete tenth, the ten images corresponding to the 10 days conforming this ten-day period will be required. In the third tenth of each month the number of days could vary depending on whether they are 28, 29 or 31-day months. In these cases, the third ten of each month will have 8, 9 or 11 days respectively. Thus, the Kc value won't be obtained until the last day of each tenth, which means that during the first 9 days of these periods, the value to calculate the actual daily evapotranspiration won't be available.

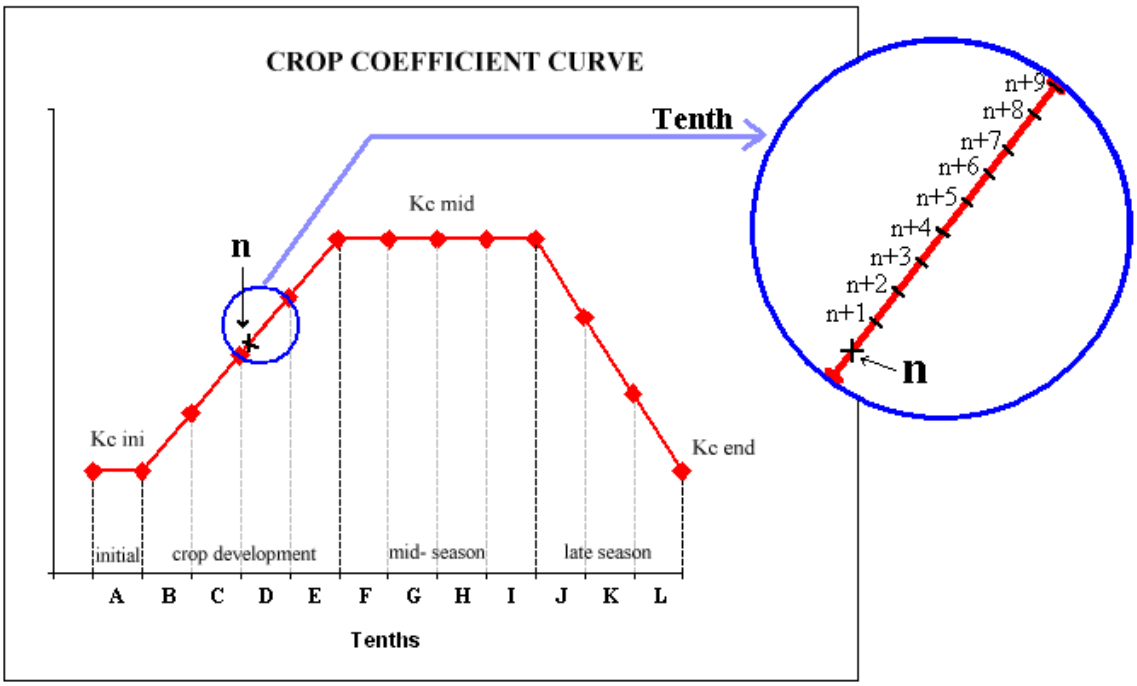

Figure 32. Crop coefficient curve.

This problem could be solved in two different ways. The first one would be to calculate the crop coefficient daily. However, this would not make much sense nor it would be feasible in many cases since the vegetation would not reflect any kind of variation in such a short period of time. Furthermore, the calculation of the daily Kc would bring up certain problems, such as the lack of data in cloudy zones or having to use very geometrically distorted zones of the MODIS-TERRA images (or even not having coverage of some areas in case of too oblique passes over the Peninsula). However, in decennial composites the distorted zones would not have to be taken into consideration since they would only provide erroneous information about the state of the crop. The second solution would be to multiply ETo by the Kc obtained in the former tenth instead of the coefficient corresponding to the present ten-day period. Due to Kc value is obtained from a 10-day maximum vegetation value composite (that is, by taking the highest pixel value), the Kc values of each tenth, during the crop development stage, should correspond with values obtained in the last images of each tenth because the vegetation will be higher. This imply that the Kc value for a concrete day "n" belonging to the tenth "D", according to Figure 32, will be comprised between the Kc value obtained for the whole tenth "D" and the value obtained in the whole former tenth "C". Obviously, depending on how early or late we are in the tenth (n, n+1, n+2…), the Kc value will be closer to the Kc value of the tenth "C" or to the Kc value of the tenth "D". Hence, it can be concluded that, in order to estimate the actual daily evapotranspiration in real time, the use of the Kc value corresponding to the former tenth could be a valid methodology, like the one used in this work.

As it is known, the evapotranspiration from a field is very difficult to be determined with accuracy, even for methods carried out "in situ" such as the lysimeters. Most evapotranspiration calculation methods (especially calculation methods at regional scale) are mere approximations of the evapotranspiration that there is at a concrete place. Thus, to make use of evapotranspiration data in applications, such as farming

watering advice, longer-period data (weeks, tenths or fifteen-day periods) are generally used (Calera *et al.*, 2005). Thus, evapotranspiration data will be more likely to adjust to the reality. In Spain, more and more public and private organisations (such as the University of Castilla La Mancha (http://crea.uclm.es/crea/index.htm) or the Local Government of Castilla y León (http://www.jcyl.es:8080/ora_riac/plsql/Proc_MuestraRecProv1?PROVINCIA=24&RIEGO=0#), for instance, offer this kind of information to farmers every 7 or 10 days through their websites. In the first one these data are obtained using both remote sensing data and field data and the second one only by means of field data.

6 CONCLUSION

- Satellite images provide essential information to carry out evapotranspiration estimations at regional scale.

- In this thesis, a model capable of estimating actual evapotranspiration at regional scale with a spatial resolution of 250m has been developed. It comes from Penman-Monteith equation by means of a model that combines both meteorological and remote-sensing data.

- The interpolation methods selected for each of the meteorological variables required in the calculation were:

    - maximum temperature → kriging with heigh correction,
    - minimum temperature → kriging,
    - mean temperature → kriging,
    - maximum relative humidity → inverse distance to a power,
    - minimum relative humidity → radial basis function,
    - mean wind velocity → radial basis with a previous decomposition of wind components.

- The relative greenness index reveals itself as a very useful tool for the estimation and monitoring of the crop coefficient.

- This model has been validated in the region of Andalusia, where the highest percentage of irrigated land in Spain is found, a type of agriculture that is also the base of the economic development of this region. For this purpose, MODIS-TERRA and SEVIRI-MSG images together with data from different meteorological stations in the zone have been used.

- A total of 28 meteorological stations situated in the main irrigated areas and 10 days from the months of July and August of 2005 have been selected. The comparison between the data calculated at the station and the ones obtained through our model shows an estimation error of ± 0.537 mm/day and an overestimation of 0.181 mm/day.

- Actual evapotranspiration maps resulting from the application of the model in Andalusia show how this model is capable of reproducing the expected regional changes.

6.1 Future improvements

For future researchs, some recommendations would be required in order to improve the final results obtained in this work.

As it has been discussed in section 5 there are uncertainties not taken into account that will affect the final results of reference and actual evapotranspiration. These uncertainties will affect both meteorological and remote sensing data.

With respect to meteorological uncertainties, to study the accuracy and calibration of the measurement instruments used in the meteorological stations should be necessary. Furthermore, inserting data from meteorological stations situated in bordering areas would be able to improve the accuracy of the interpolation methods.

Regarding remote sensing data, the crop coefficient is the highest uncertainty introduced for calculating actual evapotranspiration since it is related directly with reference evapotranspiration according the FAO equation used in this work:

$$ET\ (actual) = ETo \cdot Kc$$

In this study, the evolution of the Kc curves show oscillations with regard to the FAO curves. These oscillations should be studied in futures improvements in order to understand correctly the behaviour of the curve in the presence of, for instance, atypical meteorological factors or different climatic varieties inside the Mediterranean climate. To study these oscillations would be necessary to have available data through different years for comparing among them and to be able to relate correctly each cause with its corresponding effect over the Kc curve.

For future improvements the use of lisimetric measurements would be also necessary in order to validate actual evapotranspiration. Moreover, the use of satellite images of higher resolution would permit to carry out this study with higher accuracy.

7 REFERENCES

Ackerman S, Strabala K, Menzel P, Frey R, Moeller C, Gumley L, Baum B, Seeman SW, Zhang H. (2002). "*Discriminating Clear-Sky from Cloud with MODIS - Algorithm Theoretical Basis Document*" Products: MOD35. ATBD Reference Number: ATBD-MOD-06. http://modis-atmos.gsfc.nasa.gov/MOD35_L2/atbd.html

Aguado, I., Chuvieco, E., Martín, P., Salas, J. (2003). "*Assessment of forest fire danger conditions in southern Spain from NOAA images and meteorological indices"*. International Journal of Remote Sensing, 24 (8): pp 1653-1668.

Allen, R.G., Pereira, S., D. Raes, D. and Smith, M. (1998). "*Crop evapotranspiration"*. FAO Irrigation and Drainage Paper 56. FAO. Roma.

Allen, R.G., Smith, M., Pereira, L.S. and Perrier, A. (1994). "*An update for the calculation of reference evapotranspiration*". Journal of Irrigation and Drainage. Bulletin 43 2, pp. 35-92.

"CMA" Andalusian Department of Environment. http://www.juntadeandalucia.es/medioambiente/site/web/menuitem.fb35c303e9ce92c08d0cfd8760425ea0/?vgnextoid=5849185968f04010VgnVCM1000001625e50aRCRD

"CAP" Andalusian Department of Fish and Agriculture. "*Memoria 2003*". http://www.juntadeandalucia.es/agriculturaypesca/portal/opencms/portal/estudios?entrada=servicios&servicio=851

Bandara, K.M.P.S. (2003). "*Monitoring irrigation performance in Sri Lanka with high-frequency satellite measurements during the dry season"*. Agricultural Water Management 58: 159-170

Barranco, D., Fernández-Escobar, R., Rallo, L. (2004). "*El cultivo del olivo*". Mundi Prensa, Madrid. 5th ed. 701 pp

Bastiaansen, W.G.M., Molden, D.J., Makin, I.W. (2000). "*Remote sensing for irrigated agriculture: examples from research and possible applications"*. Agric. Water Manage. 46: pp 137-155.

Bastiaanssen, W.G.M., Pelgrum, H., Wang, J., Ma, Y., Moreno, J.F., Roerink, G.J. & van der Wal, T. (1998b). "*A remote sensing surface energy balance algorithm for land (SEBAL)"*. II Validation. International Journal of Hydrology 213–229.

Bastiaanssen, W.G.M., Menenti, M., Feddes, R.A. & Holtslag, A.A. (1998a.) "*A remote sensing surface energy balance algorithm for land (SEBAL)"*. International Journal of Hydrology 212-213.

Bastiaanssen, W.G.M., (1996). "*Diagnosis of regional evaporation by remote sensing to support irrigation performance assessment"*. Irrigation and Drainage Systems. 10(1): pp 1-23.

Bausch,W.C. (1995). "*Remote sensing of crop coefficients for improving the irrigation scheduling of corn"*. Agricultural Water Management 27: 55-68.

Bausch, W.C. (1993). "*Soil background effects on reflectance-based crop coefficients for corn"*. Remote Sensing of Environment 46: pp 213-222.

Bausch, W.C. & Neale, C.M.U. (1989). "*Spectral inputs improve corn crop coefficients and irrigation scheduling"*. Transactions of the ASAE 32: pp 1901-1908.

Bailey, J. O. (1990). "*The potential value of remotely sensed data in the assessment of evapotranspiration and evaporation"*. Remote sensing reviews, 4(2): 349–377.

Blaney, H.F. & Criddle, W.D. (1950). "*Determining water requirements in irrigated areas from climatological and irrigation data*". USDA Soil Conserv. Serv. SCS-TP 96. 44 pp.

Boegh, E., Soegaard, H., Thomsen, A., (2002). "*Evaluating evapotranspiration rates and surface conditions using Landsat TM to estimate atmospheric resistance and surface resistance"*. Remote Sensing of Environment 79: 329-343.

Brasa, A. (1997). "*Determinación mediante teledetección de la evapotranspiración en regadíos extensivos*". Tesis doctoral, Universidad de Castilla La Mancha, Cuenca 167 pp.

Brasa, A., Martín de Santa Olalla, F. and Caselles, V. (1996). "*Maximum and actual evapotranspiration for Barley (Hordeum vulgare L.) through NOAA satellite images in Castilla-La Mancha (Spain)"*. J. of Agricultural Engeneering Research, 63 (4): 283-293.

Brutsaert, W. (1984). *"Evaporation into the atmosphere: Theory, history and application"*. Kluwer Academic, Dordrecht, Holland.

Burgan, R. E., and R. A. Hartford. (1993). "*Monitoring vegetation greenness with satellite data"*. INT-297, USDA Forest Service. Intermountain Research Station.

Burman, R.D., Cuenca R.H. and Weiss, A. (1983). "*Techniques for estimating irrigation water requirements*". In Hillel, D. (ed.), Advances in irrigation, 2: pp 335-394. Academic Press, New York.

Burton, T. (2004). "*Wind energy*". John Wiley & Sons Publishers. 617 pp.

Calera, A., Jochum, A.M., Cuesta, A., Montoro, A. and López, P. (2005). "*Irrigation management from space: Towards user-friendly products"*. Irrigation and Drainage Systems 19: 337-353.

Casanova, C. (2006). "*Detección y clasificación de nubes mediante imágenes de satélite"*. Tesis Doctoral. Universidad de Valladolid. 177 pp.

Caselles, V., Artigao, M.M., Hurtado, E., Coll, C. and Brasa, A. (1998). "*Mapping actual evapotranspiration by combining Landsat TM and NOAA-AVHRR images: Application to the Barrax area, Albacete, Spain*". Remote Sensing of Environment 63: pp 1-10.

Caselles, V., and Delegido, K. (1987). "*A simple model to estimate the daily value of the regional maximum evapotranspiration form satellite temperature and Albedo images*". Int. J. Remote Sensing 8: pp 1151-1162.

Chorley, R.J. (1969). "*Introduction to Physical Hydrology*". University Paperbacks. London. 211 pp.

Choudhury, B.J., Ahmed, N.U., Idso, S.B., Reginato, R.J. & Daughtry, C.S.T. (1994). "*Relations between evaporation coefficients and vegetation indices studies by model simulations"*. Remote Sensing of Environment 50: pp 1-17.

Choudhury, B. J. (1989). "*Estimating evaporation and carbon assimilation using infrared temperature data: vistas in modelling*" Theory and applications of optical remote sensing, John Wiley & Sons. New York: pp 628–690.

Choudhury, B., Monteith, J. (1988). "*A four-layer model for the heat budget of homogeneus land surfaces"*. Quarterly Journal of the Royal Meteorological Society, 114: pp 373-398.

Chuvieco, E., Aguado, I., Cocero, D., Riaño, D. (2003). "*Design of an empirical index to estimate fuel moisture content from NOAA-AVHRR images in forest fire danger studies*". International Journal of Remote Sensing, 24 (8): pp 1621-1637.

Cleugh, H.A., Leuning, R., Mu, Q. and Running S. W. (2007). "*Regional evaporation estimates from flux tower and MODIS satellite data"*. Remote Sensing of Environment 106: pp 285-304.

Consoli, S., D'Urso, G., Toscazo, A. (2006). "*Remote sensing to estimate ET-fluxes and the performance of an irrigation district in southern Italy"*. Agricultural Water Management 81: pp 295–314.

Courault, D., Seguin, B. and Olioso, A. (2003). "*Review to estimate evapotranspiration from remote sensing data: Some examples from the simplified relationship to the use of mesoscale atmospheric models*". Proc Int. Workshop on Use of Remote Sensing of Crop Evapotranspiration for Large Regions. 54th IEC Meeting of the International Commission on Irrigation and Drainage (ICID). Montpellier, France, pp 11.

De Juan, J. A., Martín de Santa Olalla, F. (1993). "*El estrés hídrico en las plantas*". Agronomía del Riego, Ed. Mundi-Prensa-Universidad de Castilla-La Mancha, Madrid: pp 125-238.

Dingman, L. (2002). "*Physical hydrology*". Prentice Hall, second edition, New Jersey, United State of America, 644 pp.

Doorenbos, J., Kassam, A., (1986). "*Efectos del agua sobre el rendimiento de los cultivos"*. Estudios FAO Serie riego y drenaje 33, Roma, 212 pp.

Doorenbos J. & W.O Pruitt. (1977). "*Crop water requirements"*. FAO Irrigation and Drainage Paper No 24. Rome, Italy.

Duchemin, B., Hadria, R., Erraki, S., Boulet, G., Maisongrande, P., Chehbouni, A., Escadafal, R., Ezzahar, J., Hoedjes, J. C. B., Kharrou, M. H., Khabba, S., Mougenot, B., Olioso, A., Rodriguez, J. C. and Simmoneaux, V. (2006). "*Monitoring wheat phenology and irrigation in Central Morocco: On the use of relationships between evapotranspiration, crops coefficients, leaf area index and remotely-sensed vegetation indices*". Agricultural Water Management, 79: pp 1-27.

Eidenshink, J. C., Burgan, R.E. and Haas, R.H. (1990). "*Monitoring fire fuels condition by using time series composites of Advanced Very High Resolution Radiometer (AVHRR) data*". P. Resource, Ed. Washington DC: pp 68-82.

Elias F., Castellvi F. *et al.* (1996). "*Agrometeorología"*. MAPA-Mundi-Prensa. Madrid.

EUM TD 07 (2001). "*Meteosat Second Generation: System Overview*". Issue 1.1.

EUM TD 15 (2006). "*EUMETCast- EUMETSAT´s Broadcast System for Environmental Data. Technical Description*". EUMETSAT, Issue: v4. Darmstadt, Germany. 45 pp.

Felicísimo, A.M, Morán, R., Sánchez J.M., Pérez, D. (2001). "*Elaboración del Atlas climático de Extremadura mediante un sistema de información geográfica*". GeoFocus, 1: 17-23.

"FENACORE" Federación Nacional de Comunidades de Regantes de España (2005). "*Dossier corporativo"*. http://www.fenacore.org

Fernández, R., Ávila, R., López, M., Gavilán, P., Oyonarte, N.A. (2006). "*Fundamentos del riego*". Junta de Andalucía. Consejería de Agricultura y Pesca.

Gabban, A., San-Miguel-Ayanz, J., Barbosa, P., Libertà, G. (2006). "*Análisis of NOAA-AVHRR NDVI inter-annual variability for forest FIRE risk estimation*". International Journal of Remote Sensing, 27 (8): pp 1725-1732.

Gavilán, P. and Berengena, J. (2000). "*Comportamiento de los métodos Penman-FAO y Penman- Monteith FAO en el Valle medio del Guadalquivir"*. Proc. del XVIII Congreso Nacional de Riegos, Huelva, Spain.

Hardy, C.C., Burgan, R.E., Ottmar, R.D. (2000). "*A database for spatial assessments of fire characteristics, fuel profiles, and PM10 emissions*". Journal of Sustainable Forestry, 11 (1-2): pp 229-244.

Hargreaves, G.H., and Samani, Z. A. (1985). "*Reference crop evapotranspiration from temperature.*" Applied Engrg. In Agric., 1(2): pp 96-99.

Heilman, J.L., Heilman, W.E. & Moore, D.G. (1982). "*Evaluating the crop coefficient using spectral reflectance".* Agricultural Journal 74: pp 967–971.

Howell, T.A., S.R. Evett, A.D. Schneider, R.W. Todd, and J.A. Tolk. (1998). "*Evapotranspiration of irrigated fescue grass in a semi-arid environment*". ASAE Paper no. 982117.

Humes, K. S., Kustas, W. P. and Moran, M. S. (1994). "*Use of remote sensing and reference site measurements to estimate instantaneous surface energy balance components over a semiarid rangeland watershed*". Water Resources Research, 30 (5): pp 1363-1374.

Hupet, F., Vanclosooster, M. (2001). "*Effect of the sampling frequency of meteorological variables on the estimation of the reference evapotranspiration*". Journal of Hydrology, 243: pp 192-204.

Hurtado, E., Caselles, V. and Artigao, M. (1995). "*Estimating corn evapotranspiration from NOAA-AVHRR data in the Albacete area*". International Journal of Remote Sensing, 10: pp 2023–2037.

Idso, S. B., Schmugge, T. J., Jackson, R. D. and Reginato, R. J. (1975). "*The utility of surface temperature measurements for remote sensing of soil water studies*". Journal of Geophysical Research, 80 (21): pp 3044-3049.

"Inventory and Characterization of Andalusian irrigated lands" (2003). Andalusian Department of Fish and Agriculture (CD-ROM).

"Inventory and Characterization of Andalusian irrigated lands" (1999). Andalusian Department of Fish and Agriculture (CD-ROM).

Jackson, R. D., Reginato, R. J. and Idso, S. B. (1977). "*Wheat canopy temperature: A practical tool for evaluating water requirements*". Water Resources Research,13: pp 651-656.

Jensen M. E., Burman R. D., Allen R. G., (1990). "*Evapotranspiration and irrigation water requirements"*. ASCE Manual N° 70, 332 pp.

Jensen, M. E., (1974). "*Consumptive use of water and irrigation water requirements"*. Rep. Tech. Com. on Irrig. Water Requirements, Irrigation and Drainage Division, American Society of Civil Engineers, 227 pp.

Jensen, M.E., and Erie, L.J. (1971)."*Irrigation and water management*". In Johnson, R.T., *et al.* (eds.). Advances in sugarbeet production, Iowa State University Press. pp 189-222.

Joaquín Díez-Cascón Sagrado. (2003). "*Las presas en el siglo XXI"*. Ingeniería y territorio, ISSN 1695-9647 (62), pp.4-9.

Kimes, D. S., and Sellers, P. (1985). "*Inferring hemispherical reflectance of the Earth's surface for global energy budgets from remotely sensed nadir or directional radiance values*". Remote Sensing of Environonment 18: pp 205–223.

King, M.D., Closs, J., Spangler, S., Greenstone, R., Wharton, S. and Myers, M. (2000). "*EOS Data Products Handbook".* Vol.1 (revised). January 2004. EOS Project Science Office, Maryland.

Kustas, W. P., Norman, J. M. (1996). "*Use of remote sensing for evapotranspiration monitoring over land surfaces*". Hydrological Sciences. Journal des Sciences Hydrologiques 41: pp. 495-516.

Kustas, K. P., Perry, E. M., Doraiswamy, P. C. and Moran, M. S. (1994). "*Using satellite remote sensing to extrapolate evapotranspiration estimates in time and space over a semiarid rangeland basin*". Remote Sensing of Environment, 49: pp 275–286.

Kustas, W. (1990). "*Estimate of evapotranspiration with a one and two layer model of heat transfer over partial canopy cover"*. Journal of Applied Meteorology, 29: pp 704-715.

Liang, S., Chad J. Shuey, Andrew L. Russ, Hongliang Fang, Mingzhen Chen, Charles L. Walthall, Craig S.T. Daughtry, Raymond Hunt Jr. (2002). "*Narrowband to broadband conversions of land surface albedo: II.Validation"*. Remote Sensing of Environment 84: pp 25-41.

Lillesand, T.M and R.W. Kiefer, (2000). "*Remote Sensing and Image Interpretation*". 4th Ed.: John Wiley & Sons, Inc., New York.

López-Urrea, R, Martín de Santa Olalla, F., Fabeiro, C. and Moratalla, A. (2006*). "An evaluation of two hourly reference evapotranspiration equations for semiarid conditions"*. Agricultural water management 86: pp 277-282.

Lutgens, F.K., Tarbuck, E. (1998) "*The atmosphere: an introduction to meteorology*". Prentice- Hall Publishers. 7th Ed. 434 pp.

"MAPA" Spanish Ministry of Agriculture, Fishing and Feeding (2004). "*Hechos y cifras de la agricultura, la pesca y la alimentación en España".* http://www.mapa.es/es/ministerio/pags/hechoscifras/introhechos.htm

Mckenney, M., Rosenberg, N. (1993). "*Sensitivity of some potential evapotranspiration estimation methods to climate change*". Agricultural and Forest Meteorology, 64: 81-110.

Menenti, M., Jia, L. and Su, Z. (2003). "*On SEBI-SEBS validation in France, Italy, Spain, USA and China*". Proc Int. Workshop on Use of Remote Sensing of Crop Evapotranspiration for Large Regions. 54th IEC Meeting of the International Commission on Irrigation and Drainage (ICID). Montpellier, France, pp 10.

Meteosat Second Generation. "*MSG System Overview*" Eumetsat. EUM TD 07 - Issue 1.1 (2001)
http://www.eumetsat.int/groups/ops/documents/document/pdf_td07_msg.pdf

"MMA" Spanish Ministry of Environment (2005). "*Anticipar, mitigar, educar"*. Revista Ambienta. Octubre 2005. Nº 48.
http://www.mma.es/portal/secciones/biblioteca_publicacion/publicaciones/revista_ambienta/n48/index.htm

"MMA" Spanish Ministry of Environment "*Informe de Sequía"*.
http://www.mma.es/secciones/medios_comunicacion/prensa/notas_pre/2005/06/pdf/Informesequiajunio05.pdf

Monteith, J.L., and M.H. Unsworth. (1990). "*Principles of environmental physics*". 291 pp. Edward Arnold, London, England.

Moran, M. S. and Jackson, R. D. (1991). "*Assessing the spatial distribution of evapotranspiration using remotely sensed inputs*". J. Environm. Qual., 20: pp 725-737.

Moran, M.S., Inoue, Y., Barnes, E.M. (1997). "*Opportunities and limitations for image-based remote sensing in precision crop management*". Remote Sensing of Environment, 61: pp 319-346.

Naredo J.M. and Gascó J.M. (1996) "*Spanish Water Accounts"*. MOPTMA-Dirección General de calidad de aguas.

Neale, C.M.U., Bausch, W.C. & Heerman, D.F. (1989). "*Development of reflectance-based crop coefficients for corn"*. Transactions of the *ASAE* 32: pp 1891–1899.

Neale, C., Jayanthi, H.&Wright, J.L. (2005). "*Irrigation water management using high resolution airborne remote sensing"*. Irrigation and Drainage Systems 19(3/4): 321–336.

Ninyerola, M., Pons, X., Roure, J.M. (2005). "*Atlas Climático Digital de la Península Ibérica. Metodología y aplicaciones en bioclimatología y geobotánica*". Universidad Autónoma de Barcelona, Bellaterra.

Oldford, S., Leblon, B., Maclean, D., Flannigan, M. (2006). "*Predicting slow-drying fire weather index fuel moisture codes with NOAA-AVHRR images in Canada´s northern boreal forests*". International Journal of Remote Sensing, 27 (18): pp 3881-3902.

Observatorio Nacional de la sequía (2005).(ONS)
http://www.mma.es/portal/secciones/acm/aguas_continent_zonas_asoc/ons/index.htm

Olioso, A., Chauki, H., Courault, D. and Wigneron, J. P. (1999). "*Estimation of evapotranspiration and photosynthesis by assimilation of remote sensing data in SVAT models*". Remote Sensing of Environment, 68: pp 341–356.

Orgaz, F. y Fereres. (1999). "*Cultivo del Olivo*". Ed. Mundi-Prensa. Madrid, pp 267-288.

Otterman, J., and Tucker, C. J. (1985). "*Satellite measurements of surface albedo and temperature in semi-desert*". J. Clim. Appl. Meteorol. 24: pp 228–235.

Parkinson, C.L. and Greenstone, R. (2000). "*EOS Data Product: Handbook*" . Volume 2. NASA Goddard Space Flight Center, Greenbelt, Maryland. 252 pp.

Penman, H. L. (1948). "*Natural evaporation from open water, bare soil and grass*". Proceeding Royal Society London 193: pp 120-145.

Priestley, C., Taylor, R., (1972). "*On the assessment of surface heat flux and evaporation using large-scale parameters"*. Monthly Weather Review, 100(2): pp 81-92.

Rivas, R. and Caselles, V. (2004). "*A simplified equation to estimate spatial reference evaporation from remote sensing-based surface temperature and local meteorological data"*. Remote Sensing of Environment 93: pp 68-76.

Rossi, S., Gomarasca, M.A., Bocchi1, S., Rampini, A. (2006*). "Monitoring crop evapotranspiration with time series of MODIS satellite data in Northern Italy"*. 26th EARSeL Symposium, Warsaw (Poland).

Sánchez, M.L., García, M.A., Calle, A. (1994). "*Characterization of wind fields at a regional scale calculated by means of a diagnostic model using multivariate techniques*". Computer Simulation. Air Pollution II, 1: pp 57-64. Computational Mechanics Publications.

Sánchez-Toribio, M.I. (1992). "*Métodos para el estudio de la evaporación y la evapotranspiración*"**.** Ingeniería del Agua**.** Vol.6 (1).pp 63-68.

Sakhnovich, L.A. "*Interpolation theory and its applications*". Kluwer Academic Publishers, Dordrecht, Holland 1997. 1st ed. 197 pp.

Schmugge, T., French, A., Kustas, W. (2001). "*Evapotranspiration estimates using ASTER thermal infrared imagery"*. In: Proc. of SPIE EurOpto 8th Int. Symp. on Remote Sensing, Toulouse, France, 45.

Seen, D. L., Mougin, E., Rambal, S., Gaston, A. and Hiernaux, P. (1995). "*A regional sahelian grassland model to be coupled with multispectral satellite data: II toward the control of its simulation by remotely sensed indices*" Remote Sensing of Environment, 52: pp 194-206.

Seguin, B., Assad, E., Fretaud, J. P., Imbernon, J., Kerr, Y. and Lagouarde, J. P. (1989). "*Use of meteorological satellites for water balance monitoring in Sahelian regions*". International Journal of Remote Sensing, 10(6): pp 1101–1117.

Su, Z. (2002a). "*The surface energy balance system (SEBS) for estimation of turbulent heat fluxes"*. Hydrology and Earth System Sciences 6: pp 85–99.

Stewart, J.B. (1883). "*A discussion of the relationships between the principal forms of the combination equation for estimating crop evaporation*". Agric. Meteorol., 30, 111-127.

Tasumi, M., Trezza, R., Allen, R. G. and Wright, J. L. (2003). "*U.S. Validation tests on the SEBAL model for evapotranspiration via satellite*". Proc Int. Workshop on Use of Remote Sensing of Crop Evapotranspiration for Large Regions. 54th IEC Meeting of the International Commission on Irrigation and Drainage (ICID). Montpellier, France, pp 13.

Thornthwaite, C.W., (1948). "*An approach toward a rational classification of climate*". Geographical Review, 38: pp 55-94.

Turc, L., (1961). "*Estimation of irrigation water requirements, potential evapotranspiration: a simple climatic formula evolved up to date".* Annals of Agronomy, 12: pp 13-14.

Ventura, F., Spano, D., Duce, P. and Snyder, R. L. (1999). "*An evaluation of common evapotranspiration equations"*. Irrigation Science 18: pp 163-170.

Vicente-Serrano, S.M, Saz-Sánchez, M.A, Cuadrat, JM. (2003). "*Comparative analysis of interpolation methods in the middle Ebro Valley (Spain): application to annual precipitation and temperature*". Climate Research, 24: 161-180 pp.

Wang, L., Sousa, W.P., Gong, P., Binging, G.S., (2004). "*Comparison of IKONOS and Quick Bird images for mapping mangrove species on Caribbean coast of Panama"*. Remote Sensing Environ. 91: pp 432-440.

Wang, S., Grant, R.F., Verseghy, D.L. and Black, T.A. (2001). "*Modelling plant carbon and nitrogen dynamics of a boreal aspen forest in CLASS-the Canadian Land Surface Scheme*", *Ecol. Model.* 142: pp. 135-154.

Weng D, Sun Z. (1984). "*A preliminary study of the lapse rate of surface air temperature over mountainous regions of China*". Geographical Research 3 (2): pp 24-34.

Willmott, C.J., Matsuura, K. (2006). "*On the use of dimensioned measures of error to evaluate the performance of spatial interpolators*". International Journal of Geographical Information Science, 20 (1): pp 89-102.

Willmott, C.J., Matsuura, K. (1995). "*Smart interpolation of annually averaged air temperatura in the United States*". Journal of Applied Meteorology, 34: pp 2577-2586.

World Meteorological Organization (1997) "*Guide to meteorological instruments and methods of observation*" 6th Ed. http://www.wmo.int

Websites cited in the text

URL-1: Andalusian Department of Environment (CMA).
http://www.juntadeandalucia.es/medioambiente/web/Bloques_Tematicos/Publicaciones_Divulgacion_Y_Noticias/Publicaciones_Periodicas/IMA/2005/pdfs/007_Capitulo_02_Clima.pdf

http://www.juntadeandalucia.es/medioambiente/site/web/menuitem.fb35c303e9ce92c08d0cfd8760425ea0/?vgnextoid=5849185968f04010VgnVCM1000001625e50aRCRD

URL-2: Andalusian Department of Fish and Agriculture (CAP):
http://www.juntadeandalucia.es/innovacioncienciayempresa/ifapa/ria/servlet/FrontController

http://www.juntadeandalucia.es/agriculturaypesca/portal/opencms/portal/estudios?entrada=servicios&servicio=851

URL-3: EUMETSAT:
http://www.eumetsat.int/Home/Main/Access_to_Data/Meteosat_Image_Services/SP_1123237865326

URL-4: Local Government of Castilla y León.
http://www.jcyl.es:8080/ora_riac/plsql/Proc_MuestraRecProv1?PROVINCIA=24&RIEGO=0#

URL-5: NASA.
http://modis-atmos.gsfc.nasa.gov/MOD35_L2/atbd.html

URL-6: National Institute of Meteorology (INM).
www.inm.es

URL-7: Spanish Federation of Irrigation Communities (FENACORE).
http://www.fenacore.org

URL-8: Spanish Ministry of Agriculture (MA).
http://www.mapa.es/es/ministerio/pags/hechoscifras/introhechos.htm

URL-9: Spanish Ministry of Environment (MMA)
http://www.mma.es/secciones/medios_comunicacion/prensa/notas_pre/2005/06/pdf/Informesequiajunio05.pdf

URL-10: Spanish Ministry of Environment (MMA)
http://www.mma.es/portal/secciones/biblioteca_publicacion/publicaciones/revista_ambienta/n48/index.htm

URL-11: Spanish Observatory of the Drought. (ONS).
http://www.mma.es/portal/secciones/acm/aguas_continent_zonas_asoc/ons/index.htm

URL-12: University of Castilla la Mancha.
http://crea.uclm.es/crea/index.htm

URL-13: World Meteorological Organization (WMO)
http://www.wmo.int

8 APPENDICES

➢ APPENDIX I – CHARACTERISTICS OF MODIS AND SEVIRI SENSORS

Some general information about bands contained in the MODIS-TERRA and SEVIRI-MSG sensors are summarized in Tables 8 and 9.

PRIMARY USE	BAND	BANDWIDTH	RESOLUTION (m)
Land/Cloud/Aerosols Boundaries	1	620 – 670 nm	250
	2	841 – 876 nm	250
Land/Cloud/Aerosols Properties	3	459 – 479 nm	500
	4	545 – 565 nm	500
	5	1230 – 1250 nm	500
	6	1628 – 1652 nm	500
	7	2105 – 2155 nm	500
Ocean Color/ Phytoplankton/ Biogeochemistry	8	405 – 420 nm	1000
	9	438 – 448 nm	1000
	10	483 – 493 nm	1000
	11	526 – 536 nm	1000
	12	546 – 556 nm	1000
	13	662 – 672 nm	1000
	14	673 – 683 nm	1000
	15	743 – 753 nm	1000
	16	862 – 877 nm	1000
Atmospheric Water Vapor	17	890 – 920 nm	1000
	18	931 – 941 nm	1000
	19	915 – 965 nm	1000
Surface/Cloud Temperature	20	3.660 – 3.840 μm	1000
	21	3.929 – 3.989 μm	1000
	22	3.929 – 3.989 μm	1000
	23	4.020 – 4.080 μm	1000
Atmospheric Temperature	24	4.433 – 4.498 μm	1000
	25	4.482 – 4.549 μm	1000
Cirrus Clouds Water Vapor	26	1.360 – 1.390 μm	1000
	27	6.535 – 6.895 μm	1000
	28	7.175 – 7.475 μm	1000
Cloud Properties	29	8.400 – 8.700 μm	1000
Ozone	30	9.580 – 9.880 μm	1000
Surface/Cloud Temperature	31	10.780 – 11.280 μm	1000
	32	11.770 – 12.270 μm	1000
Cloud Top Altitude	33	13.185 – 13.485 μm	1000
	34	13.485 – 13.785 μm	1000
	35	13.785 – 14.085 μm	1000
	36	14.085 – 14.385 μm	1000

Table 8. MODIS spectral bands (Lillesand and Kiefer, 2000).

PRYMARY USE	CHANNELS	NOMINAL SPECTRAL BAND	RESOLUTION
Cloud detection, scene identification, cloud tracking, aerosol observation, vegetation monitoring.	VIS 0.6	0.56 - 0.71 μm	3 km
Cloud detection, scene identification, cloud tracking, aerosol observation, vegetation monitoring.	VIS 0.8	0.74 - 0.88 μm	3 km
Discriminates between snow and cloud, ice and water clouds. Aerosol information.	IR 1.6	1.50 - 1.78 μm	3 km
Low cloud and fog detection, measurement of land and sea surface temperature.	IR 3.9	3.48 - 4.36 μm	3 km
Discriminates between snow and cloud, ice and water clouds.	IR 8.7	8.30 - 9.10 μm	3 km
Measurement of earth surface and cloud top temperatures. Detection of cirrus and inference of total precipitable WV over sea.	IR 10.8	9.80 - 11.80 μm	3 km
Measurement of earth surface and cloud top temperatures. Detection of cirrus and inference of total precipitable WV over sea.	IR 12.0	11.00 - 13.00 μm	3 km
Water vapour channel	WV 6.2	5.35 - 7.15 μm	3 km
Water vapour channel	WV 7.3	6.85 - 7.85 μm	3 km
Ozone absorption channel	IR 9.7	9.38 - 9.94 μm	3 km
CO_2 absorption channel	IR 13.4	12.40 - 14.40 μm	3 km
Broadband visible channel	HRV	0.5 - 0.9 μm	1 km

Table 9. SEVIRI spectral bands (EUMETSAT website).

➢ APPENDIX II – INTERPOLATED MAPS

In this appendix are shown some examples of interpolated maps obtained through the selected spatial interpolators.

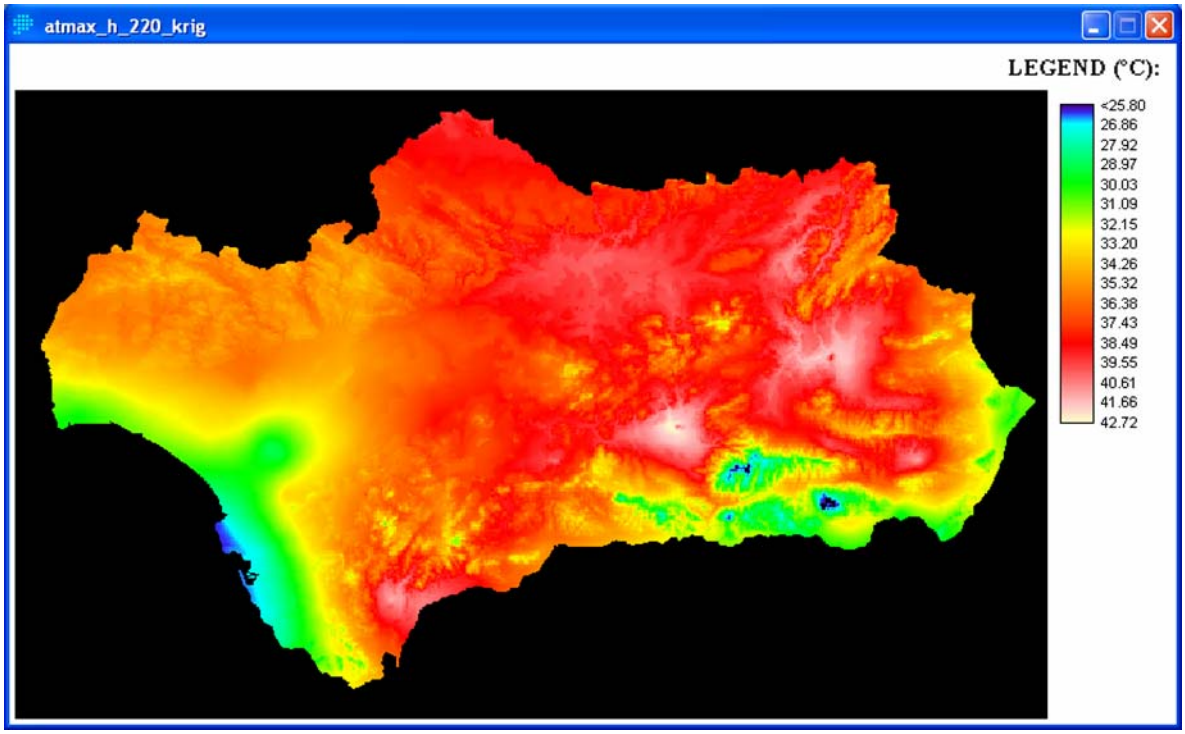

Figure 33. Interpolated map of maximum air temperature obtained by means of kriging method and height correction.

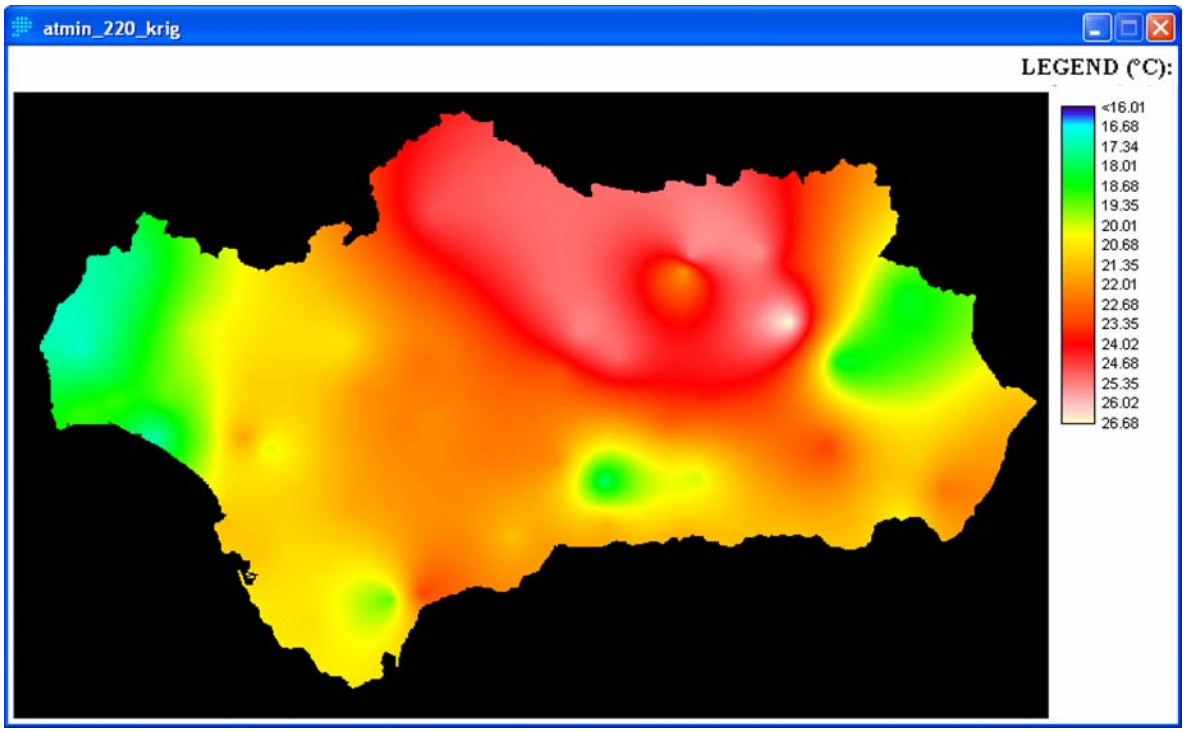

Figure 34. Interpolated map of minimum air temperature obtained by means of kriging method.

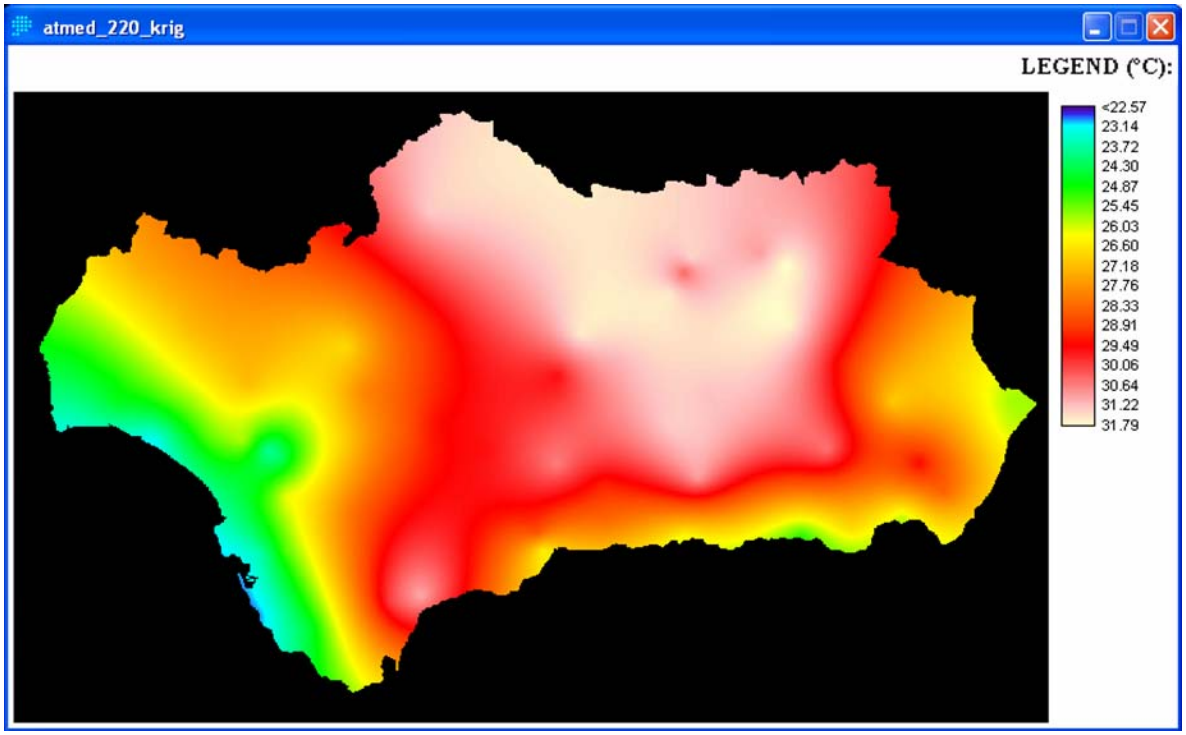

Figure 35. Interpolated map of mean air temperature obtained by means of kriging method.

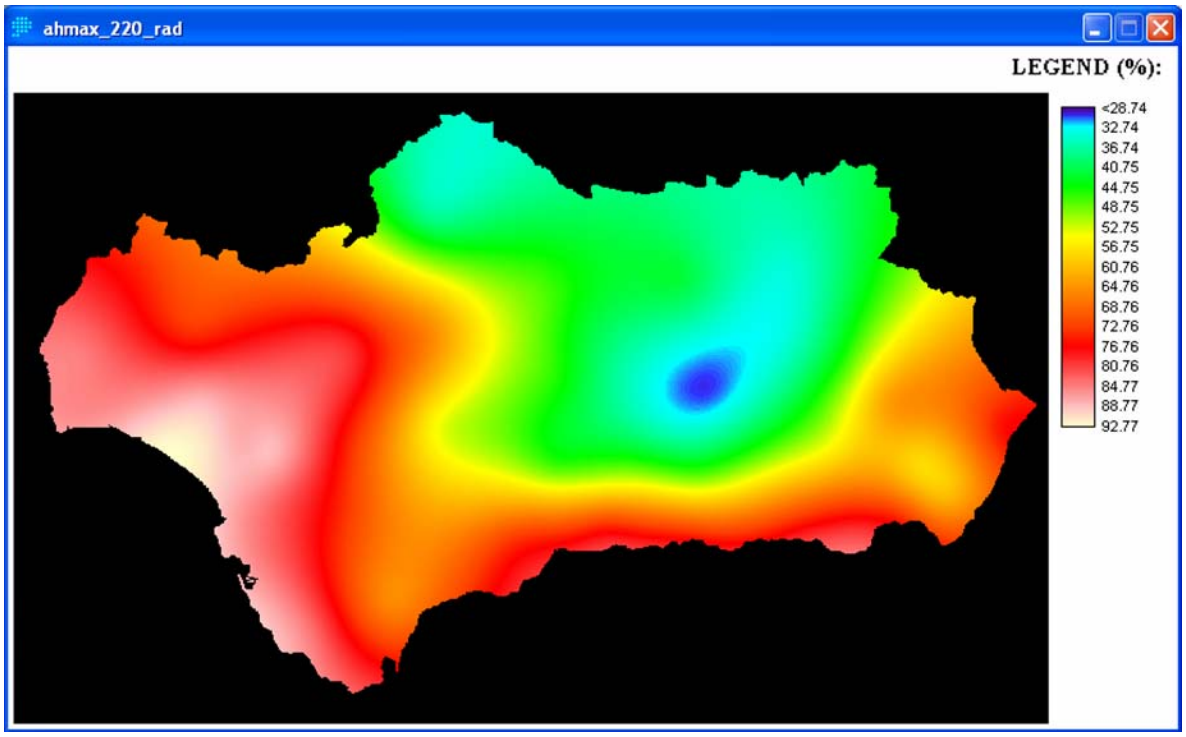

Figure 36. Interpolated map of maximum relative humidity obtained by means of inverse distance to a power method.

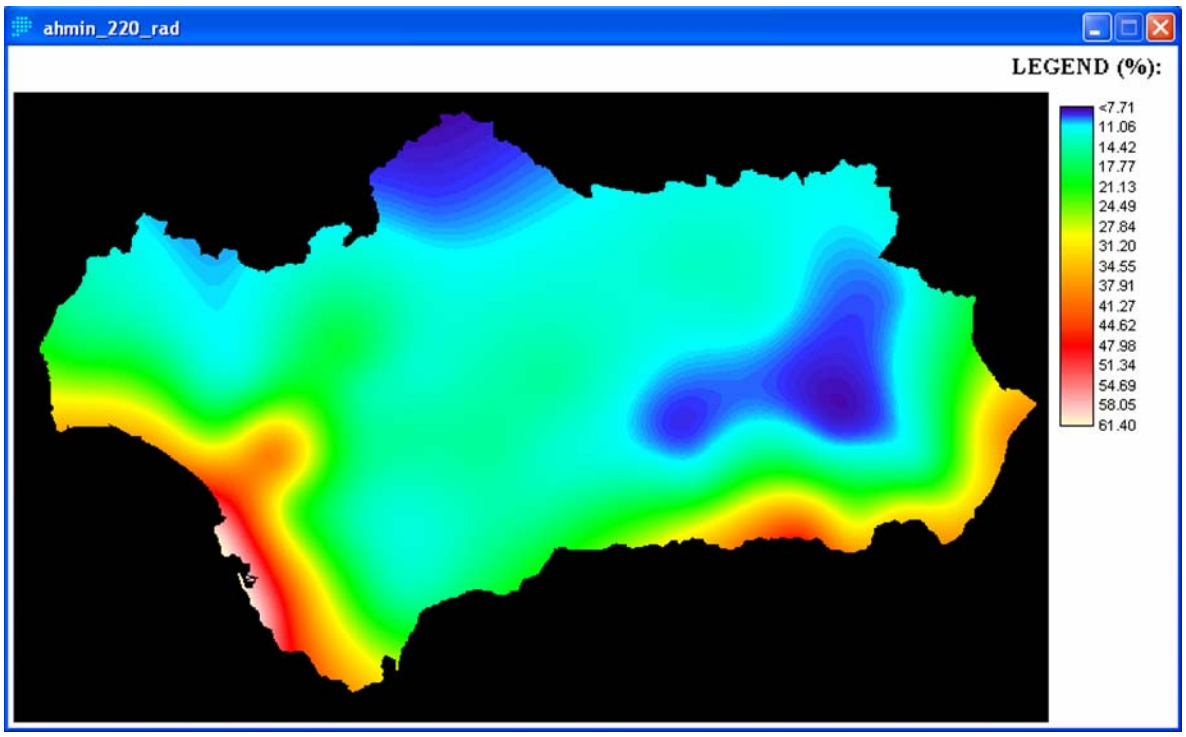

Figure 37. Interpolated map of minimum relative humidity obtained by means of radial basis method.

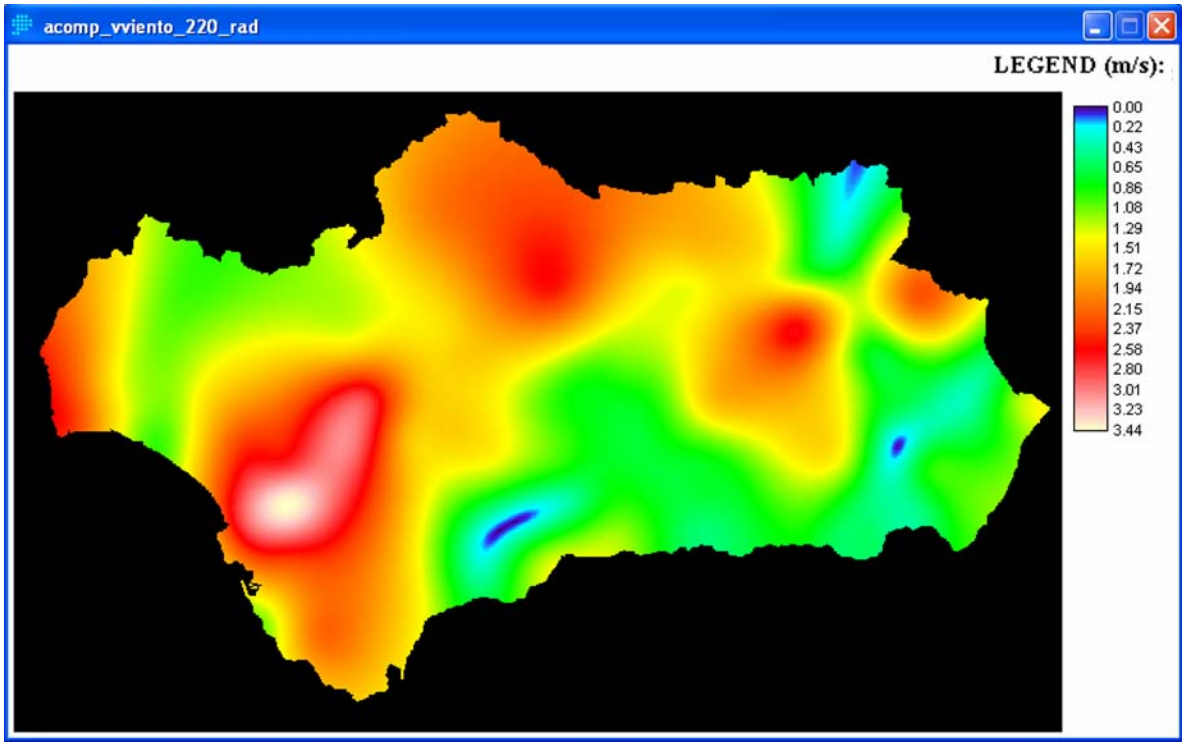

Figure 38. Interpolated map of wind velocity obtained by means of radial basis method and decomposition of wind components.

➢ APPENDIX III – REFERENCE AND ACTUAL EVAPOTRANSPIRATIONS MAPS

Here are shown some examples of reference and actual evapotranspiration maps obtained by means of the methodology proposed in this thesis.

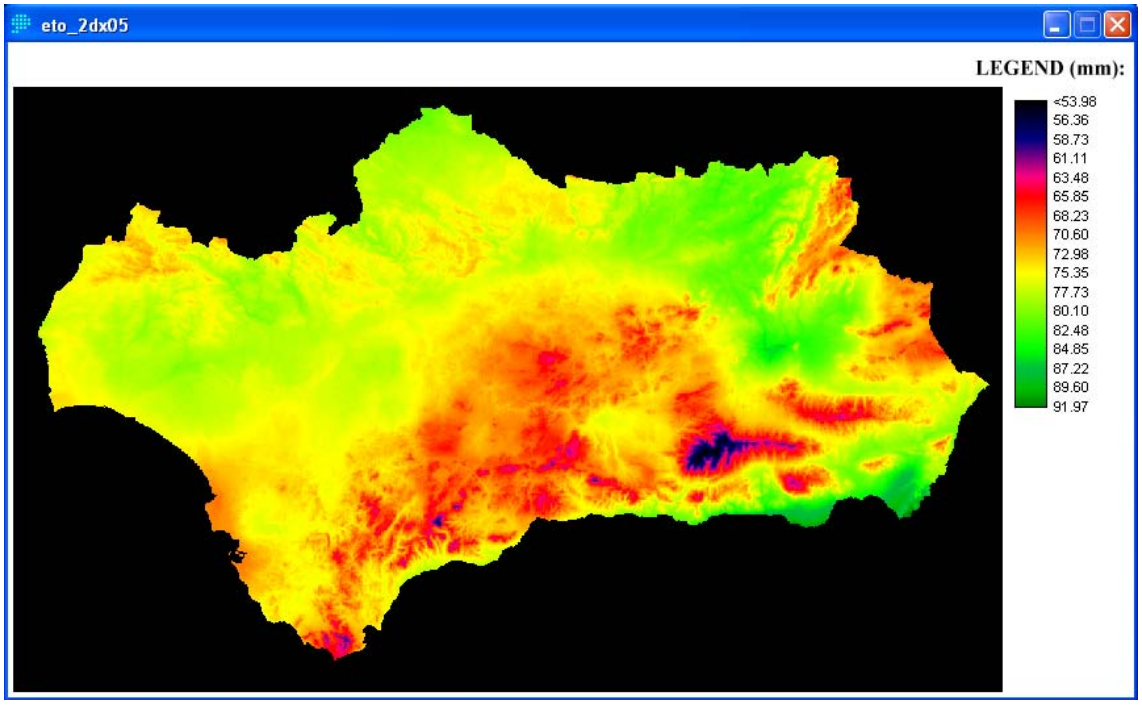

Figure 39. Reference evapotranspiration accumulated through the second tenth of 2005.

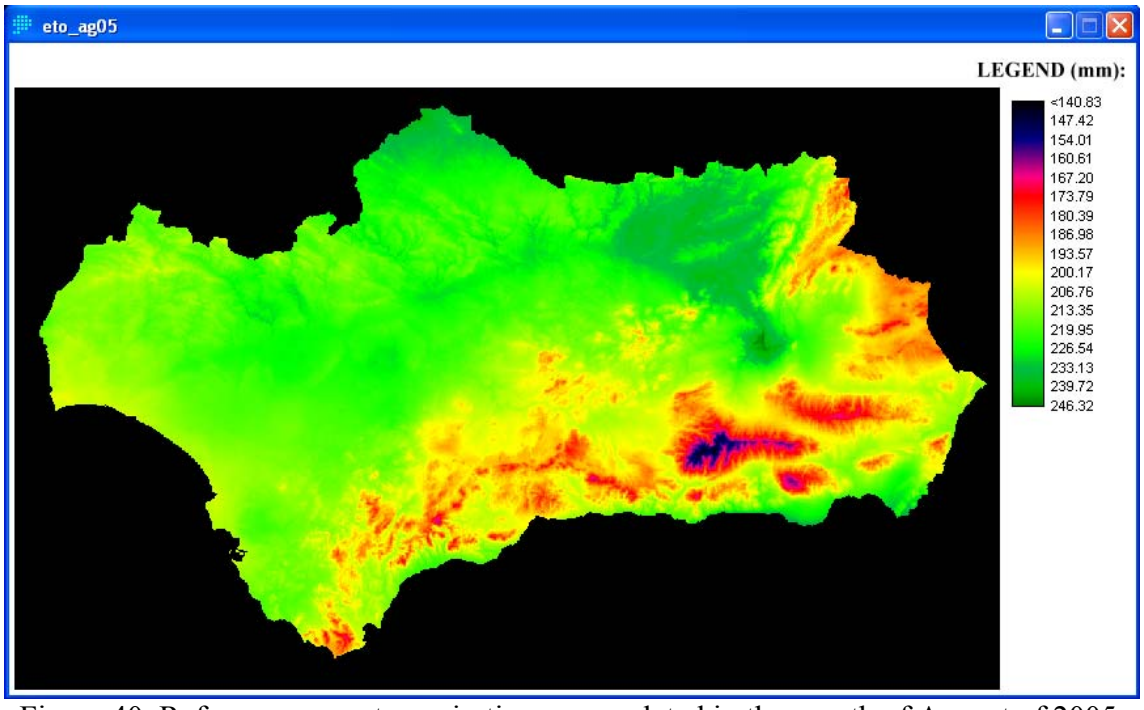

Figure 40. Reference evapotranspiration accumulated in the month of August of 2005.

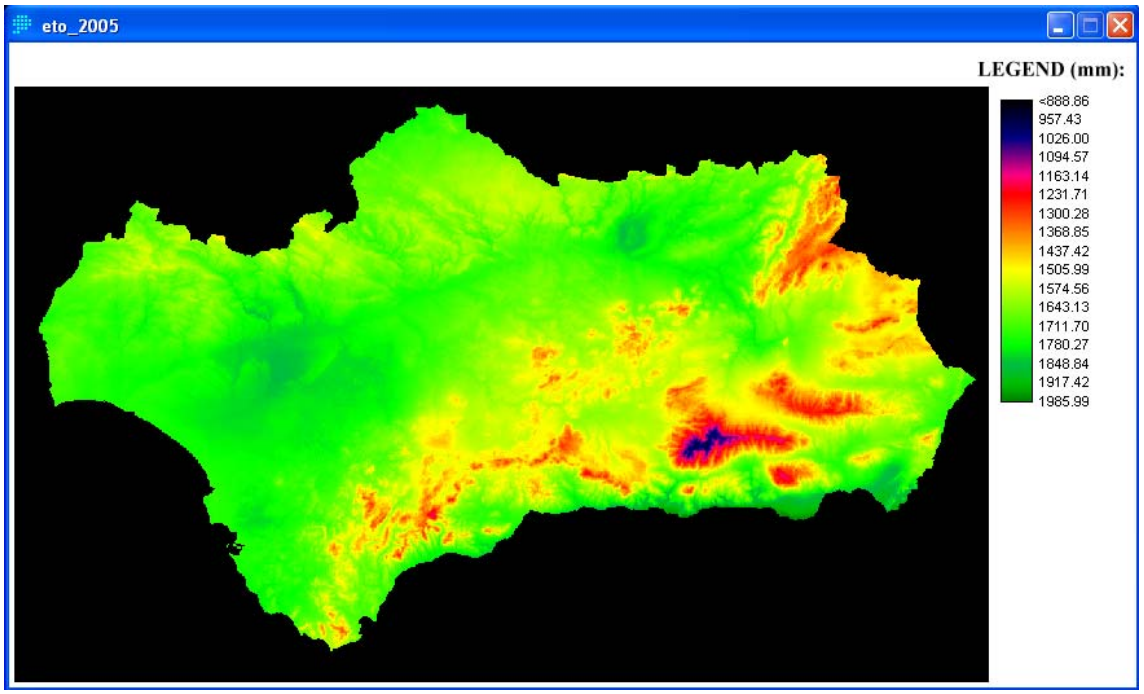

Figure 41. Reference evapotranspiration accumulated in the year 2005.

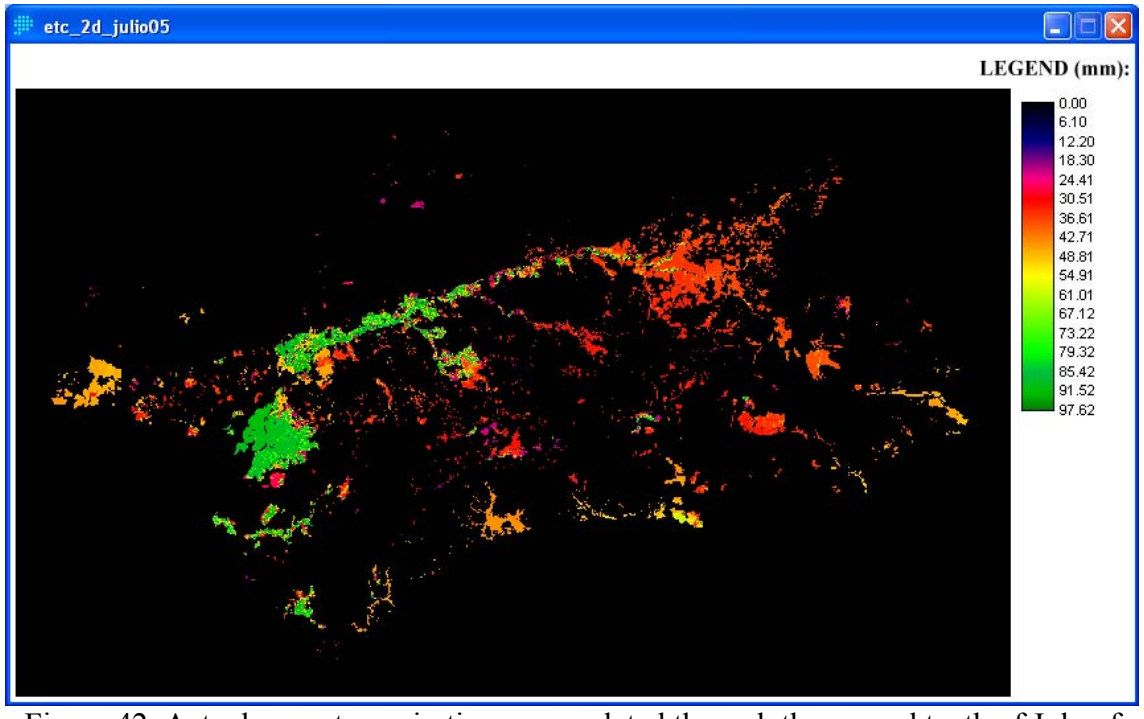

Figure 42. Actual evapotranspiration accumulated through the second tenth of July of 2005.

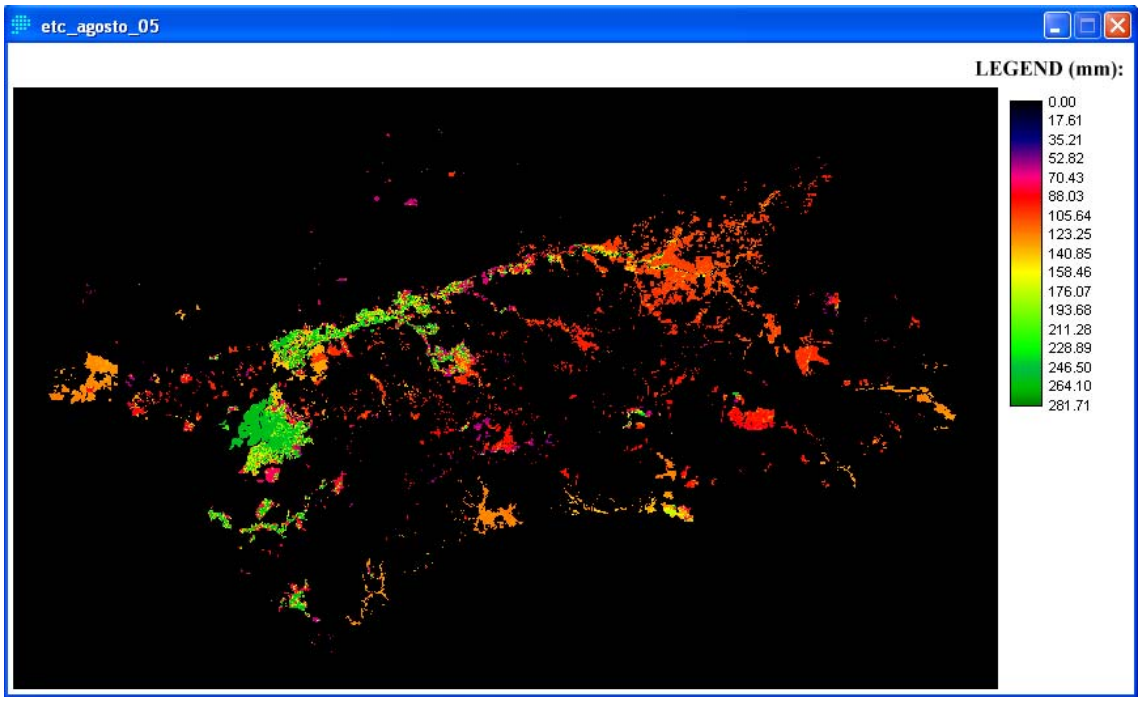

Figure 43. Actual evapotranspiration accumulated in the month of August of 2005.

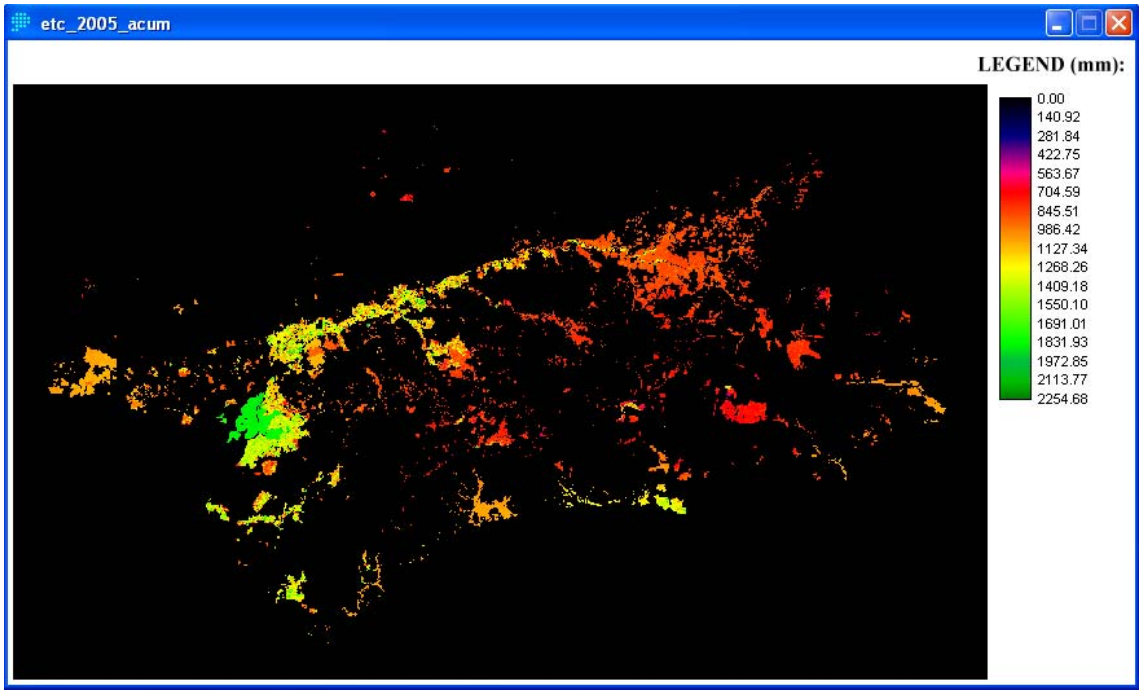

Figure 44. Actual evapotranspiration accumulated in the year 2005.

➢ APPENDIX IV – CROP CEFFICIENT CURVES

Comparisons between Kc curves obtained by means of our model and the ones established by FAO for the some of the selected crops are presented in this Appendix.

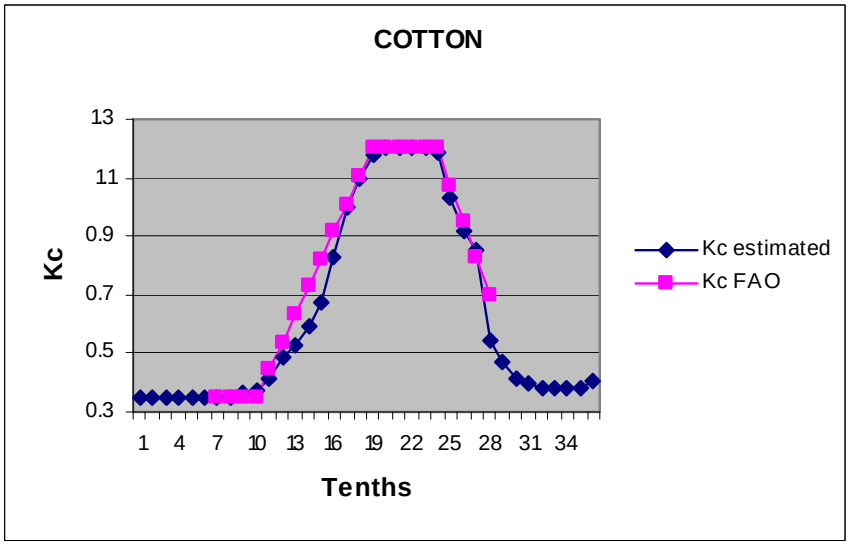

Figure 45. Evolution of cotton Kc through the year 2005.

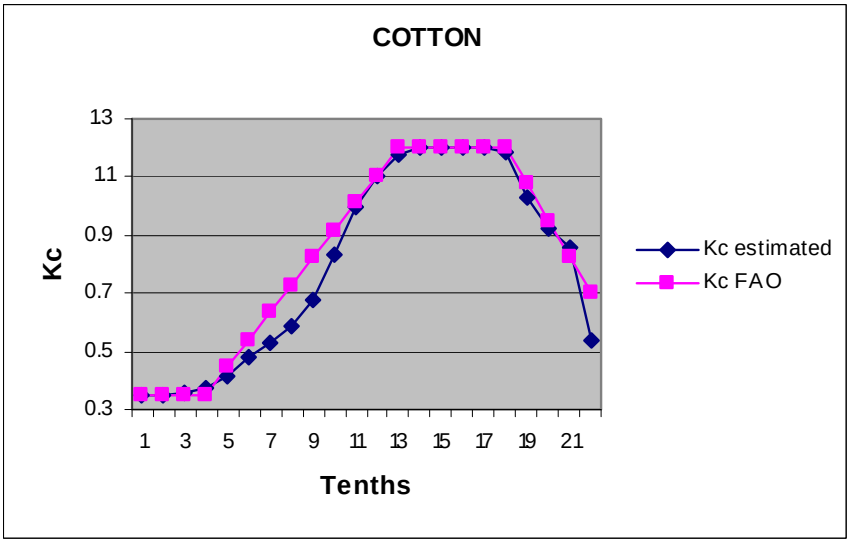

Figure 46. Kc curves in the growing period (from March to October).

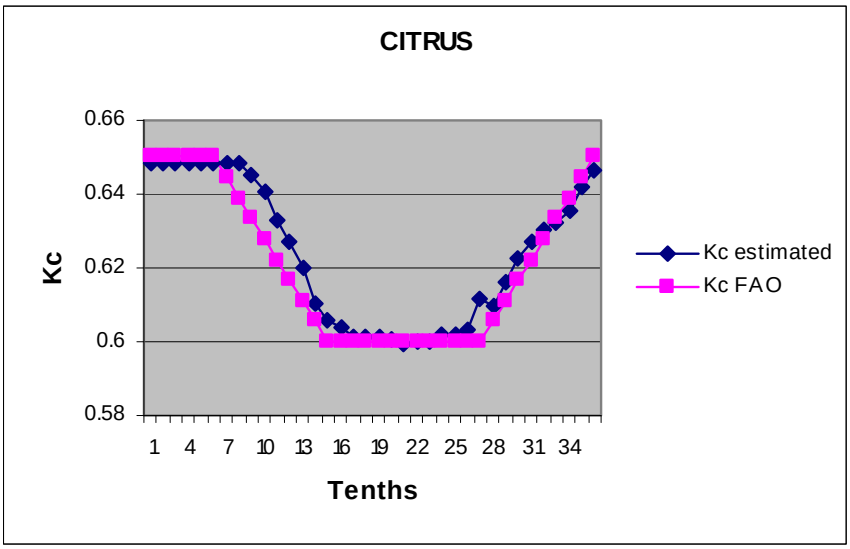

Figure 47. Evolution of citrus Kc through the year 2005 (growing period from January to December).

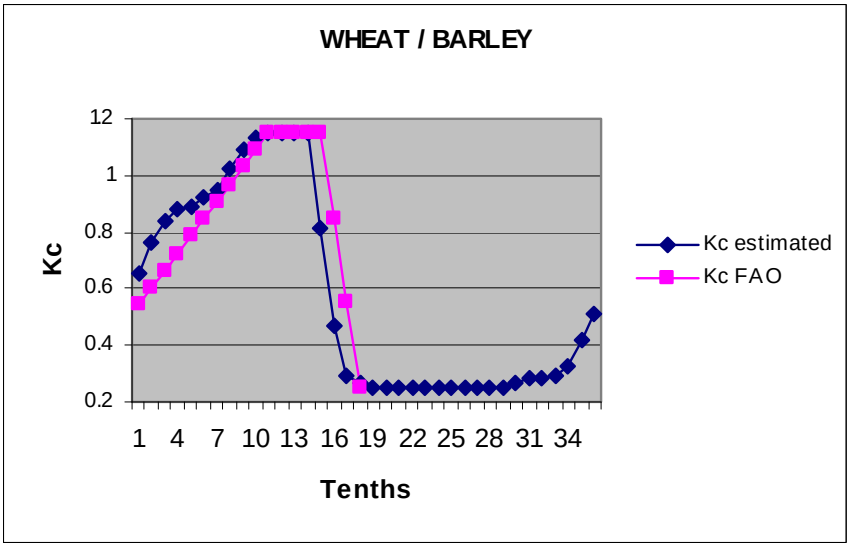

Figure 48. Evolution of wheat/barley Kc through the year 2005.

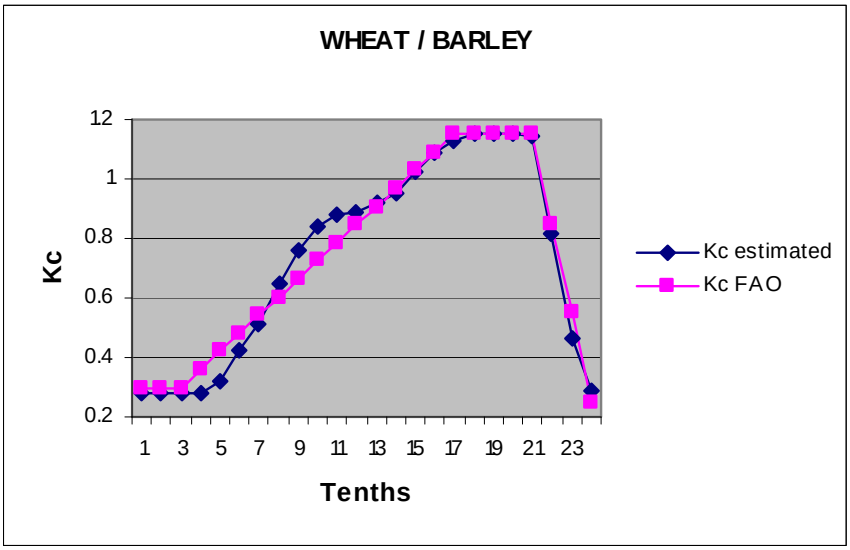

Figure 49. Adjustment between both curves in the growing period (from November to June).

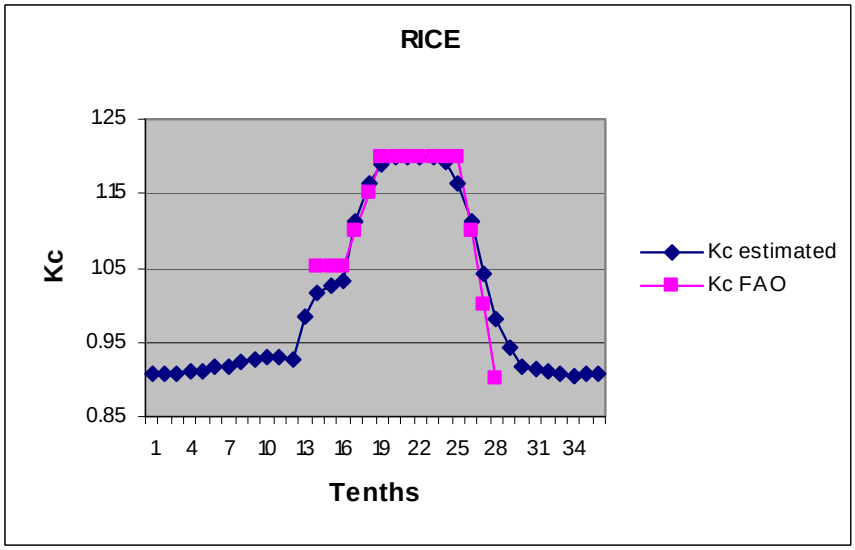

Figure 50. Evolution of rice Kc through the year 2005.

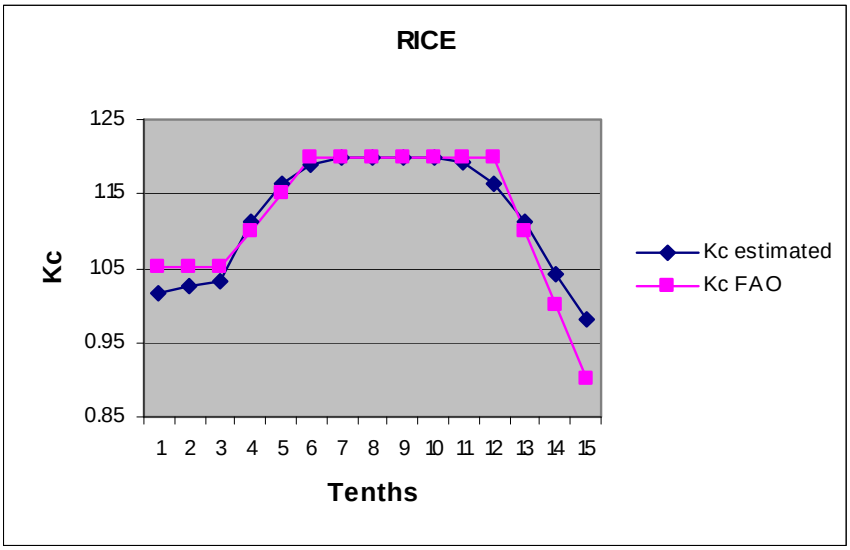

Figure 51. Kc curves in the growing period (from May to October).

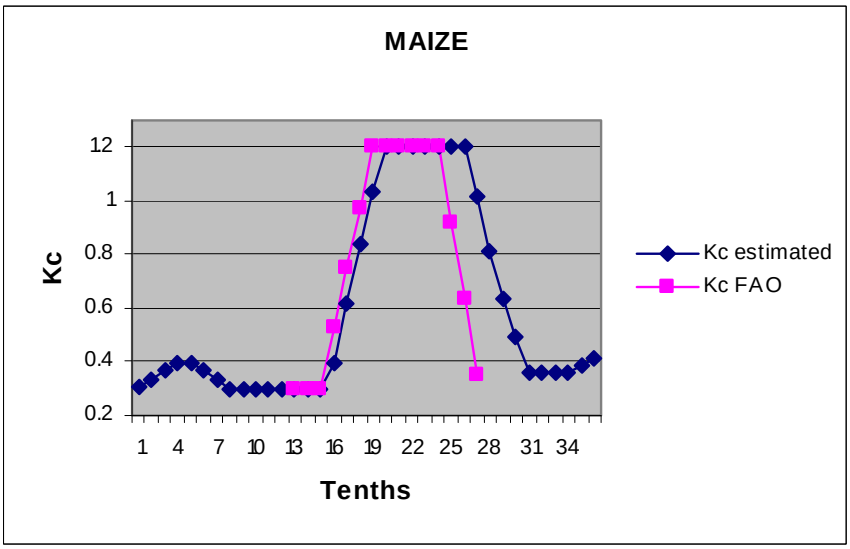

Figure 52. Evolution of maize Kc through the year 2005.

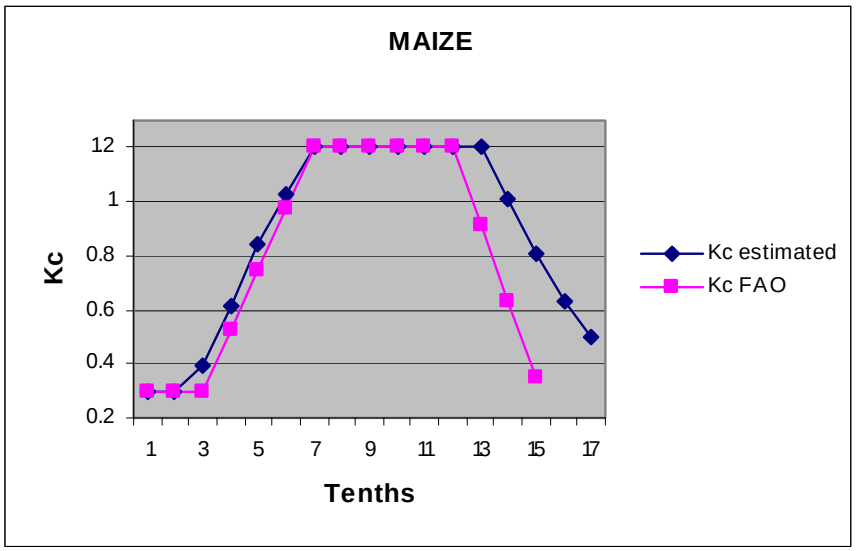

Figure 53. Adjustment between both curves in the growing period (from April to August).

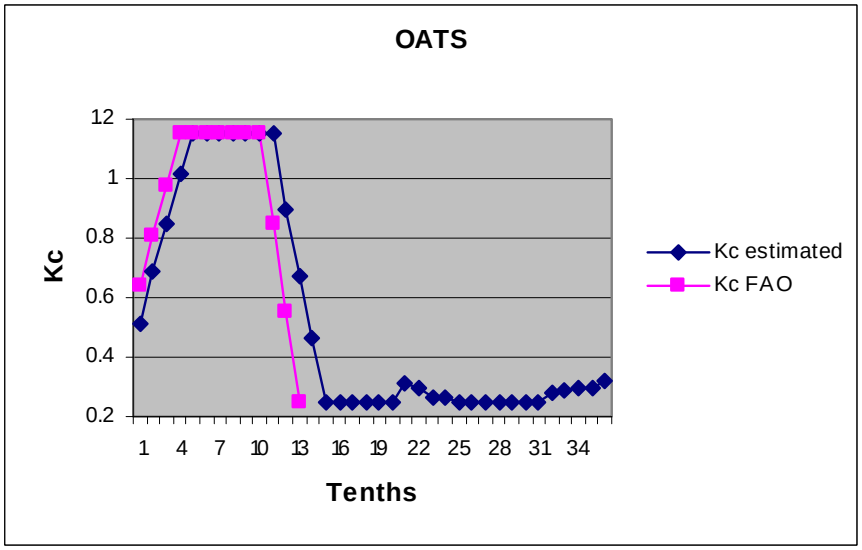

Figure 54. Evolution of oats Kc through the year 2005.

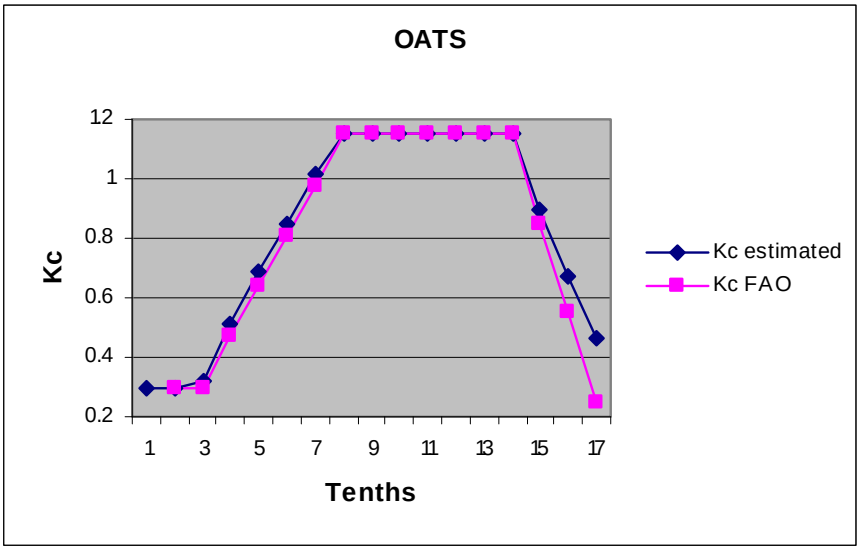

Figure 55. Adjustment between both curves in the growing period (from December to May).

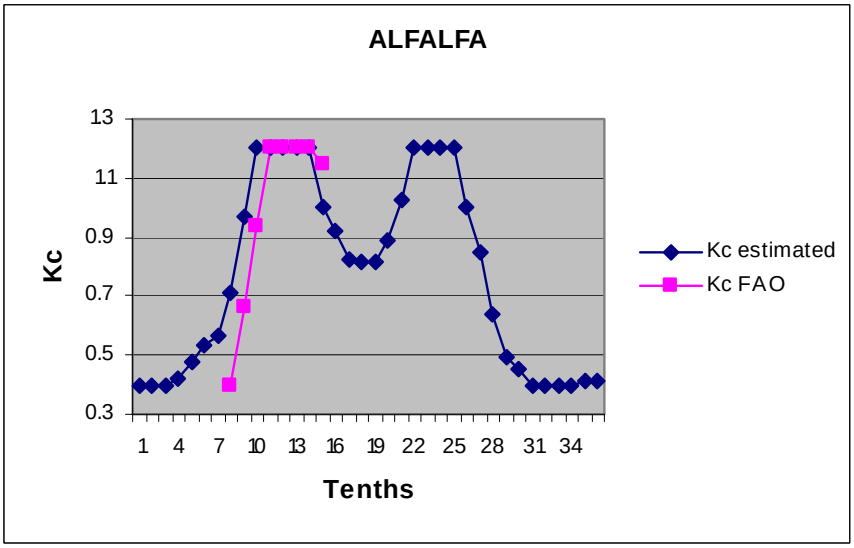

Figure 56. Evolution of alfalfa Kc through the year 2005.

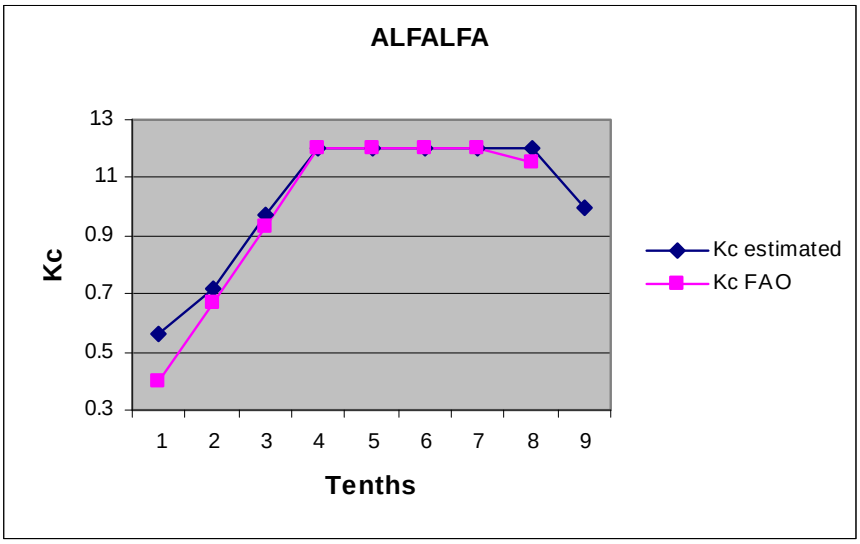

Figure 57. Adjustment between both curves in the growing period (from April to June for the first cutting cycle).

The curves obtained for avocado and strawberry crops could not be validated since the FAO does not establish the length of the different crop phases. Other reliable information sources could not be found either. However, we present the curves obtained below (Figure 58 and Figure 59).

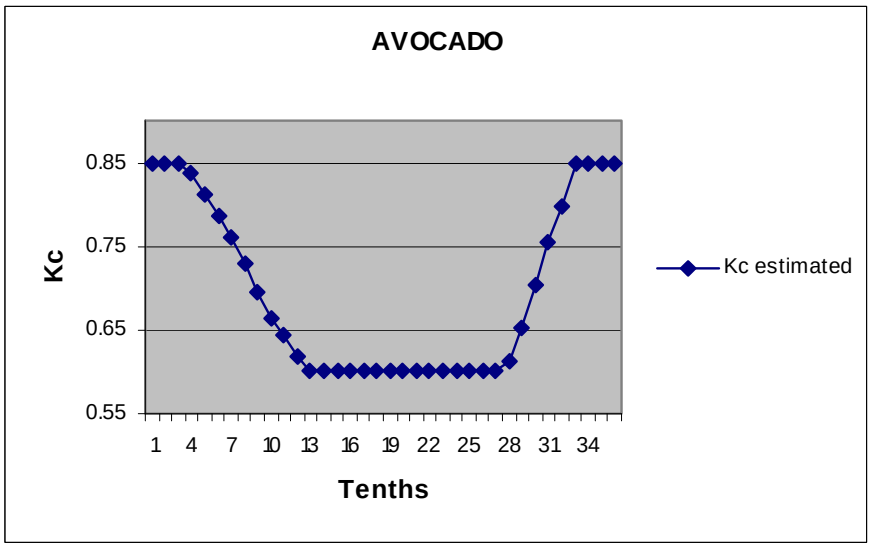

Figure 58. Evolution of avocado Kc through the year 2005.

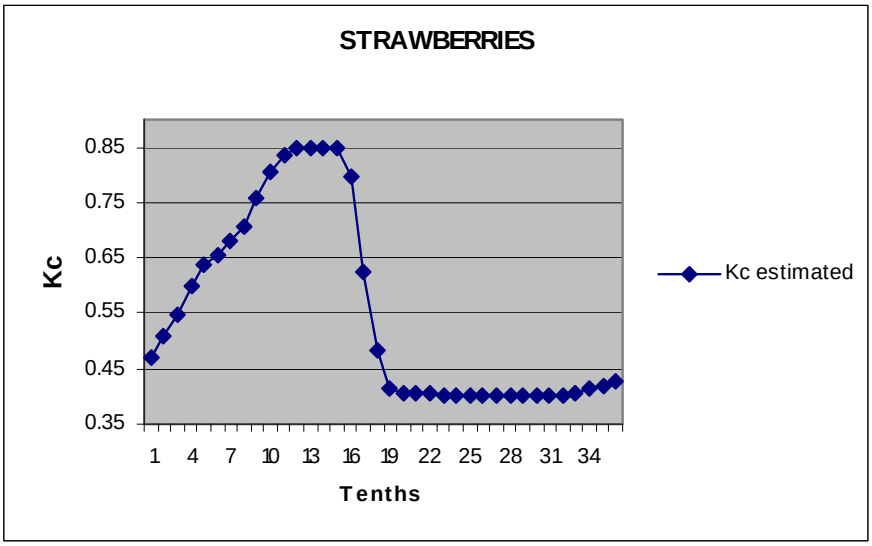

Figure 59. Evolution of strawberries Kc through the year 2005.